MASSACHUSETTS INSTITUTE OF TECHNOLOGY
NAVAL SUPERSONIC LABORATORY

Technical Report 303

A HIGH TEMPERATURE STREAM TUBE FOR A SUPERSONIC WIND TUNNEL

by

Richard H. Adams

May 1958

MASSACHUSETTS INSTITUTE OF TECHNOLOGY
Naval Supersonic Laboratory
Cambridge, Massachusetts

Technical Report 303

A HIGH TEMPERATURE STREAM TUBE FOR A SUPERSONIC WIND TUNNEL

Fifth Quarterly Progress Report
Contract Nonr 1841(40)
February, March, April 1958

Sixth Quarterly Progress Report
Contract AF33(616)-3909
February, March, April 1958

This report describes the design, construction, and calibration of a hot core circuit for the supersonic wind tunnel at the Naval Supersonic Laboratory (NSL). This work was supported out of NSL funds. However, the need for this device was clearly established in the course of work under our infrared contracts and it will be used extensively in tests for these projects. Accordingly, it seems appropriate to identify this as an Infrared Progress Report since knowledge of this facility will assist in a better understanding of tests that will be described later in this series and it may also suggest to those active in the infrared field, realistic environmental tests that might be made of their equipment.

MASSACHUSETTS INSTITUTE OF TECHNOLOGY
Naval Supersonic Laboratory
Cambridge, Massachusetts

Technical Report 303

A HIGH TEMPERATURE STREAM TUBE FOR A SUPERSONIC WIND TUNNEL

May 1958

By: Richard H. Adams
Richard H. Adams

Eugene S. Rubin
Eugene S. Rubin, Project Engineer

Approved: John R Markham
John R. Markham, Director

FOREWORD

This report was submitted in thesis form in partial fulfillment of the requirements for the degrees of Bachelor of Science and Master of Science in the Department of Aeronautical Engineering at the Massachusetts Institute of Technology, May 26, 1958. Professor John R. Markham served as Thesis Advisor.

ABSTRACT

The increasing desirability of obtaining aerodynamic heating data at supersonic Mach numbers led to the development of a method of injecting a high temperature stream tube into a supersonic wind tunnel. A "core" of high temperature air injected slightly downstream of the throat of the Naval Supersonic Laboratory Supersonic Wind Tunnel's Mach 3.5 nozzle produces a relatively constant Mach number and temperature region in the 18 inch x 18 inch test section. This region of 900°F stagnation temperature air was approximately 7 inch x 7 inch and caused no appreciable heating of the tunnel structure. The 7 inch x 7 inch "hot" test area is approximately the blocking area of the test section. Thus by heating only one-sixth of the total mass flow of air in the test section the same aerodynamic heating models may be tested as if the entire mass flow were heated.

TABLE OF CONTENTS

TABLE OF CONTENTS (Concluded)

LIST OF ILLUSTRATIONS

LIST OF ILLUSTRATIONS (Continued)

LIST OF ILLUSTRATIONS (Concluded)

LIST OF SYMBOLS

C_p	Specific heat at constant pressure for air
D	Diameter of hot core stilling section
$\bar{F}$	Scaling factor
h_c	Half-height of hot core
h_t	Half-height of test section
$\bar{h}$	Nozzle generating function
k	Thermal conductivity of air
ℓ	Distance between oblique shock and pitot shock
L	A characteristic length
M	Mach number
$\bar{M}$	Mach number on nozzle axis
p	Pressure
p_p	Pitot pressure
p_{p_s}	Pitot pressure behind an oblique shock
Pr	Prandtl number
Re	Reynolds number
T	Temperature
T_1	Absolute temperature of the flow at velocity U
u, U	Stream velocity in x-direction
U_0	u of surrounding stream
U_1	Largest u in jet
U_{10}	$u - U_0$
U'	Resultant velocity in diverging nozzle
v	Stream velocity in y - direction
w	Mass flow
x, y, z	Cartesian coordinates
x_i, y_i	Coefficients in power series expansion for streamlines
α	$\sqrt{\mu_0 / \rho_0 \mu_0}$
γ	Specific heat ratio for air
δ	Wedge angle
δ'	Effective wedge angle (including boundary layer)

ϵ	Emissivity
η	Streamline parameter
μ	Coefficient of viscosity
ξ	Potential line parameter
ρ	Density
ω	Mass flow

Subscripts

0	Stagnation
c	Conditions in core
s	Conditions in stream surrounding core

Superscripts

*	Condition at nozzle throat

1. INTRODUCTION

As the Mach numbers of aircraft and missiles increase, it is becoming more important to duplicate the aerodynamic heating which vehicles will encounter in flight through the atmosphere It is well known that the vehicle is aerodynamically heated by high stagnation temperature air and that this heating is partially balanced by radiation to the cold surrounding medium.

The obvious tool for duplicating flight conditions is a high stagnation temperature wind tunnel. However, many difficulties arise when an attempt is made to obtain high stagnation temperatures by heating the wind tunnel air stream. Mechanical and structural difficulties arise in the wind tunnel when it is exposed to high temperatures, especially in the nozzle which distorts with thermal stresses unless an intricate cooling system is employed. Valves and other moving parts must be able to operate at the high temperatures to which they are exposed. Due to the loss of strength and the phenomenon of scaling at high temperatures it is necessary to employ stainless steel or other high temperature alloys throughout the system which are costly and difficult to machine. Large wind tunnels (100 in^2 test sections and up) used for testing reasonably sized models require large mass flow rates of air. The expense of heating the mass flow rates required is very high and in many cases where electric heaters would be used the power required is not available.

The Naval Supersonic Laboratory (NSL) is currently operating a hypersonic wind tunnel at a stagnation temperature of 1000°F. However, it was desirable to have heat transfer data on larger models than can be tested in this tunnel Heating the main 18" x 18" supersonic wind tunnel air stream was undesirable due to the above mentioned problems.

A method of alleviating these problems is to heat only the central portion of the airstream to which the model is exposed. This reduces the high temperature mass flow to a fraction of the total mass flow and confines mechanical and structural difficulties due to heating to a relatively small circuit necessary to carry this small mass flow. It also provides the aerodynamically heated model with a cold surrounding medium to which it radiates, namely the cold test section walls

The NACA Lewis Flight Propulsion Laboratory has shown through a preliminary investigation that a heated core wind tunnel is feasible (Reference 1). Upon the basis of this investigation and the increasing desirability to obtain aerodynamic heating data on large models, a heated core installation was undertaken at NSL. This installation was to make use of existing equipment at NSL to the fullest extent possible. Any additions were not to hinder the use of the supersonic wind tunnel under ordinary operation. Any equipment that could hinder the use of the supersonic wind tunnel was to be easy to install and remove.

2. NOTES ON THE THEORY OF MIXING BETWEEN A HIGH TEMPERATURE STREAM TUBE AND A SURROUNDING COLD STREAM

Although the method of approach to obtaining an operational heated core installation was primarily empirical it should be noted that the problem of mixing has been solved for various cases due to the interest in jet and rocket propelled aircraft. A general knowledge of what to expect of a stream tube in a wind tunnel may be obtained from these solutions.

Consider the problem of introducing a stream tube of high temperature air into a supersonic wind tunnel. The core of heated air must be introduced into the main stream via a nozzle which itself can be formed to follow the stream tube. In the absence of viscosity and by matching pressures and Mach numbers at the exit of an infinitesimally thin heated core nozzle, the heated air will follow the stream tube of the area at which it is introduced into the supersonic stream. However the exhausting nozzle must be of finite thickness, and large velocity and temperature differences may exist between the core and the surrounding stream. Thus it is reasonable to suspect that between the core and the surrounding stream there will exist a mixing region, due to slight turbulence caused by the finite size of the exhausting nozzle, viscous effects, boundary layer from the exhausting nozzle and heat transfer.

Since the exhausting nozzle may be fabricated relatively thin and tapered to zero thickness, turbulence induced by the nozzle may be considered negligible as a first approximation. As a first approximation the boundary layer will also be neglected. Consider a nozzle exhausting uniform

velocity flow into a uniform velocity stream. The temperature and velocity distribution throughout the flow may be considered governed by the solution of the problem of two dimensional laminar jet mixing of a viscous compressible fluid.

The equation of motion governing this mixing is

$$\rho u \frac{\partial u}{\partial x} + \rho v \frac{\partial u}{\partial y} = \frac{\partial}{\partial y}\left(\mu \frac{\partial u}{\partial y}\right) \tag{2.1}$$

The equation of continuity is

$$\frac{\partial \rho u}{\partial x} + \frac{\partial \rho v}{\partial y} = 0 \tag{2.2}$$

The energy equation is

$$\rho u \frac{\partial C_p T}{\partial x} + \rho v \frac{\partial C_p T}{\partial y} = \frac{\partial}{\partial y}\left(k \frac{\partial T}{\partial y}\right) + \mu \left(\frac{\partial u}{\partial y}\right)^2 \tag{2.3}$$

These equations describe two dimensional laminar jet mixing and have been solved by Pai (Reference 2) for the case of a two dimensional jet in a uniform stream of velocity U_0 by the method of successive approximations.

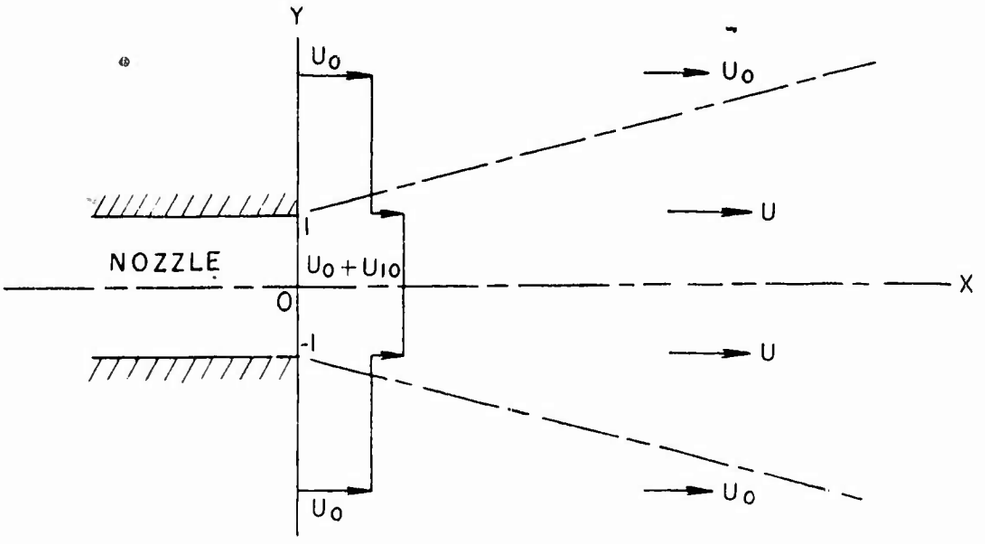

This is the same type of problem encountered in the case of the heated core except for the fact that the heated core is an expanding stream tube, increasing in velocity in the x - direction, as illustrated below.

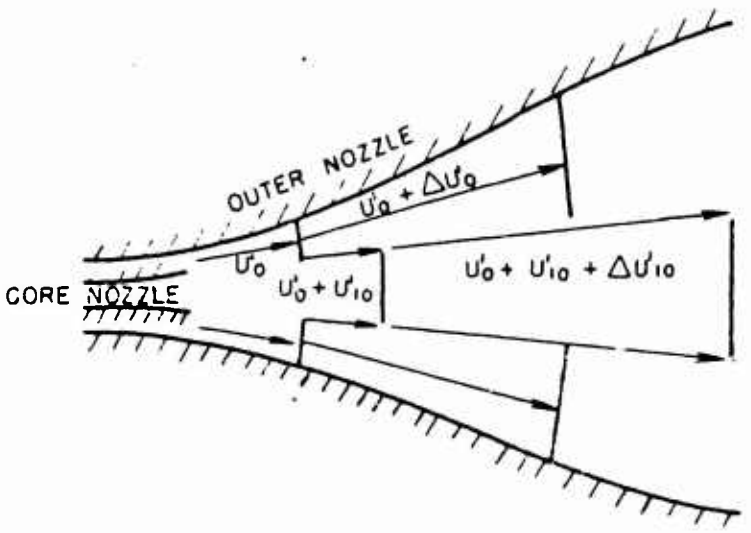

Without actually solving the latter case, which is complicated by the varying x - velocity, we may conclude that the shape of the temperature and velocity distribution curves in the mixing region of the former case will be similar to that of the heated core. Typical temperature and velocity distribution curves reproduced from Reference 3 are shown in Figure 1. Note that the temperature curve is slightly wider than the corresponding velocity distribution curve.

3. THE NACA LEWIS LABORATORY HEATED CORE SUPERSONIC WIND TUNNEL

The NACA Lewis Laboratory made a preliminary investigation into heating the central core of air in the test section of a supersonic wind tunnel (References 1 and 4).

This investigation was carried out at Mach numbers 1.9 and 3.0. The test section for each nozzle was 18 inches by 18 inches. Air for the heated core portion of the test section was heated to 500° F in a parallel arrangement of four jet-engine combustors using JP-4 fuel. The core nozzle was designed to parallel the streamlines induced by the walls of the subsonic portion of the main tunnel nozzle in order to avoid choking upstream of the throat. This nozzle which was entirely convergent in order

to create sonic flow at its exit, theoretically would create a 9 inch by 9 inch core in the test section.

The NACA did investigate partially:

1. Four axial locations of the core nozzle exit plane, i.e., 3 inches upstream, 1 inch upstream, 1 inch downstream of the tunnel throat, and at the tunnel throat.
2. A rectangular core nozzle exit.
3. Various stagnation pressure ratios of core to cold stream.
4. Temperature and Mach number profiles at several stations in the test section region.

The NACA did not investigate in detail:

1. Diffusion of the interface layer separating the hot and cold streams.
2. Effect of the area of the core nozzle exit.
3. Effect of the geometry of the core nozzle exit.
4. Positioning of the exit plane in the supersonic region.
5. Reflection strengths.
6. Possible canting or vibrations of the core inlet nozzle.
7. Mixing of the streams in and downstream of the supersonic diffusor.

The flow in the test section was surveyed with a wall to wall rake of alternately spaced temperature and pitot probes. In addition five static-pressure orifices were located on the rake within 4 1/4 inches of the tunnel wall.

A typical Mach number and temperature profile illustrating the NACA's results is reproduced in Figure 2.

The NACA concluded that the cross-sectional area of the core within 90 per cent of the stagnation temperature of the core air was about 35 per cent of theoretical for Mach number 1.9 and 25 per cent of theoretical for Mach number 3.0. The location of the core nozzle exit plane for the Mach number 3.0 tests was considerably upstream of its location for the Mach number 1.9 tests. Data indicated that the best core shapes and sizes were obtained with the core nozzle exits located at the tunnel throats or slightly downstream. The variation of the core to cold stream stagnation pressure ratio had little effect on the core size and shape.

The above summarized heated core wind tunnel was pursued no further after its preliminary investigation and at the present is inoperative.

4. DESCRIPTION OF EXISTING EQUIPMENT

Since the design philosophy on the heated core installation was to use existing equipment, several definite limits were placed on the performance of the installation. A brief description of the existing equipment is presented below in two categories, the supersonic wind tunnel and the hypersonic wind tunnel circuit.

4.1 Supersonic Wind Tunnel

Characteristics of the Naval Supersonic Laboratory Wind Tunnel are as follows:

Operating cycle	Continuous
Test section	18 in × 24 in to Mach 2.5 18 in × 18 in to Mach 4.0
Nozzle blocks available	For Mach numbers 1.5, 1.7, 2.0, 2.25 2.5, 2.75, 3.0, 3.25, 3.5 and 4.3. Also transonic blocks provide a continuous Mach-number range from M = 0.5 to 1.2.
Test-section window size	30-inch (24-inch diameter largest currently available)
Optical apparatus	30-inch schlieren or shadowgraph
Balance	Strain gage with automatic readout
Mach-number range	0.5 to 4.3, approximately
Reynolds-number range	0.05×10^6 to 10×10^6/ft
Stagnation-pressure range, p_0	1.5 to 42 psia
Stagnation-temperature range, T_0	100 to 130° F (normal operating temperature 110 degrees)
Drive horsepower	Electricity 10,000 hp rated 12,500 hp for 2 hours

Main compressors	4,000 hp 4-stage centrifugal
	6,000 hp 4-stage centrifugal
	Operable in parallel or series
	Outlet temperature limit-500° F

4.2 Hypersonic Wind Tunnel Circuit

Included in the hypersonic wind tunnel circuit and pertinent to the heated core installation are the Chicago pneumatic compressers capable of drawing 1.7 pounds of air per second from atmosphere and raising it to a pressure of 100 psia and a temperature of 100° F. Approximately one pound per second of this air after passing through driers, passes through a total pressure control and into 270 kilowatt heaters. These heaters are capable of raising a continuous mass flow of air of one pound per second to a stagnation temperature of 1000° F. This is the maximum mass flow of air available for the heated core portion of the flow in the supersonic test section, the remaining 0.7 pounds per second of air being used in the air seals of the supersonic wind tunnel compressors.

Figure 3 is a schematic diagram of the circuit used for the operation of a hot core installation. The main tunnel circuit depicted as a block in Figure 3 is broken down into components in Reference 5, but is not pertinent to the discussion at hand.

5. THEORETICAL PERFORMANCE CALCULATIONS

All performance calculations for the heated core were based on the performance of the apparatus discussed in the preceding section. Throughout all calculations the hot core and stream stagnation pressures were assumed identical. Also the Mach number of the core in the test section was assumed identical to the Mach number of the cold stream. These are reasonable design criteria since with isentropic, one-dimensional, non mixing flow and the above conditions the core may be dealt with as a stream tube separated from the cold stream flow. For the purpose of these performance calculations, i.e. to obtain the design criterion, the specific heat ratio γ can be assumed to be 1.4 without considerable loss of accuracy.

Performance characteristics based on the above assumptions are presented in Reference 6 and in Figures 4 through 10. Assuming a core mass flow of one pound per second and a core stagnation temperature of 1000°F, Figure 4 presents the theoretical heated test section area possible, as a function of Mach number and stagnation pressure. Figure 5 gives the temperature of the completely mixed flow, downstream of the test section as a function of Mach number and stagnation pressure, assuming a cold stream stagnation temperature of 100°F. Figure 6 shows the temperature of the mixed flow as a function of the cold stream mass flow for various core stagnation temperatures. The effect of stagnation pressure and Mach number on the cold stream mass flow is indicated in Figures 7 and 8. The variation of theoretical test section area with stagnation temperature of the core for typical fixed parameters is given in Figure 9. Since the simulation of aerodynamic heating was the ultimate goal and the heating of the tunnel structure and the compressors could cause difficulties, Figure 10 is presented to indicate the heated theoretical test section area available for an allowable mixed flow temperature.

6. DESIGN COMPROMISES BASED ON EXISTING EQUIPMENT AT NSL

6.1 Design Parameters

The theoretical performance curves of the heated core installation, as is pictured schematically in Figure 3, depict the range of parameters possible using existing equipment. The only additional equipment necessary was a circuit and nozzle to inject the heated air into the supersonic test section as shown in Figures 11 through 13.

Section 4.1 indicates that the outlet temperature limit of the main compressors is 500°F. Thus knowing the efficiency of the compressors the inlet temperature limit may be obtained. As Figure 10 indicates this will set a limit on the hot core test section area obtainable for a given hot core stagnation temperature. Appendix A yields a compressor efficiency of approximately 77 per cent and a maximum intake temperature of 233°F for Mach 3.5 operation. From Figure 10 this temperature limit gives a possible test section area of 80 in^2 at a stagnation temperature of 800°F. It is reasonable to suspect that the actual inlet temperature will be considerably lower than the mixed flow temperature due to the heat dissipated

to the piping between the diffuser and the compressors. Thus a choice of a theoretical test section area of 80 in^2 will allow stagnation temperatures in the hot core of at least 800° F, and possibly 1000° F without harm to the main compressors.

It was felt that the highest Mach number conveniently possible should be chosen for the heated core installation. NSL has had considerable favorable experience with the operation of the supersonic wind tunnel with the Mach 3.5 blocks. These blocks have a throat large enough for convenient installation of an inner, hot core nozzle. A Mach number of 3.5 at a stagnation temperature of 1000° F also simulates actual flight conditions of missiles and aircraft very well.

Figure 4 indicates that under optimum theoretical conditions of T_{0_c} = 1000° F, ω_c = 1 #/sec, A_c = 80 in^2 and M = 3.5, the stagnation pressure of the core will be about 6 psia.

The test section for Mach 3.5 is 18 in x 18 in or 324 in^2. Since this test section is square the theoretical heated core test section was designed so as to be square. That is 8.94 in x 8.94 in or 80 in^2.

6.2 Additions to the Existing NSL Piping Circuit

The additional circuitry shown schematically in Figure 11 is necessary to supply the core air from the HWT (Hypersonic Wind Tunnel) heaters to the main tunnel. Appendix B includes a detailed report of the design conditions considered and met in the construction of this additional circuit.

To transport the air heated in the HWT heaters to the wind tunnel required approximately 75 feet of pipe. Conceivably this pipe must withstand 1000° F temperatures and be insulated so as to keep heat losses to a minimum.

A p_0 control located upstream of the heaters would allow use of a "cold" valve. However this would mean the use of large pipe since the heated core is operated at about 6 psia. By carrying the air at 100 psia and locating p_0 control valves just upstream of the core stilling chamber, as is shown in Figure 12, it is possible to use 2" inch pipe. This 2" inch line is insulated with three inches of "Kaylo 20" on the radius. Approximate calculations show that under equilibrium conditions with one pound per second of 1000° F air a total temperature loss of 75° F is expected in the 75 foot line.

Design codes do not permit the use of steel under stresses encountered in 1000° F service. Another problem encountered at high temperatures is the phenomenon of scaling. The most practical solution to the problem of a choice of material for the pipe seems to be the use of chrome molybdenum steel. At 1000° F the pipe expands axially about one inch for every 10 feet of pipe. This expansion is taken up with flexible hose (stainless steel wire woven about stainless steel bellows). Such a hose provides practically no reaction.

The 75 foot line may be preheated by passing hot air to atmosphere through a bypass located just upstream of the entrance of the hot core line into the main tunnel (Figure B.1). This allows the core to be operated at maximum temperature shortly after supersonic flow is obtained in the test section. To allow rapid shutdown and provide for cooling of the model, provisions are made to pass cold air through the hot core stilling section and nozzle using the existing pre-drying system as a source (Figure B.1).

6.3 Heated Core Stilling Section

The location of the heated core stilling section immediately upstream of the heated core nozzle limits the physical size and shape of the section since it passes through the plug valve upstream of the supersonic test section (see Figure 12). Any area taken up by the heated core stilling section thus increases the velocity of the cold air through the plug valve. This cold air conceivably cools the heated core stilling section, causing a heat loss in the hot core system. It was necessary in considering the design of the heated core stilling section therefore to keep in mind the following problems in addition to the conventional problems.

1. Structural problems of the stilling section are aggravated by the high temperature requirements.
2. There are heat losses from the heated core air which may be alleviated by insulating the stilling section.
3. Size and shape of the section affect not only the flow properties of the hot air but the cold air as well.
4. The supporting structure of the stilling section should be kept aerodynamically "clean" as there is cold air flowing past the outside of the section.
5. The downstream end of the stilling section should be anchored so that thermal-expansion of the section will cause no motion of the hot core nozzle.

For structural purposes the stilling section was chosen to be fabricated from # 304, 12 gauge stainless steel, rolled into a 12 inch O.D. cylinder. Such a cylinder, approximately 10 feet long, will support itself at each end and withstand pressure differences on the order of 20 psia. at 1000° F. Normally, pressure differences will be no greater than 3 or 4 psia.

A conservative estimate of the heat loss from a 10 foot cylinder with one inch of insulation under typical operating conditions, as given in section 6.1, indicates a temperature drop of 18° F. These calculations are given in Appendix C. An 18° F temperature loss might suggest a need for greater insulation. However in order to provide for large contraction ratios in the cold and hot nozzles and to keep the Reynolds Number low in the stilling chamber it was not possible to add more insulation. The fact that the 18° F loss is a conservative estimate is encouraging however.

The 12 inch stilling chamber with one inch of insulation provides Reynolds numbers of about 5×10^4 inside of the stilling chamber and 1.4×10^5 outside of the stilling chamber. Velocities are on the order of 100 feet per second. The insulation around the stilling section was covered with thin sheet metal to assure smooth flow over the outside of the stilling section. The contraction ratio for the hot core nozzle is 9.6 and the contraction ratio for the cold stream nozzle is 11.1. These are generally accepted ratios.

The upstream end of the stilling section is suspended from the top of the main tunnel stilling chamber by two cables. A third spring loaded cable running to the bottom of the stilling chamber anchors the upstream end of the section in the vertical and horizontal planes, but allows motion in the axial direction (Figures 12 and 13). Two sets of triangularly arranged struts anchor the downstream end of the stilling section. See Figure 12. Each set fastens at a common point on the tunnel floor and ceiling and is angulated in the vertical plane so that radial expansion of the section will not cause binding in the system. With this arrangement the nozzle end of the stilling chamber is fixed, except for minute motion in the axial direction due to radial expansion of the stilling chamber and the angular arrangement of the downstream struts. The struts are circular rods.

However, due to their location and the flow direction of the cold air they are "seen" elliptically streamlined by the flow. All cables and struts supporting the stilling chamber contain turnbuckles in order to allow proper centering of the nozzle which is fastened by stainless steel screws onto the square end of a transition section (Figure 12). In order to assure precise positioning of the core nozzle a special gauge and set of levels are used at the time of installation of the stilling section and nozzle. Photographs of the heated core stilling section and nozzle installation are shown in Figures 14 through 16.

6.4. Core Nozzle Design

The ideal nozzle for the injection of a heated stream tube should follow the stream tube of the air it is replacing in the test section. Since the parameters used to design the Mach 3.5 nozzle blocks for Naval Supersonic Laboratory's supersonic wind tunnel were available, it was possible to accomplish this design condition. The design of the nozzle blocks at NSL by the Friedrichs Method and computation tables for the flow field through the nozzle are summarized in Reference 7.

In the figure below the supersonic nozzle block contour is represented by the streamline $\eta = \eta_d$. The contour the core nozzle should follow is determined by h_c and is represented by $\eta = \eta_c$. Conceivably, a scaling factor, $\overline{F}$, must be determined. $\overline{F}$ is given by

$$\overline{F} = \frac{h_T}{yQ} \tag{6.4.1}$$

where

$$yQ = \frac{(M_d^2 + 5)^3}{216\, M_d}\, \eta_d \tag{6.4.2}$$

M_d is the design Mach number, and η_d is given in Reference 7 for $M_d = 3.5$.

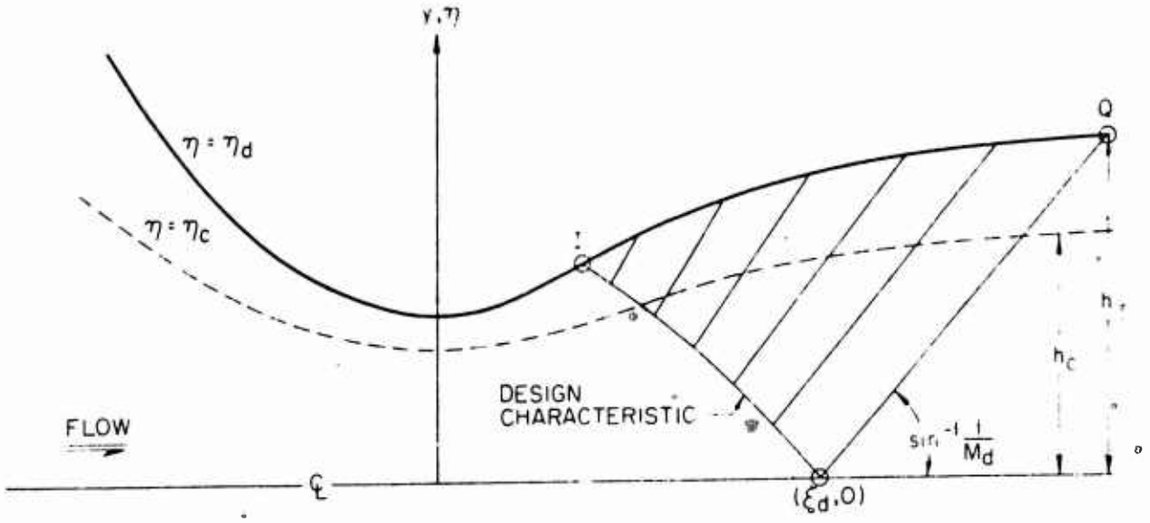

Upstream of the inflection point, I, which is the region in which the heated core nozzle is installed, the flow properties are assumed in the series form:

$$x = \xi + x_2 \eta^2 + x_4 \eta^4 \qquad (6.4.3)$$

$$y = y_1 \eta + y_3 \eta^3 + y_5 \eta^5$$

The nozzle generating function used in the design of the nozzle for the Naval Supersonic Laboratory is

$$\overline{h} = 1 + \xi^2$$

Assuming this generating function the coefficients y_i are given by:

$$y_1 = 1 + \xi^2$$

$$y_3 = \frac{y_1}{3}\left[y_1 (A - 2) + 2 \right]$$

$$y_5 = \frac{y_1}{5}\left\{ y_1^2 \left[B/2 - 2A + 2/3 (1 - 2C) \right] + 2y_1 \left[A + 2/3(C - 1) \right] + A\delta_4 + 2/3 \right\}$$

where

$$A = \overline{M}^2 - 1$$

$$B = \gamma \overline{M}^4 - \overline{M}^2 + 2$$

$$C = \frac{(\gamma + 1)\overline{M}^4}{\overline{M}^2 - 1} - 1$$

$$D = \frac{(\gamma - 1)\overline{M}^2 + 2}{\overline{M}^2 - 1}$$

$$\delta_4 = \frac{y_1}{6}\left[3y_1 (A + C + 2) - 2C + \frac{(y_1 - 1)}{A}(2D)(C + 1)(A - 1)\right]$$

At $\xi = 0$, or at the nozzle throat:

$$y = \frac{h_c^*}{\overline{F}} \tag{6.4.4}$$

Now if $\eta \ll 1$, from equation (6.4.3)

$$\eta \cong {}^{y}/_{y_1}(0)$$

$$\cong \frac{h_c^*}{\overline{F}}$$

as a first approximation. As a second approximation assume $\eta = \eta_1$ and solve for η_2 in equation (6.4.3):

$$\eta_2 = \frac{y - y_5 \eta_1^5}{y_1(0)}$$

Using this procedure until convergence, which occured at η_2, a value of η was found. Knowing η and picking values of ξ, equations (6.4.3) were solved for values of x and y with the aid of the tabulated values for x_i and y_i found in Reference 12.

Since the tabulated values of x_i and y_i were given in the subsonic portion, upstream to about M = 0.3, the remainder of the nozzle was faired in according to the area ratio of the cold stream area to the hot core area, the the last point found. The core nozzle was extended downstream of the throat 10 percent of the distance to the end of the NSL Mach 3.5 nozzle blocks. This

distance was about 5 inches. The choice was based upon the fact that the NACA heated core showed increased performance with the core nozzle exit downstream of the throat. The core nozzle coordinates are listed in Appendix D.

The core nozzle was machined from four # 304 stainless steel plates bent to the proper contours and screwed together.

7. CALIBRATION OF THE HEATED CORE

The primary purpose of the heated core installation being the simulation of aerodynamic heating places the desirability of a total temperature survey in the test section first in importance. Conceivably a Mach number survey is of great importance also. Such properties as flow angularity were considered to be of relative unimportance at this time. The calibration of the heated core test section was further complicated over the calibration of a conventional supersonic test section due to the certainty of the existence of a turbulent mixing region, high temperatures, and varying low Reynolds numbers. The low Reynolds numbers are present due to the low p_0 (6 psia) design condition. The range of Reynolds numbers existing in the test section, for a given stagnation temperature of the core, is illustrated in Figure 17.

7.1 Instrumentation

The primary instrumentation for the calibration of the heated core test section consists of a rake of pitot probes and a rake of total temperature probes in a "biplane" arrangement extending eight inches to either side of the test section centerline (Figures 18 and 19). In addition to these probes a sonic orifice mass flow probe, to measure local total temperature, and a wedge-pitot probe, to measure local Mach number, were mounted on the rake. By mounting this rake on a special calibration mount, which can be remotely moved in the vertical and axial direction, a Mach number and total temperature survey up to a few inches from the tunnel wall was obtained in a region extending from 16 inches upstream of the schlieren centerline to 14 inches downstream of the schlieren centerline. Stagnation pressure and stagnation temperature were measured in the stilling chamber by a pitot probe and a single shielded iron-constantan thermocouple. The shield

around the thermocouple was platinum plated to cut down radiation errors. These probes, which were mounted about the centerline of the downstream end of the stilling chamber, are shown in Figure 20. The photograph, Figure 20, was taken after the probes had been run at 900° F temperatures for about 20 hours. The discoloration noticeable is of unknown cause.

A schematic diagram of the wind tunnel instrumentation for the heated core calibration is presented in Figure 21.

7.1.1 Total Temperature Probes

The total temperature probes on the rake were placed in a row, at one-half inch spacings up to five inches from the center of the rake and at one inch spacings from there on. This arrangement called for a sum of 26 total temperature probes. Thus it was neccessary in picking a total temperature probe to emphasize the importance of simplicity in the design. The probe used is shown in Figure 22. It is a Pratt and Whitney type probe similar to the design found in Reference 8. The shielded probe was fabricated from thin walled stainless steel tubing with an iron-constantan thermocouple held inside by Sauerisen, an insulating cement which will withstand high temperatures. Three vent holes of total area equal to the entrance area, were placed around the circumference of the shield. Thus at Mach 3.5 operation the thermocouple junction was exposed to a Mach number of about 0.45, the Mach number behind the normal shock. This is slightly high by standards. However, since the probe was to be used at essentially one Mach number any error due to the slightly high velocity would be corrected for in the recovery factor determined at the time of the calibration tests. Radiation errors are cut down by plating the outside of the shield with platinum, which has a very low emissivity. The thermocouple junction is placed well ahead of the vent holes in the shield so that it cannot radiate to the cold walls directly through the vent holes. These probes were fabricated with relative simplicity.

7.1.2 Mass Flow Probe

Due to the difficulty in calibrating temperature probes properly, a sonic orifice mass flow probe to determine temperature looked attractive.

The mass flow probe used is shown in Figure 23. It consists of an orifice and a ring opening around the orifice at which pitot pressure was measured. The mass flow is determined by connecting the probe to an eva tank and measuring the pressure and temperature in the tank before and after a measured period of time. The final pressure in the tank must be less than the necessary pressure to maintain sonic flow in the orifice, whi when in a supersonic stream is behind a normal shock. Knowing the mass flow through the sonic orifice, the effective area of the orifice, and the stagnation pressure, the local stagnation temperature may be obtained independent of the usual thermocouple errors induced by radiation, conduct and convection. However, results are extremely sensitive to mass flow and orifice area. There was considerable difficulty in setting up the necessary leak proof mass flow probe system and in calibrating the probe for an effective orifice area (on the order of 3×10^{-4} in^2). Due to the complication of the system and the desirability to have a check on the temperature probes a single mass flow probe was placed in the center of the rake (Figure 18). This probe was to obtain an accurate temperature reading at several points in the test section with which the thermocouple readings could be compared. Thus it was the intent to calibrate the total temperature probes near the center of the rake against the mass flow probe

7.1.3 Mach Number Measurements

A row of pitot probes at one inch spacings extending eight inches to either side of the tunnel centerline were placed on the rake one inch above the total temperature probes (Figure 18). From the ratio of pitot pressure, p_p, and stagnation pressure p_0, Mach number may be determined. However this method of measuring Mach number assumes that the stagnation pressur in the stilling chamber is identical to the stagnation pressure at every point in the test section. That is, isentropic flow must exist throughout the test section, a condition not obvious in a stream tube whose boundaries are subject to turbulence and mixing.

To calibrate a wind tunnel independent of the above assumption another local measurement is necessary in addition to the local pitot pressure. Due to the low Reynolds numbers and low pressures inherent in the heated core operation the local measurements of such parameters as

cone static or wedge static pressures will acquire great inaccuracies. These inaccuracies are induced by the displacement effect of the boundary layer on the cone or wedge and in the measurement of such low pressures. Pitot probes have acquired a reputation of accurate measurements as long as their free stream Reynolds number is greater than 10^3 and their hole diameter is less than one half of the tube diameter. Since pitot pressure is higher than static pressure, the pressure measurement accuracy is increased also. Pitot pressure thus seems to be the pressure which may be most accurately measured in this flow.

Reference 9 recommends the measurement of pitot pressure, p_{p_s}, behind a known oblique shock. This pressure is a function of the shock angle θ (Figure 25). However, the pressure in question displays a maximum for some value of θ close to that which gives equal values of specific entropy rise across the oblique and pitot shocks. Near this point the variation of p_{p_s} with the shock angle θ is slight. Figure 26 shows the optimum shock angle at M = 3.5 and γ = 1.36 to be 39.5°. The assumption of γ = 1.36 for Mach 3.5 flow with a stagnation temperature of 1000° F is in error. Reference 10 reveals that the calorically imperfect equations are more closely approximated by γ = 1.4 for these conditions, which would yield an optimum θ of 38.4°. However, Figure 27, which represents flow for γ = 1.4, shows that the error induced in measuring the Mach number with a one degree error in the shock angle is negligible.

A single wedge-pitot probe was mounted on the calibration rake above the central pitot probe. Thus by moving the rake, the pitot pressure, P_p, and the wedge-pitot pressure, P_{p_s}, could be found at a given point. From the ratio of p_{p_s}/p_p Mach number at that point could be determined. The wedge-pitot probe is shown in Figure 25 and Figure 28. Notice that the optimum shock angle is determined by δ', the effective wedge angle comprised of the physical wedge angle plus an approximation to the boundary layer angle. This boundary layer angle correction amounted to one degree. Thus the pitot tube angle in Figure 28 is one degree greater than the wedge angle. An error is induced in the wedge-pitot measurements because the oblique shock and the pitot shock are not at the same point in the flow, but are separated by a distance, ℓ. There are expansion and compression

waves in the flow behind the oblique shock due to non uniformity of the flow in the test section and due to disturbances from the boundary layer on the wedge. Thus the Mach number just upstream of the pitot shock is not identical to the Mach number just downstream of the oblique shock. A correction for these effects was made possible by making the pitot probe on the wedge adjustable for different values of ℓ at which several measurements could be taken. By extrapolating data to $\ell = 0$ the distance effect could be nullified.

7.2 Data Reduction

The primary goal in the calibration of the heated core was to obtain to the highest degree of accuracy, practically feasible, a temperature and Mach number survey in the heated core portion of the test section. The core is defined here as the region in which a constant stagnation temperature exists. Exploration of the mixing region was considered of secondary importance. Mach number and temperature surveys were taken in vertical planes with the rake described in the preceding section, at five axial, x-stations. The coordinate system used in the survey is illustrated below.

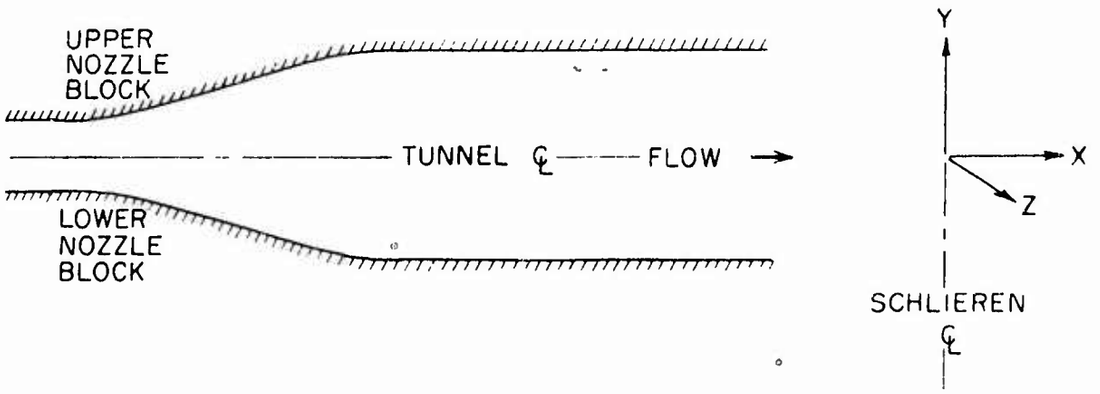

7.2.1 Temperature Data

The iron-constantan stilling chamber thermocouple shown in Figure 20 is shielded to cut down radiation effects, which are small since the walls of the stilling chamber are hot. Thus, the stagnation temperature measured in the stilling chamber, T_{0_c}, should be accurate within one-half of one per cent. As is shown in Figure 21 the temperatures indicated by the temperature probes in the test section were read on Brown self-balancing potentiometers with bucking voltages fed in by Rubicon hand potentiometers. These temperatures were hand recorded, as were the hot core and cold stream stilling chamber temperatures. Unfortunately, the mass flow probe data has not yet been interpreted. However, work is being carried out at NSL on this data. The orifice coefficient, an efficiency index of the orifice, seems to be in error as the data yields consistent low readings for the test section total temperature.

The absence of the temperatures with expected high accuracies, determined by the mass flow probe, required that the total temperature probes be calibrated by the next best method. This was to assume that the constant total temperature core of air existing in the test section must be equal to the stagnation temperature in the stilling section. This is a good assumption since the data showed a definite constant temperature region with a distinct edge (Figure 37).

The recovery factors of the probes were not defined in the usual manner since they were used at only one Mach number and were based upon the core stagnation temperature. The recovery factor, r, was defined as the ratio of the indicated thermocouple temperature, in the core at the Schlieren centerline, to the core stagnation temperature. This ratio was .94 ± .005 for all temperature probes in the core except for the probes at $z = \pm 1/2$. The recovery factors for these two probes were .91 ± .005 and .92 ± .005 respectively. One would expect these two probes to have a lower recovery factor than the others. They are located near a larger heat sink than the other probes are, the large mass of the sting holding the rake. Since all probes in the core but the two central probes gave a fairly consistent recovery factor it is reasonable to assume the recovery factor of the probes outside of the core are the same, i.e., .94 ± .005.

Such an uncertainty in the recovery factor as ± .005 coupled with the reading accuracies in the data reduction yield an overall accuracy of the total temperature data in the core of one per cent. The data outside of the core may be slightly less accurate due to the uncertainty of the recovery factor of the probes in that region. The temperature data after the application of the above recovery factors is presented in Appendix E.

7.2.2 Mach Number Data

The pitot pressures in the test section were read out on a 10 centistoke silicone manometer board and recorded by photographs. These photographs could be read to ± .05 inches of silicone or ± .002 psia. Stagnation pressures were read on the Wallace and Tiernan Gages to ± .01 psia. With the assumption that the stagnation pressure indicated in the stilling chamber exists throughout the test section these accuracies in pressures yield, by the method of Reference 11, a Mach number accuracy of ± .2 per cent.

In using the calorically perfect equations to obtain Mach number at the 900°F core temperatures however, there is another error induced. The compression of the fluid through the pitot shock is at such a high time rate, under some conditions, that there is not sufficient time to establish the distribution of energy between the various degrees of freedom corresponding to an isentropic process. In other words the degree of freedom corresponding to the intramolecular vibration has a finite "relaxation time". Also due to the variation of the static temperature as the air passes from the stilling chamber and expands through the nozzle, the specific heat ratio, γ, is not constant at every point throughout the process. These effects cause caloric imperfections in the process which are not completely understood. Reference 10 presents calorically imperfect equations and a method to correct for caloric imperfections in terms of the ratio of pitot pressure to stagnation pressure in supersonic flow. This correction was applied to the data obtained and amounted to dividing the pressure ratio in question by a factor of 0.98, a step in the right direction but not considered exact. It is possible that this combined with the other Mach number inaccuracies will yield a final Mach number accuracy of ± 0.3 per cent

again based on the assumption of a constant stagnation pressure. The Mach number data reduction was carried out on the Naval Supersonic Laboratory's Bendix G-15 computer. This data is compiled in Appendix F.

On the x = 0, z = 0 line, values of the wedge pitot pressure, p_{p_s}, were recorded for three positions of the wedge pitot probe at six y-stations. The corresponding pitot pressures were also found for these points and thus the ratio p_{p_s}/p_p determined. The ratios found at each point for the three values of ℓ are plotted in Figures 29 through 34. Figures 30 and 34 show the points falling in fairly straight lines with about the same slopes, as expected. Thus extrapolations to $\ell = 0$ were obtained. Figure 35 is an enlarged schlieren photograph of the wedge pitot probe set at $\ell = 0.1$ inches. Notice in this figure that the oblique shock is interfering with the pitot shock and touching the pitot probe. A very likely possibility exists that this interaction interferes with the streamline entering the pitot probe causing a p_{p_s} to be read which is too low. The schlieren evidence is enough to justify eliminating the $\ell = 0.1$ point in Figures 29 and 32. With the elimination of these two points the extrapolations to $\ell = 0$ yields slopes in agreement with Figures 30 and 34. The $\ell = 0.2$ point in Figure 31 and the $\ell = 0.3$ point in Figure 33 were eliminated as bad points in light of the fact that the previous extrapolations agree well "slopewise", and the elimination of these points would make all the extrapolations agree in this sense as expected. Based on the previously stated accuracies of pressure measurements and the accuracy of extrapolation techniques the wedge-pitot determined Mach number measurements have an accuracy of about ± 0.3 per cent.

7.3 Results and Discussion

The calibration of the heated core was carried out in three phases: studies of the core at Mach 3.5 with matched stagnation pressures in the core and cold streams; studies of the core under unmatched stagnation pressure conditions; and studies of the core with the NSL Mach 3.0 nozzle blocks used with the Mach 3.5 core nozzle.

Thermocouples placed on the nozzle blocks and upstream of the

l compressor showed no excessive heating at these critical points.

7.3.1 Studies of the Core at Mach 3.5 Matched Stagnation Pressures

Figures 36 through 38 present the temperature distribution in the test section at three axial stations through the use of the parameter θ, a total temperature difference ratio. This data repeats well over the axial distance of 22 inches. The isotherms shown in these figures reveal that the core has a cross sectional area with nearly constant stilling chamber temperature of approximately 50 square inches, or 60 per cent of the theoretical area. This is an improvement of at least 30 per cent over the similar NACA heated core data presented in Reference 1. The lower temperatures noticeable in the upper right hand corner of the figures are contributed by the disturbance in the flow caused by the stilling section temperature and pressure probes and their leadout lines installed in the corresponding location in the core stilling section (Figure 14). A decrease in the temperature slope in Figure 36, x = 16, to Figure 38, x = 6, indicates a slight broadening of the mixing region. The mixing region appears to be about three inches on the radius of the core.

A curve of the Mach number distribution in the expansion plane of the tunnel at the schlieren centerline is presented in Figure 39. This figure shows agreement of the Mach numbers as determined by pitot probes and the Mach numbers as determined by the wedge-pitot probe to be well within the accuracies of the data in the core region ($3\frac{1}{2}$ inches to either side of the tunnel centerline). Thus it was concluded that within the core the assumption that the stilling chamber stagnation pressure exists in the test section is valid. The design of the calibration rake did not permit wedge data to be taken in the mixing region beyond y = $-4\frac{1}{2}$. However, the point shown at y = $-4\frac{1}{2}$ suggests that the Mach numbers determined by the pitot probes outside of the core might not be valid. As was stated previously though the primary interest in this calibration was in the core itself. Figure 40 shows a comparison of the variation of the Mach number and the total temperature at the schlieren centerline. The values at z = ± 8 are definitely invalid, as they fall in the boundary layer region of the tunnel wall. The sharp discontinuity in the Mach number in the mixing region may be attributed to either a discontinuity in the stagnation pressure in this region or a true discontinuity in the Mach number itself. In light of Figure 36

it is felt that there is a discontinuity in the stagnation pressure in the mixing region. Comparison of Figures 41 and 42 shows the increasing Mach number variation in the streamwise direction. This is attributed to the growth of the mixing region, which evidently influences the Mach number. Mach number data shows a consistently higher Mach number than the design Mach number of 3.5. It was concluded therefore that the effect of the core nozzle in the throat had caused a change in the Mach number. The material of the core nozzle occupies about three square inches of the throat. This causes A/A^*, the ratio of test section area to throat area, to change from 6.79, corresponding to Mach 3.5, to 7.25 corresponding to Mach 3.57. Adding on an allowance in Mach number of 0.04 for the fact that the NSL 3.5 blocks yield a 3.54 test section Mach number (Reference 7), an expected Mach number of 3.61 is arrived at. This is very close to the mean Mach number which the data yields.

The Mach number data shows variations in the core as great as ± 0.1 in Mach number. These are larger variations than are generally accepted in force tests in a supersonic wind tunnel. However in aerodynamic heating tests such variations can well be tolerated. The large core of high temperature air suggests that a hemispherical model of the blocking area of the NSL wind tunnel (approximately a six inch diameter hemisphere) could be run at constant stagnation temperatures over 900° F, at Mach 3.64 ± 0.1 .

7.3.2 Studies of the Core at Mach 3.5-Unmatched Stagnation Pressures

In an attempt to obtain a smoother Mach number distribution in the core the cold stream stagnation pressure was varied. It is seen from Figure 43 that this variation had relatively little effect on the Mach number distribution in the core, a large decrease in cold stream pressure causing a slight increase in Mach number. The Mach number distribution outside of the core is presented based on both stagnation pressure of the core, p_{0_c}, and stagnation pressure of the cold stream, p_{0_s}. The temperatures in the core showed little change with variation of the pressures. The above observations support the findings of the NACA (Reference 1) that the variation of the ratio p_{0_c}/p_{0_s} had little effect on the core, an increase in the ratio producing a slight increase in the core Mach number.

7.3.3 Studies of the Core Using Mach 3.0 Blocks with the Mach 3.5 Core Nozzle

During the calibration tests the Mach 3.0 nozzle blocks were inserted in place of the Mach 3.5 nozzle blocks to determine the feasibility of operating the heated core installation at Mach 3.0, an off-design condition. During this test neither the heated core nozzle nor its location was changed. Thus the throats of the core nozzle and the tunnel nozzle did not match. Two axial stations were surveyed under these conditions, $x = -16$ and $x = 0$ Representative temperature and Mach number data taken at these stations is presented in Figures 44 and 45. These two figures reveal that mixing in the streamwise direction is much more prominent with these off-design conditions. The constant temperature core at the schlieren centerline, $x = 0$, is reduced to less than four square inches, while the Mach number shows less peaking in the core than with the Mach 3.5 blocks. The greater mixing at Mach 3.0 is further revealed by the comparison of Figure 46 with Figure 47. Figure 46 is a schlieren photograph of the calibration rake in operation at Mach 3.5, the design condition. Notice the shock waves are quite smooth and the core mixing region is not visible. Figure 47 is a schlieren photograph of the rake in operation at Mach 3.0, the off-design condition. Notice the distinct core region. The edge of this region seems to be about four inches from the centerline or as Figure 45 shows, on the outer edge of the mixing region. The bending of the shock waves suggests that beyond this region the Mach number increases, the opposite of what Figure 45 suggests. Due to the evidence in the schlieren photograph of a Mach number increase it is suspected that the stagnation pressure beyond the mixing region is higher than stilling chamber stagnation pressure. Thus, Figure 45 is in error for the region outside of the core. The additional instrument below the calibration rake in Figure 47 is a mirror placed in the stream to determine if the flow was free from foreign matter. The mirror was run in the stream for an hour and a half with no appreciable dulling occuring.

8. CONCLUSIONS AND RECOMMENDATIONS

From the design, construction, and calibration of the NSL heated core installation it is concluded that the injection of a high temperature stream tube into a supersonic wind tunnel is a practical way to obtain aerodynamic heating data. The Naval Supersonic Laboratory Supersonic Wind Tunnel proved to be an ideal facility for the heated core installation, considering the high temperature air source and compressing equipment available in the laboratory.

With respect to the results from the calibration of the heated core, the following is concluded:

1. The NSL Mach 3.5 heated core installation produced a 50 in^2 uniform temperature (900°F) core, which is about 60 per cent of the theoretical heated core area.

2. The Mach numbers at the schlieren centerline varied as much as ± 2.5 per cent about a mean Mach number of 3.64, a peak occuring at the center of the core. The Mach number distribution flattens out proceeding upstream of the schlieren centerline.

3. Stagnation pressure within the core does not vary noticeably from stilling chamber stagnation pressure.

4. Mach numbers increase slightly in the core with increases in the ratio of p_{0_c}/p_{0_s}.

5. Operation of the heated core installation at the off design condition of Mach 3.0 reduces the core to about 20 per cent of the theoretical area, but produces a more constant Mach number distribution in the core.

6. In light of conclusions 2.0 and 5.0 it is concluded that the percentage of the throat that the core nozzle material occupies influences the Mach number distribution unfavorably.

As an immediate improvement on the Mach 3.5 heated core installation it is recommended that the exposed stilling chamber stagnation pressure and stagnation temperature leads (Figure 14) be run under the

insulation on the stilling section. This should smooth out the flow over the stilling section considerably and thus eliminate the reduced temperature area noticeable in the upper right hand corner of Figure 37.

Further, it is recommended that a second heated core nozzle be fabricated of thinner wall thickness and that it be extended downstream from the throat ten per cent of the distance to the end of the Mach 3.5 nozzle blocks, instead of the present five per cent. By making this nozzle of one-half the cross sectional area of the existing nozzle the stagnation pressure upper limit could be increased to 12 psia, instead of the present 6 psia. This nozzle should furnish a relatively constant 900° F test section of 25 in^2 cross sectional area, with less variation in Mach number across the core and a greater stagnation pressure range.

REFERENCES

1. Rousso, M.D., and Beheim, M.A. Preliminary Investigation of a Technique of Producing a Heated Core in a Supersonic Wind-Tunnel Stream. NACA Rm E54K02, February 18, 1955.

2. Pai, Shih-I. Fluid Dynamics of Jets. New York: D. Van Nostrand Company, Inc., 1954.

3. Pai, Shih-I. Two-Dimensional Jet Mixing of a Compressible Fluid. JAS, 1949, 16, 463.

4. Adams, R. H. and Baron, J.R. Heated Core, MTP, and Free Convection Conferences at Lewis Laboratory, NACA. (Unclassified Title). Massachusetts Institute of Technology, Naval Supersonic Laboratory, A and R Memo 179, September 26, 1957. CONFIDENTIAL

5. Adams, R.H. A Description of the 18" x 24" Tunnel Circuit. Massachusetts Institute of Technology, Naval Supersonic Laboratory, A and R Memo 159, October 15, 1956.

6. Adams, R.H. A Heated Core Installation in the Naval Supersonic Laboratory Supersonic Wind Tunnel and the Theoretical Performance Characteristics. Massachusetts Institute of Technology, Naval Supersonic Laboratory, A and R Memo 245, October 8, 1957.

7. Baron, J.R. Analytic Design of a Family of Supersonic Nozzles by the Friedrichs Method. Massachusetts Institute of Technology, Naval Supersonic Laboratory, WTR 66, WADC Technical Report 54-279, June 1954.

8. Ladenburg, R. W., Lewis, B., Pease, R.N., and Taylor, R.N. Physical Measurements In Gas Dynamics and Combustion. Princeton University Press, 1954.

9. Hill, J.A.F. On the Calibration of Supersonic Wind Tunnels. JAS, 1955, 22, 441.

10. Ames Research Staff. Equations Tables, and Charts For Compressible Flow. NACA Report 1135, 1953.

11. Hill, J.A.F., Baron, J.R., and Schindel, L.H. Mach Number Measurements in High-Speed Wind Tunnels. Massachusetts Institute of Technology, Naval Supersonic Laboratory, TR 145, January 1956.

12. L'Hommedieu, J. Mechanical Design of the "Hot Core" Circuit Massachusetts Institute of Technology, Naval Supersonic Laboratory, A and R Memo 236, March 25, 1958.

13. Mc Adams, W. H. Heat Transmission. New York: Mac Graw-HillBook Company, Inc., 1954.

14. Adams, R.H. Estimated Performance of the Naval Supersonic Laboratory's Hypersonic Wind Tunnel. Massachusetts Institute of Technology, Naval Supersonic Laboratory, A and R Memo 174, March 13, 1957.

15. Ross, D.H. Compressor Operating Characteristics. Massachusetts Institute of Technology, Naval Supersonic Laboratory Wind Tunnel, Memo WT-M102-14, March 28, 1952.

16. Sherman, F.S. New Experiments on Impact-Pressure Interpretation in Supersonic and Subsonic Rarefied Air Streams. NACA TN 2995, September 1953.

17. Leupold, M.J. Specific Gravity of Manometer Fluids. Massachusetts Institute of Technology, Naval Supersonic Laboratory Wind Tunnel, Memo WT-M-110-25, February 28, 1958.

18. Baker, R. L. Hot Core Operation and Modifications to Permit Operation. Massachusetts Institute of Technology, Naval Supersonic Laboratory, A and R Memo 232, March 26, 1958.

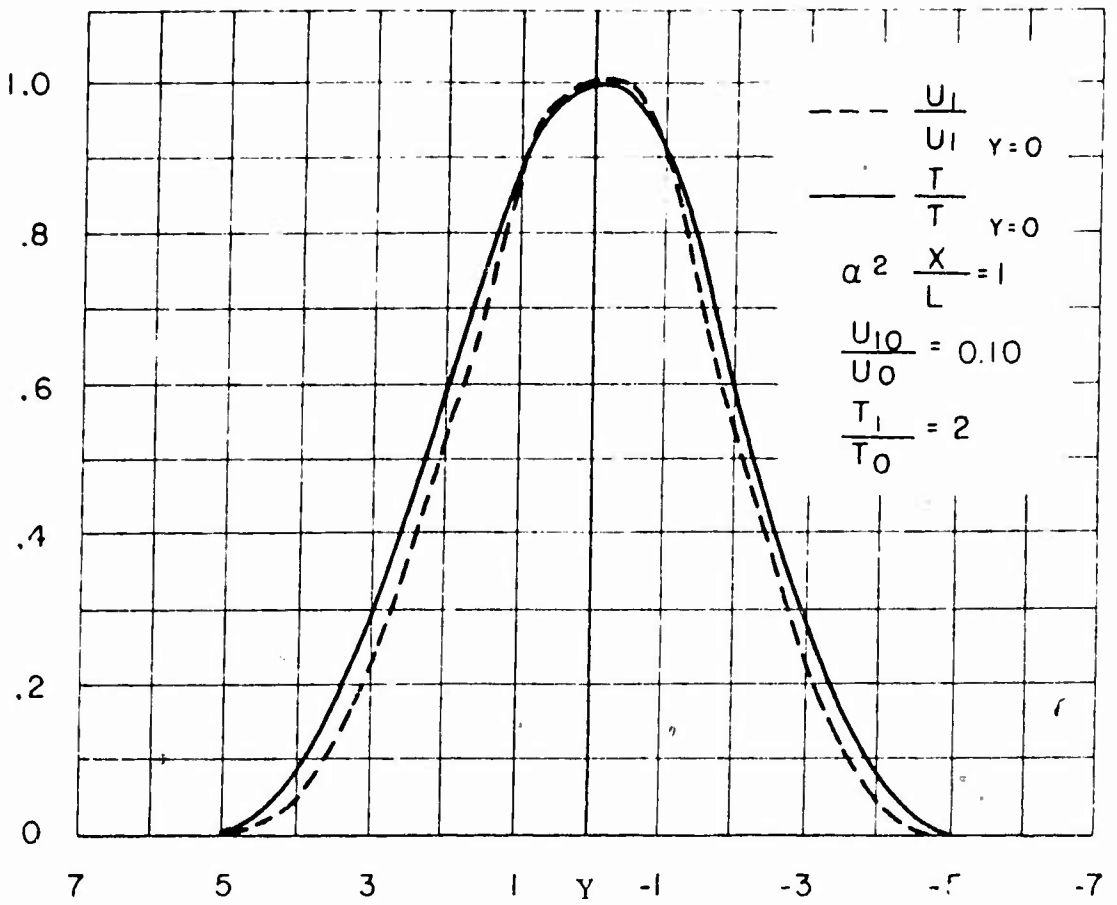

Figure 1. Temperature distribution in the jet of flow from a two-dimensional nozzle.

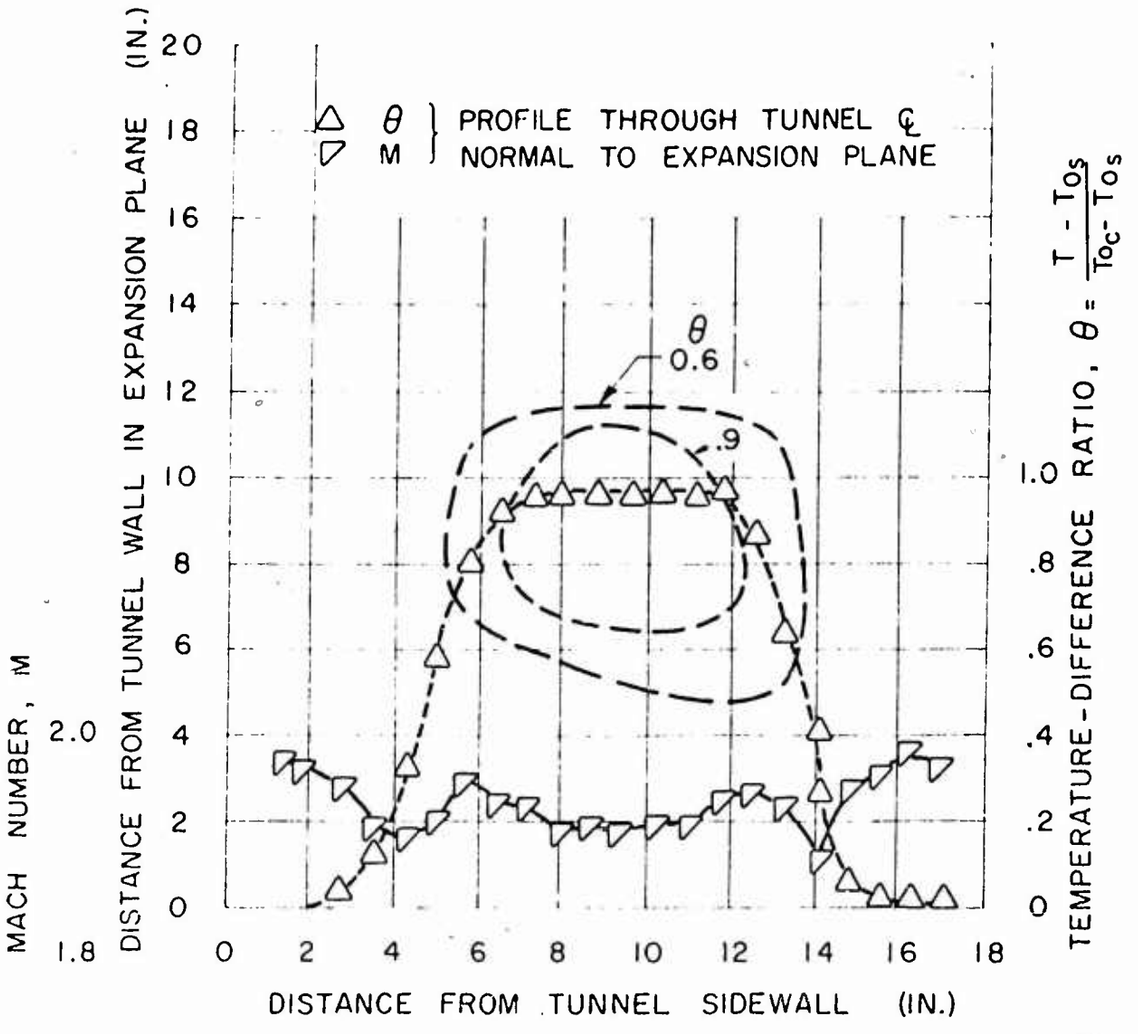

Figure 2. Temperature and Mach number distribution in the NACA Mach 1.9 heated core tunnel.

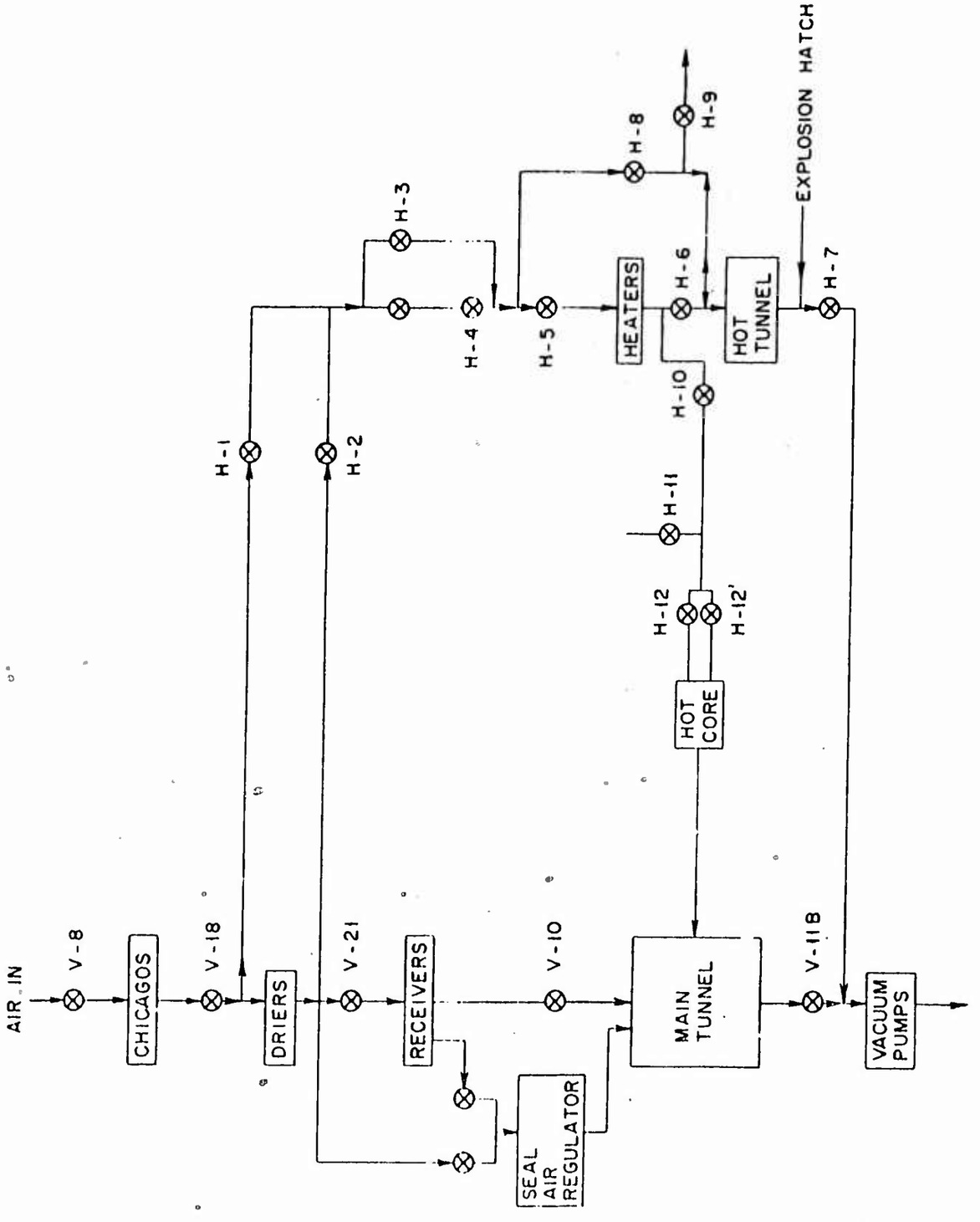

Figure 3. NSL heated core circuit - schematic diagram.

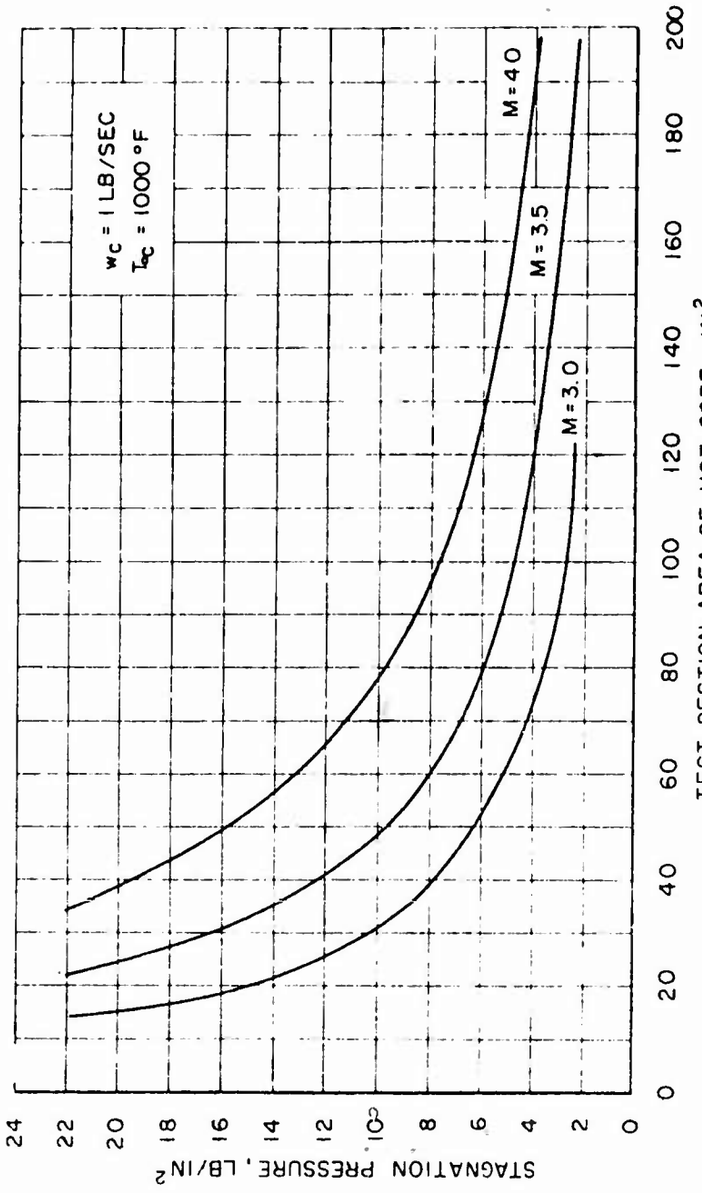

Figure 4. Theoretical test section area of hot core versus stagnation pressure.

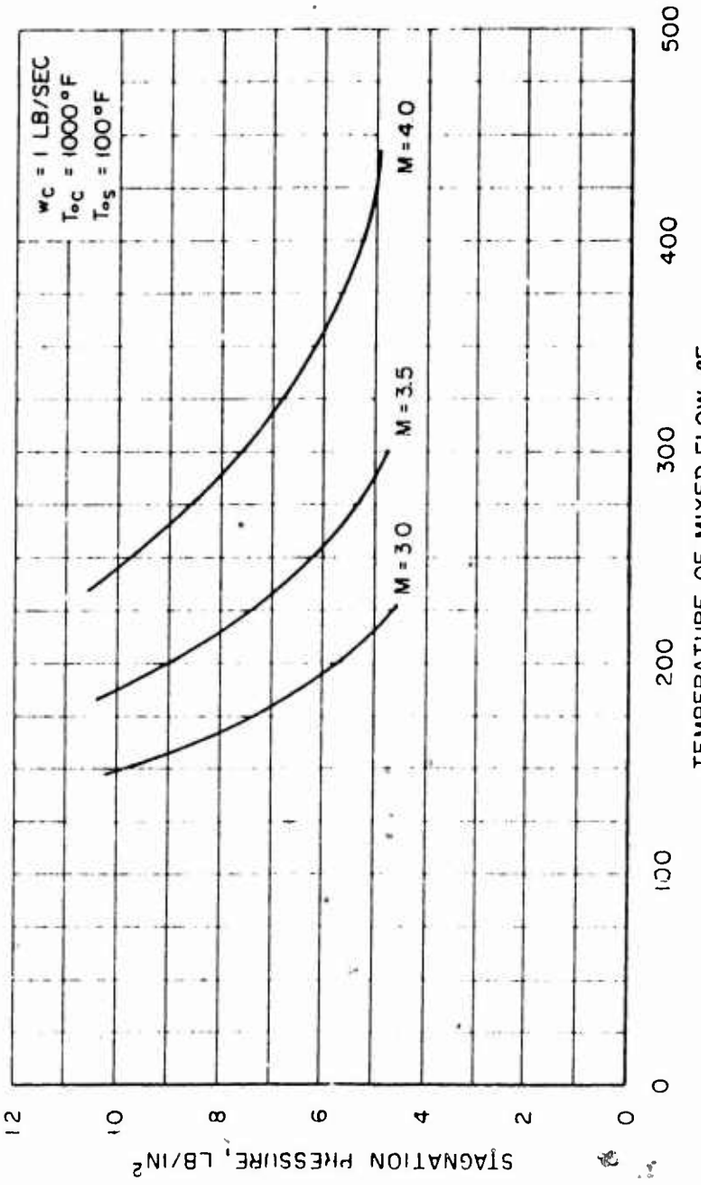

Figure 5. Theoretical temperature of mixed flow versus stagnation pressure.

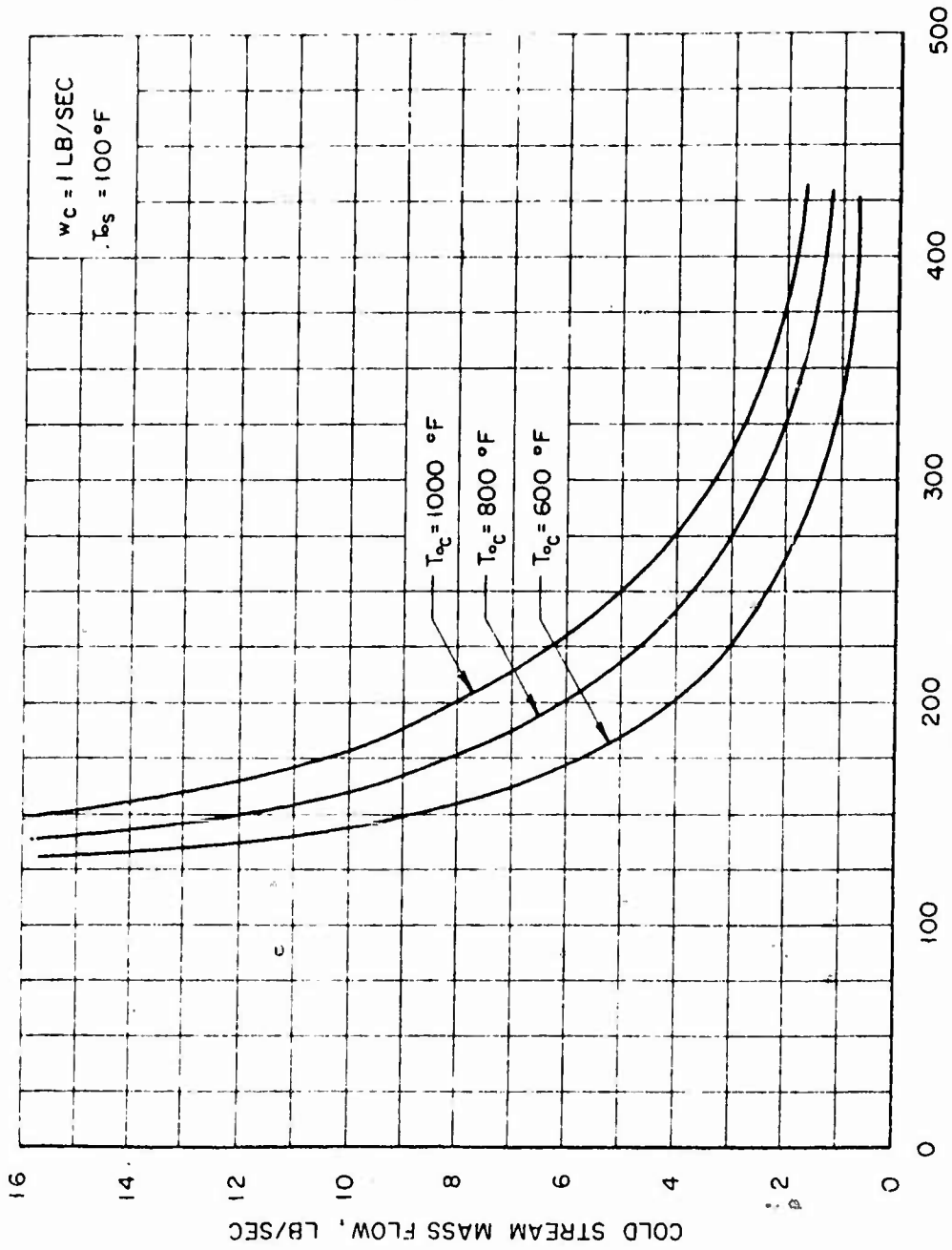

Figure 6. Theoretical temperature of mixed flow versus cold stream mass flow.

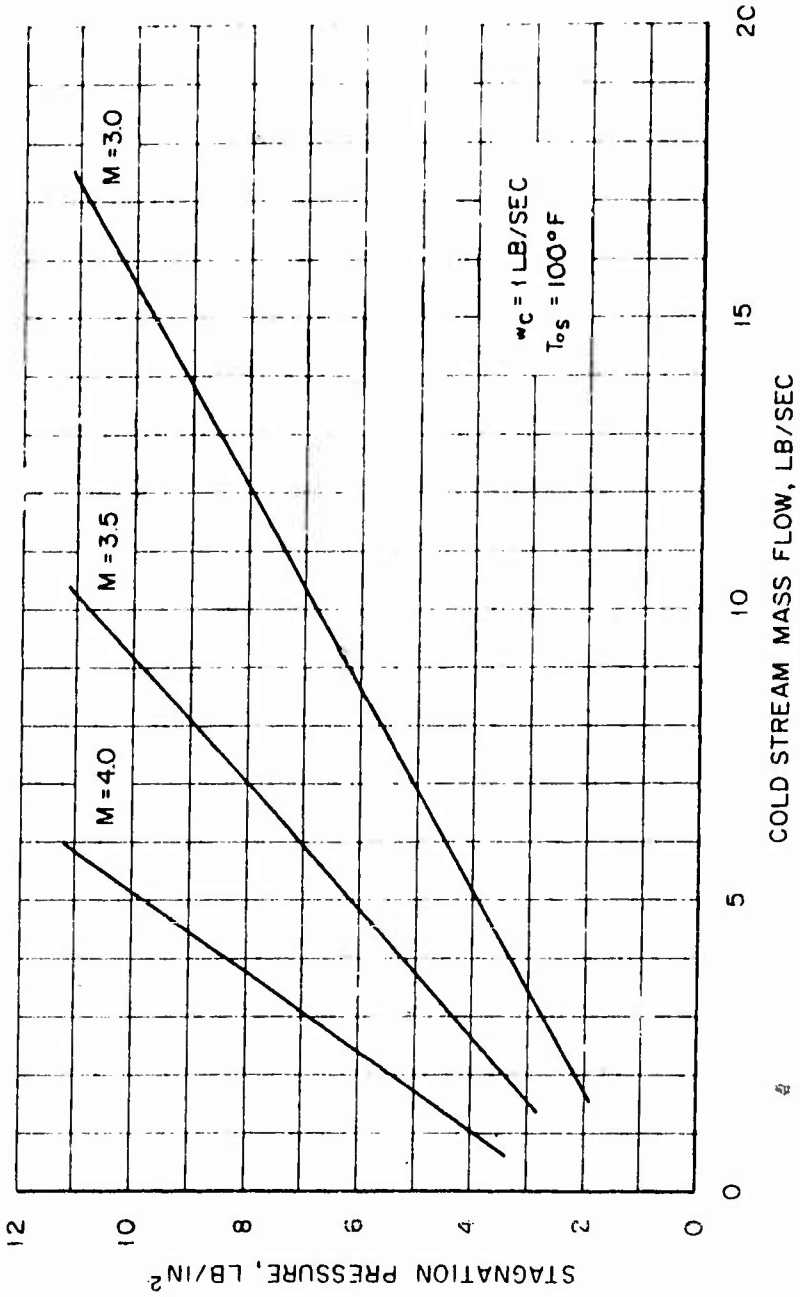

Figure 7. Cold stream mass flow versus stagnation pressure.

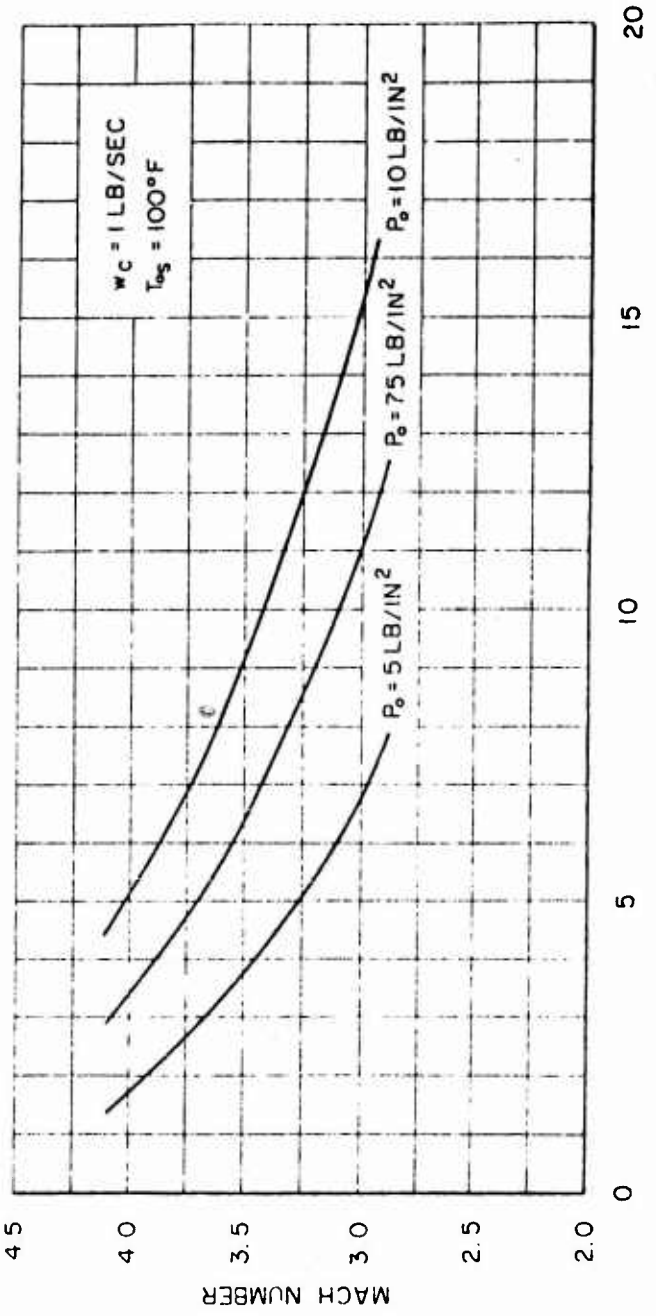

Figure 8. Cold stream mass flow versus Mach number.

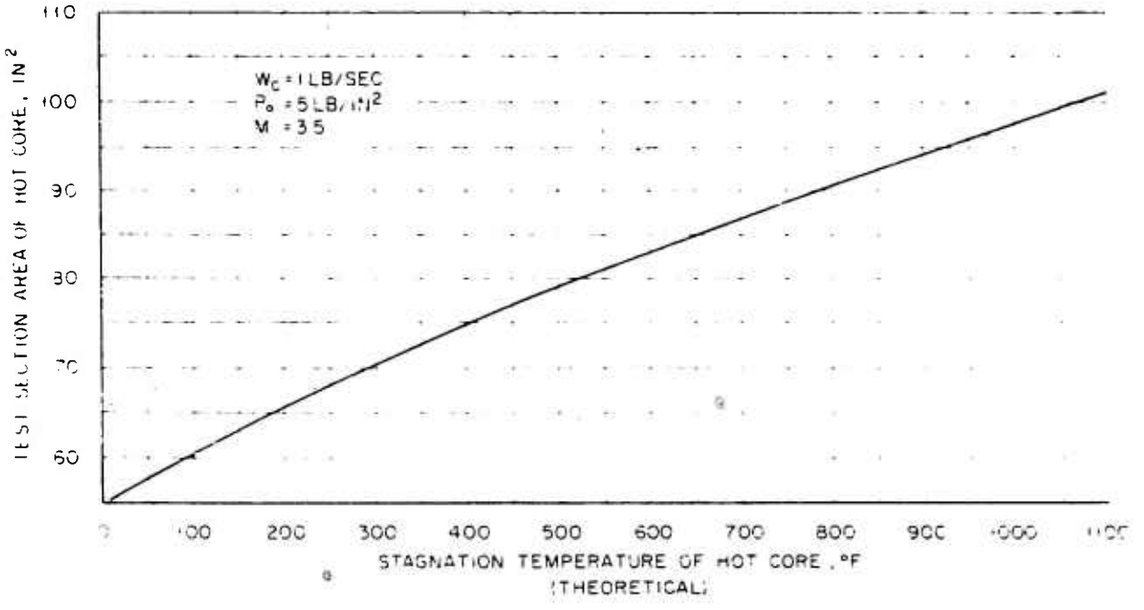

Figure 9. Theoretical test section area of hot core versus stagnation temperature

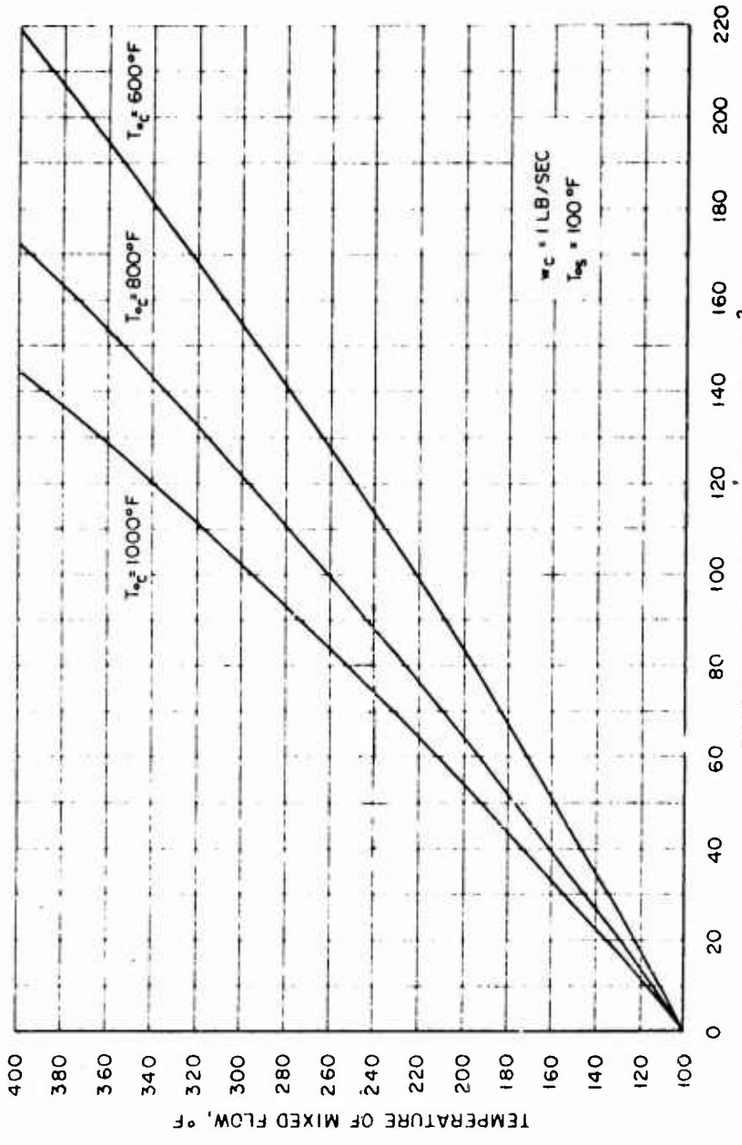

Figure 10. Theoretical test section area of hot core versus temperature of mixed flow.

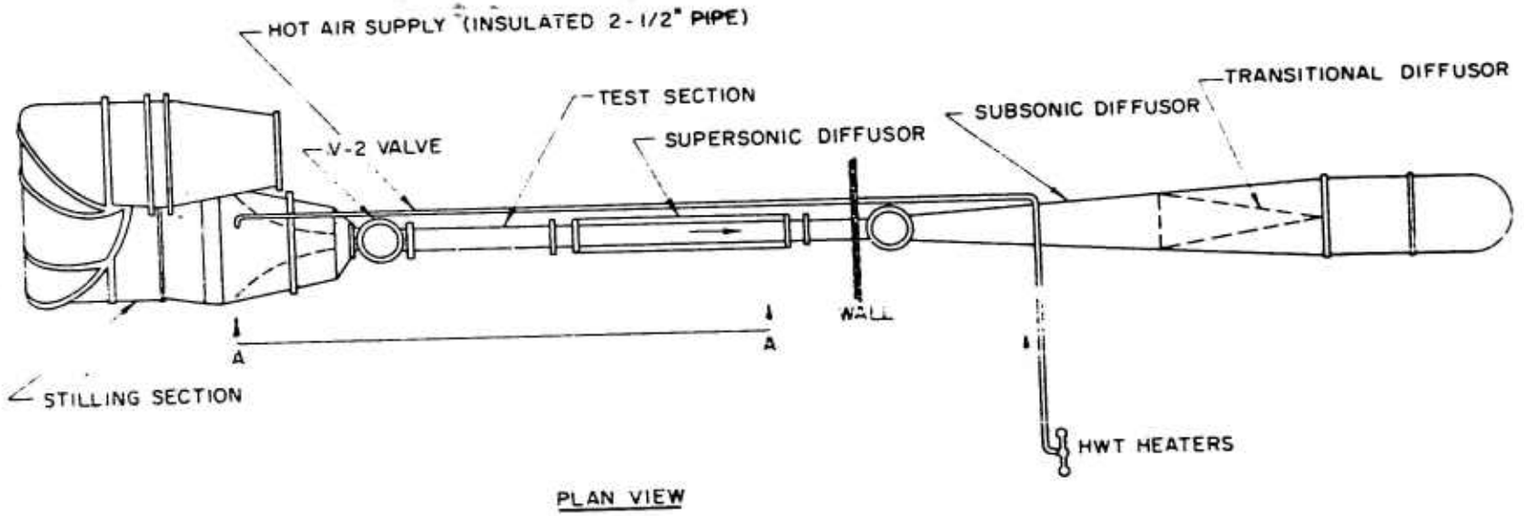

Figure 11. The NSL Mach 3.5 heated core installation – schematic diagram.

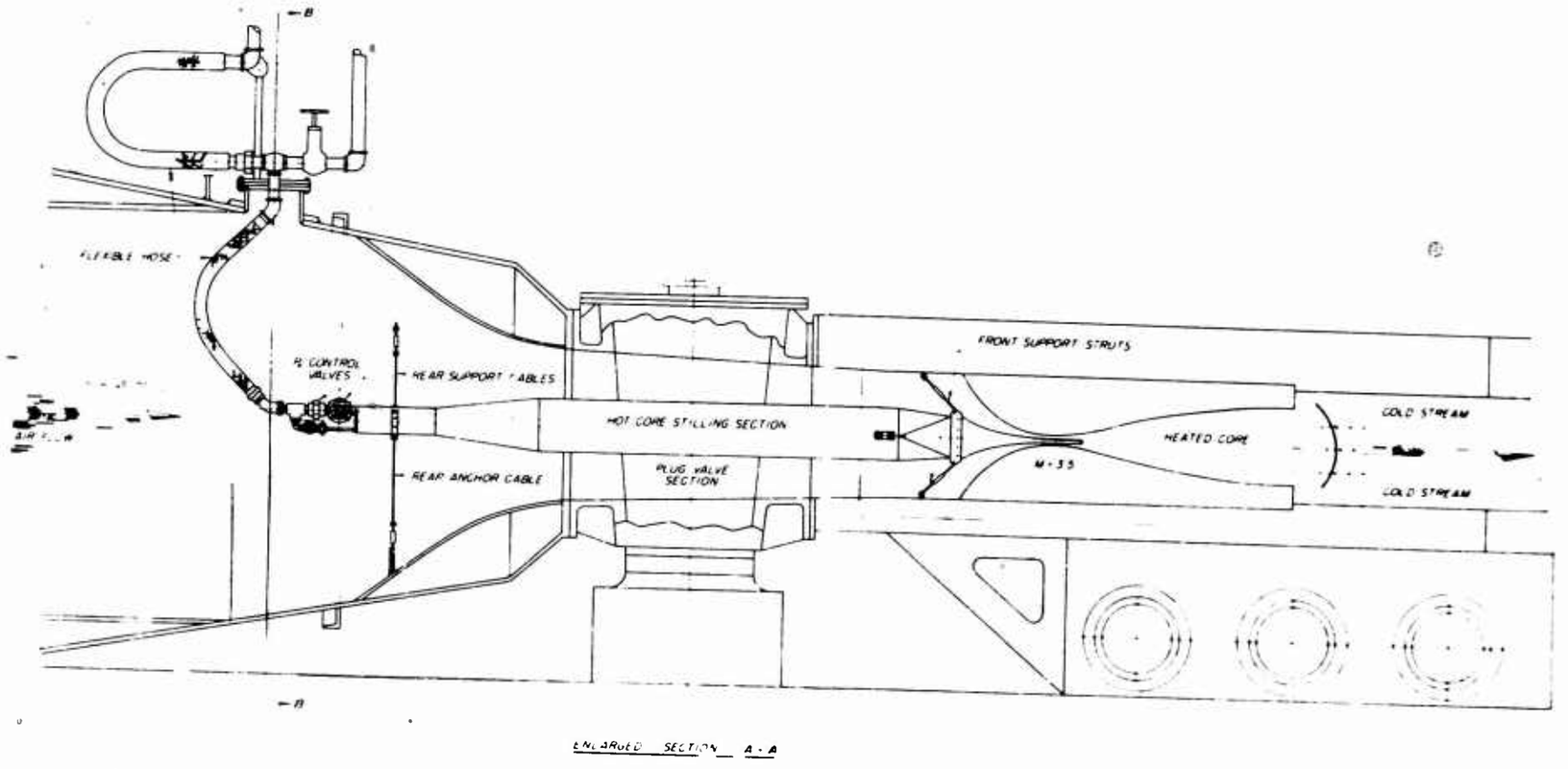

Figure 12. The NSL Mach 3.5 heated core installation – enlarged section A–A.

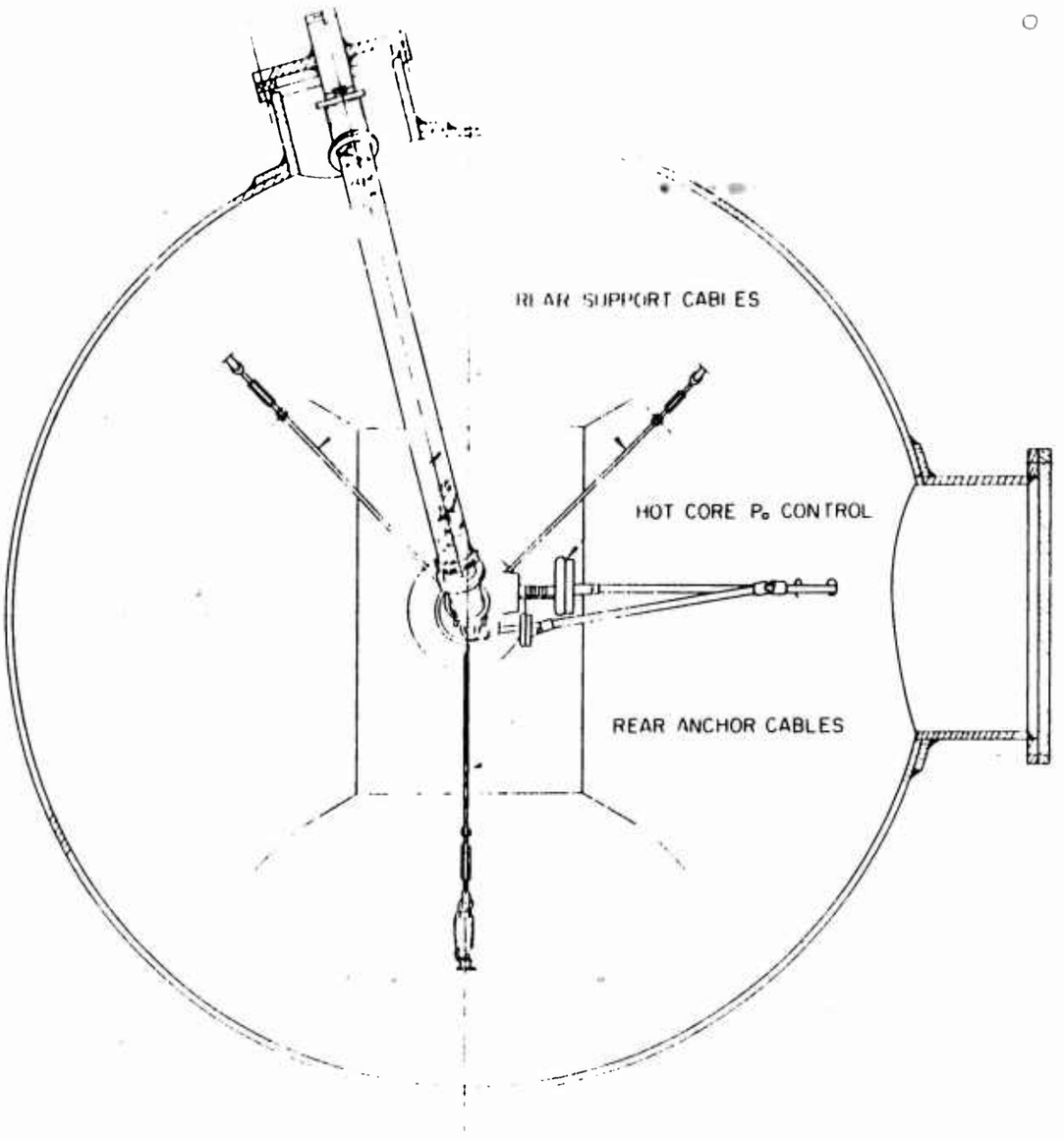

Figure 13. The NSL Mach 3.5 heated core installation – enlarged section B–B.

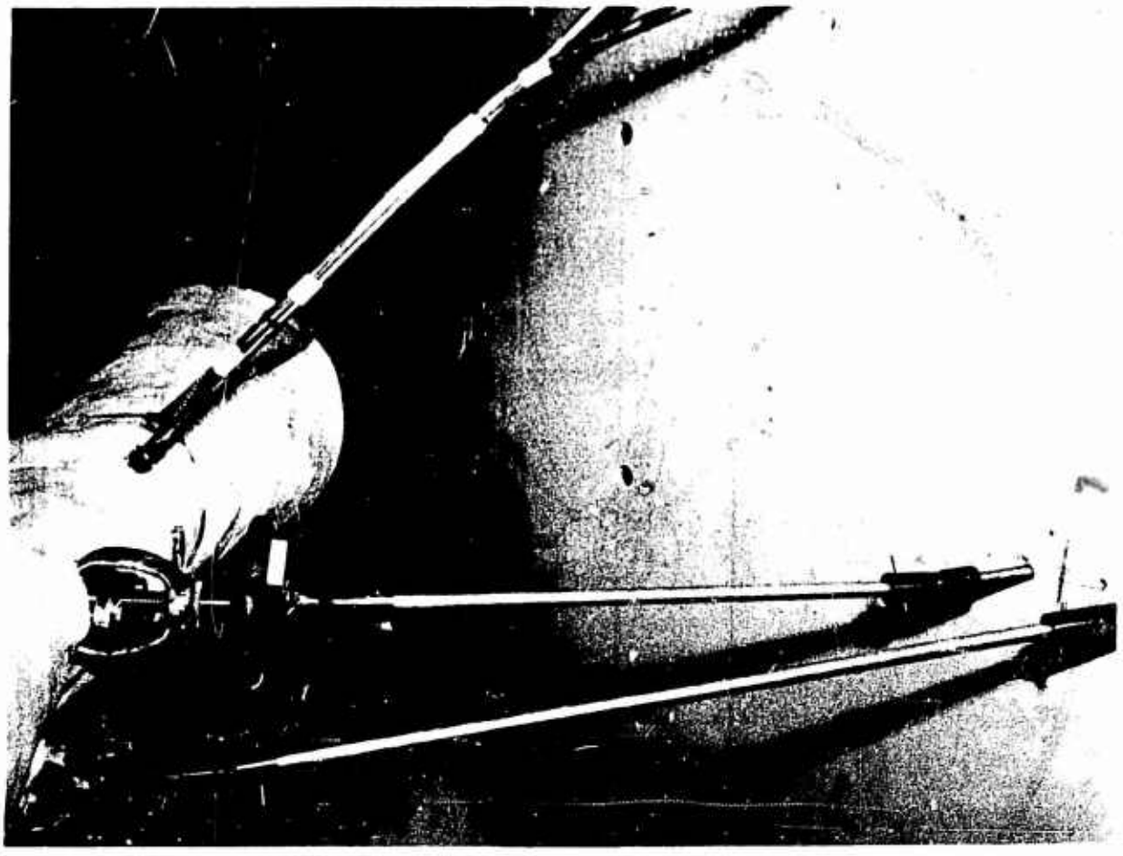

Figure 14. Installation of insulated heated core stilling section – looking downstream.

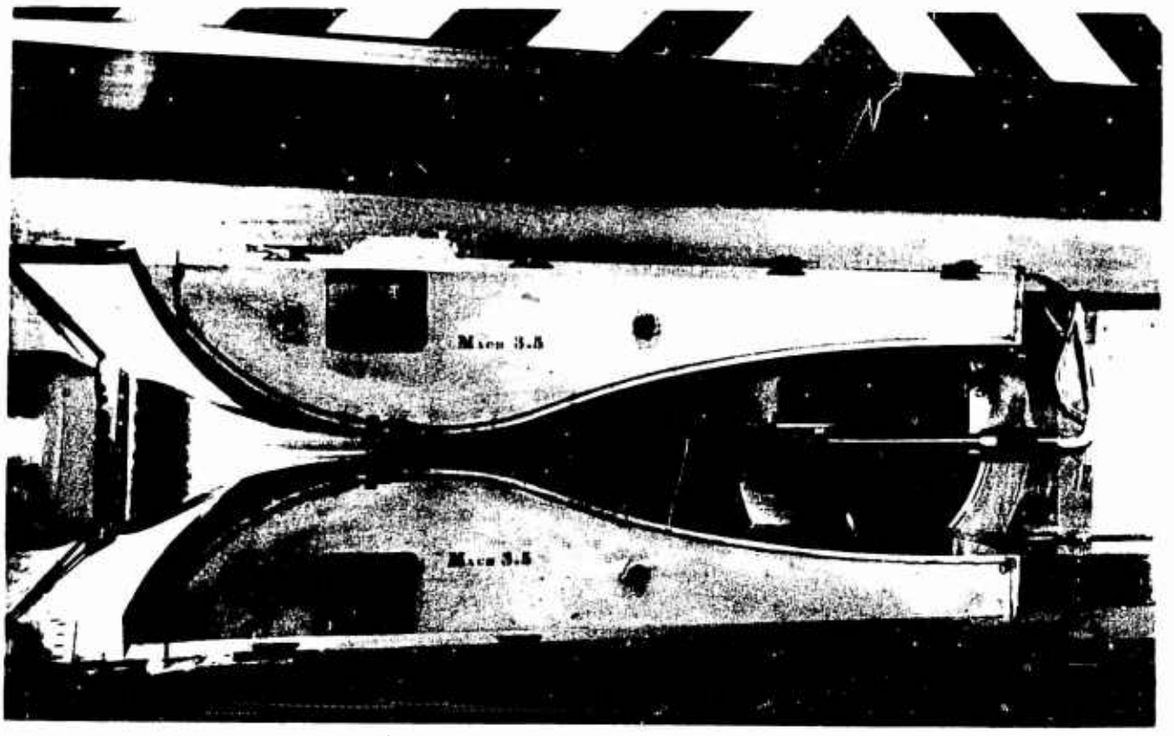

Figure 15. NSL heated core nozzle installation and calibration rake – side view.

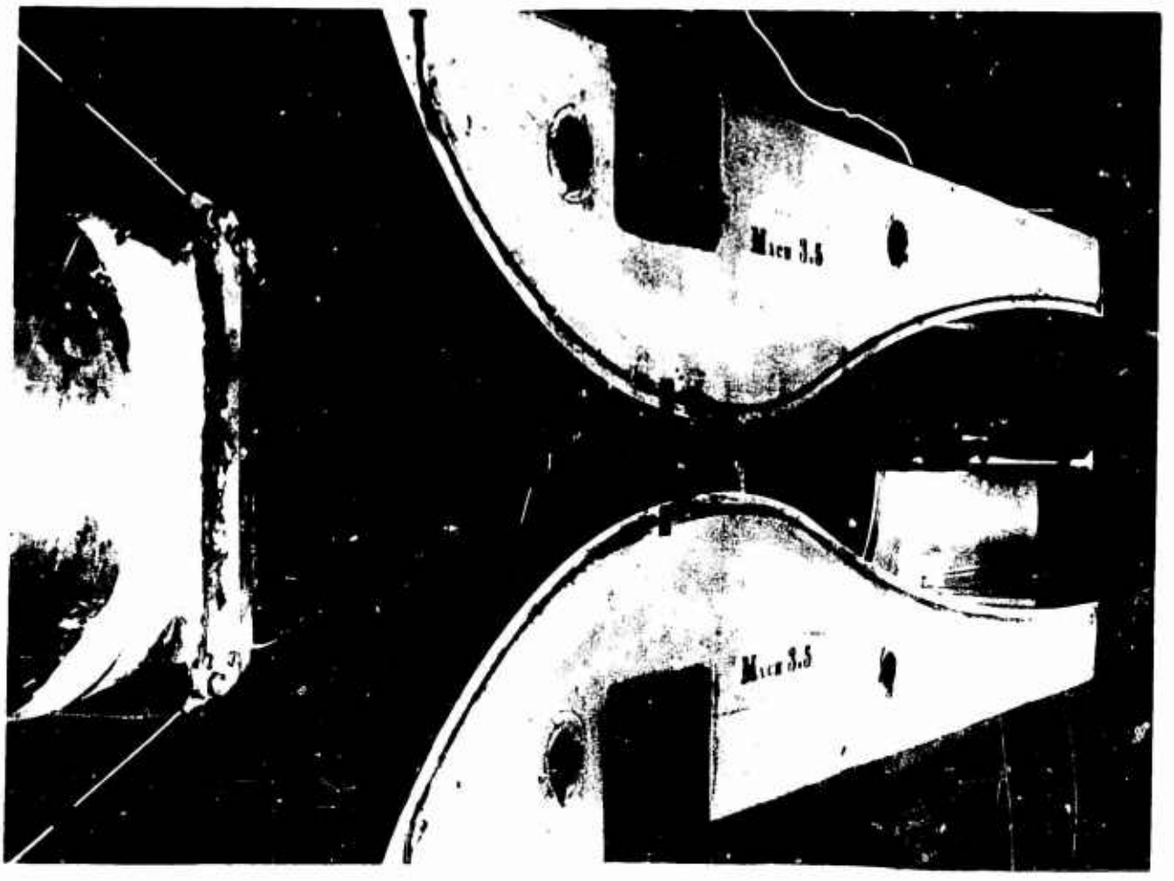

Figure 16. NSL heated core nozzle installation – looking downstream at calibration rake.

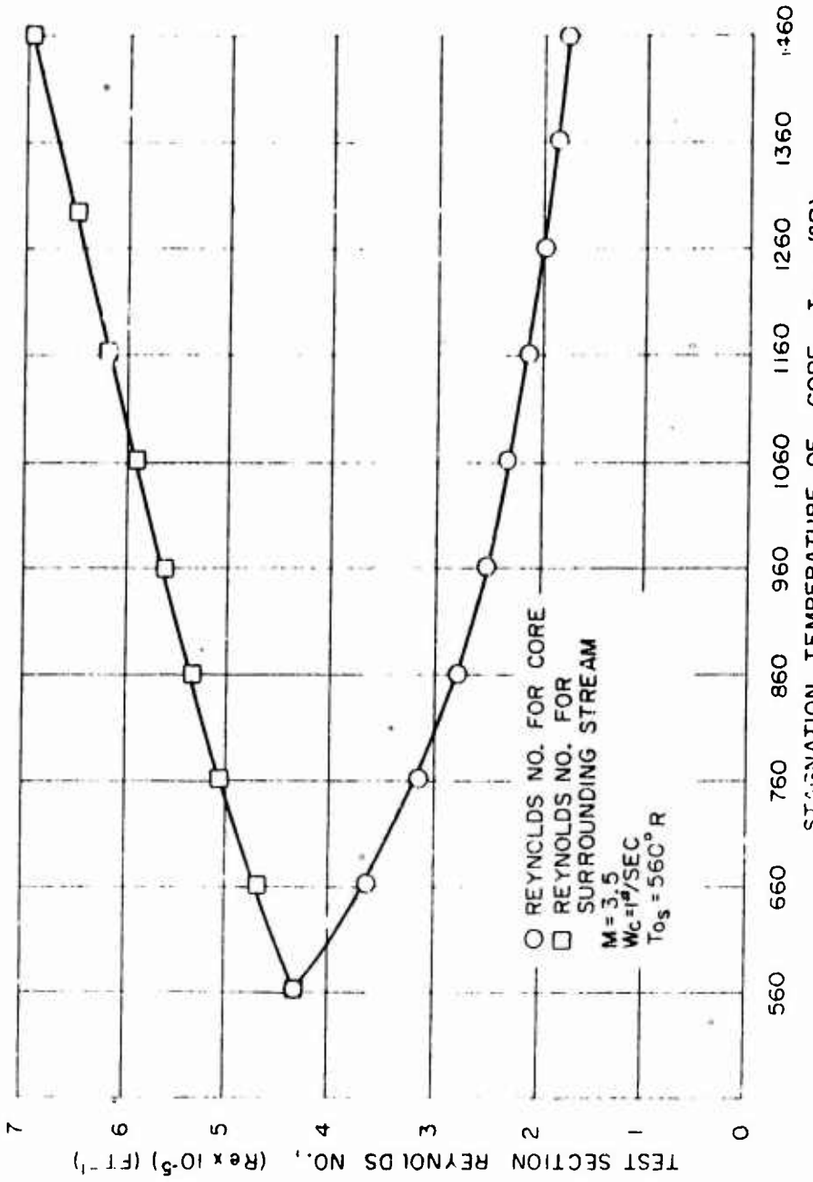

Figure 17. Reynolds numbers encountered during operation of the NSL heated core installation.

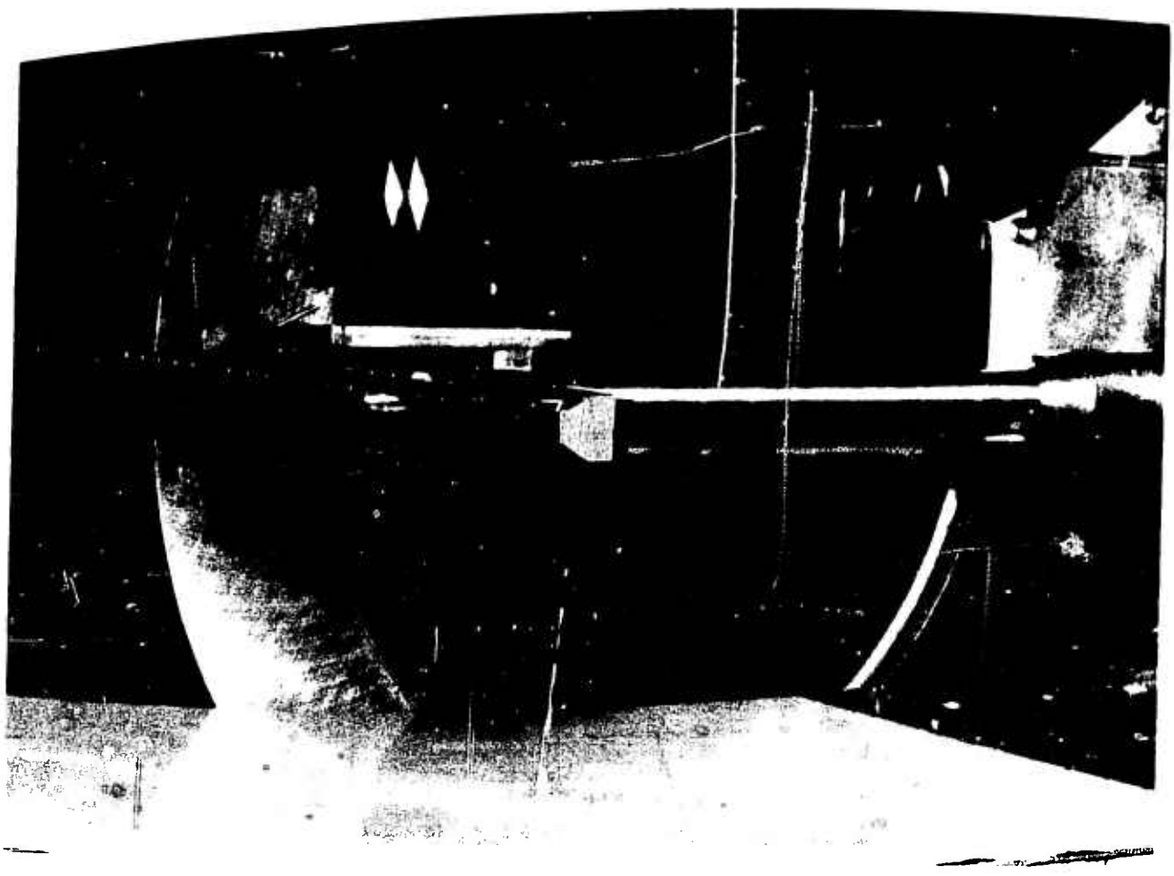

Figure 18. Calibration rake installed in the NSL Mach 3.5 test section.

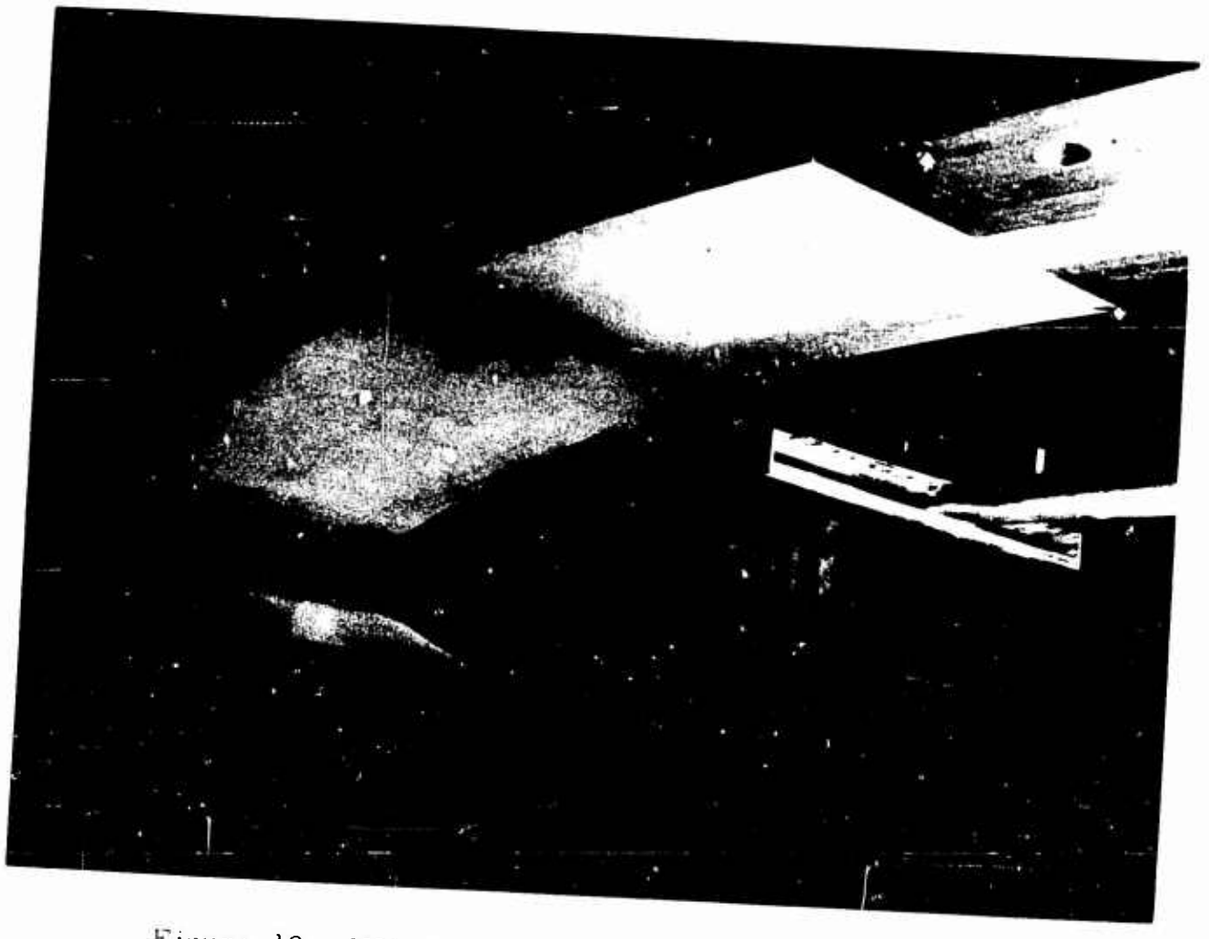

Figure 19. NSL heated core calibration rake - looking upstream at the core nozzle.

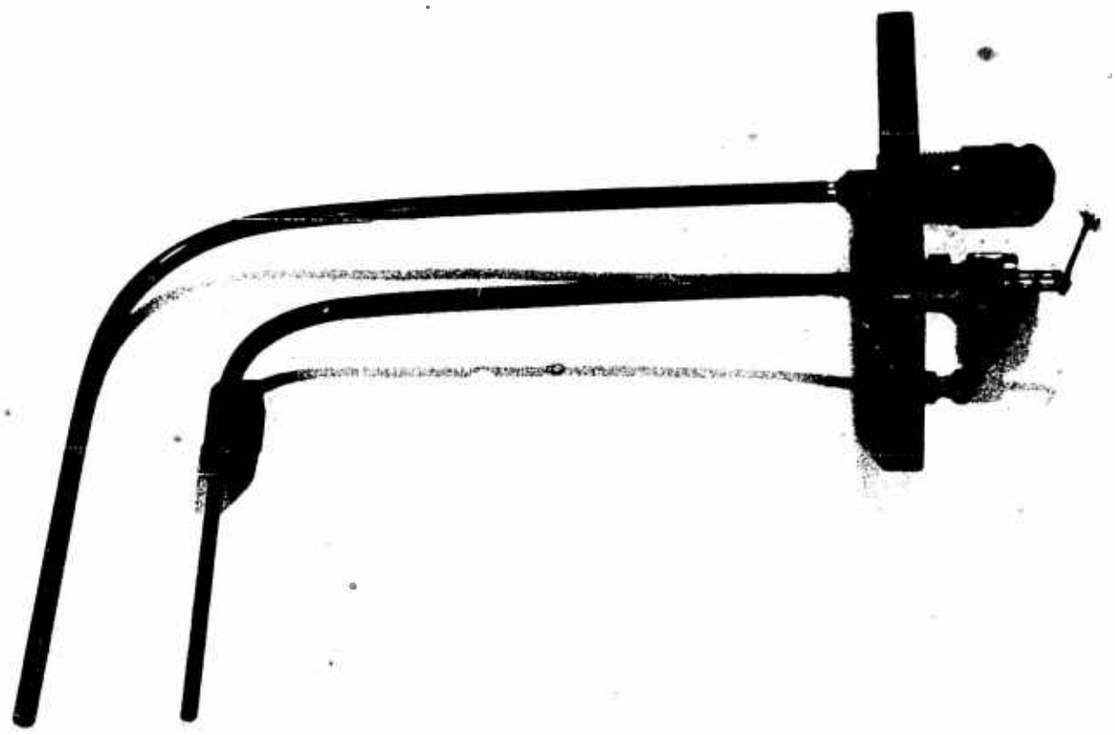

Figure 20. Heated core stilling chamber stagnation pressure and stagnation temperature probes.

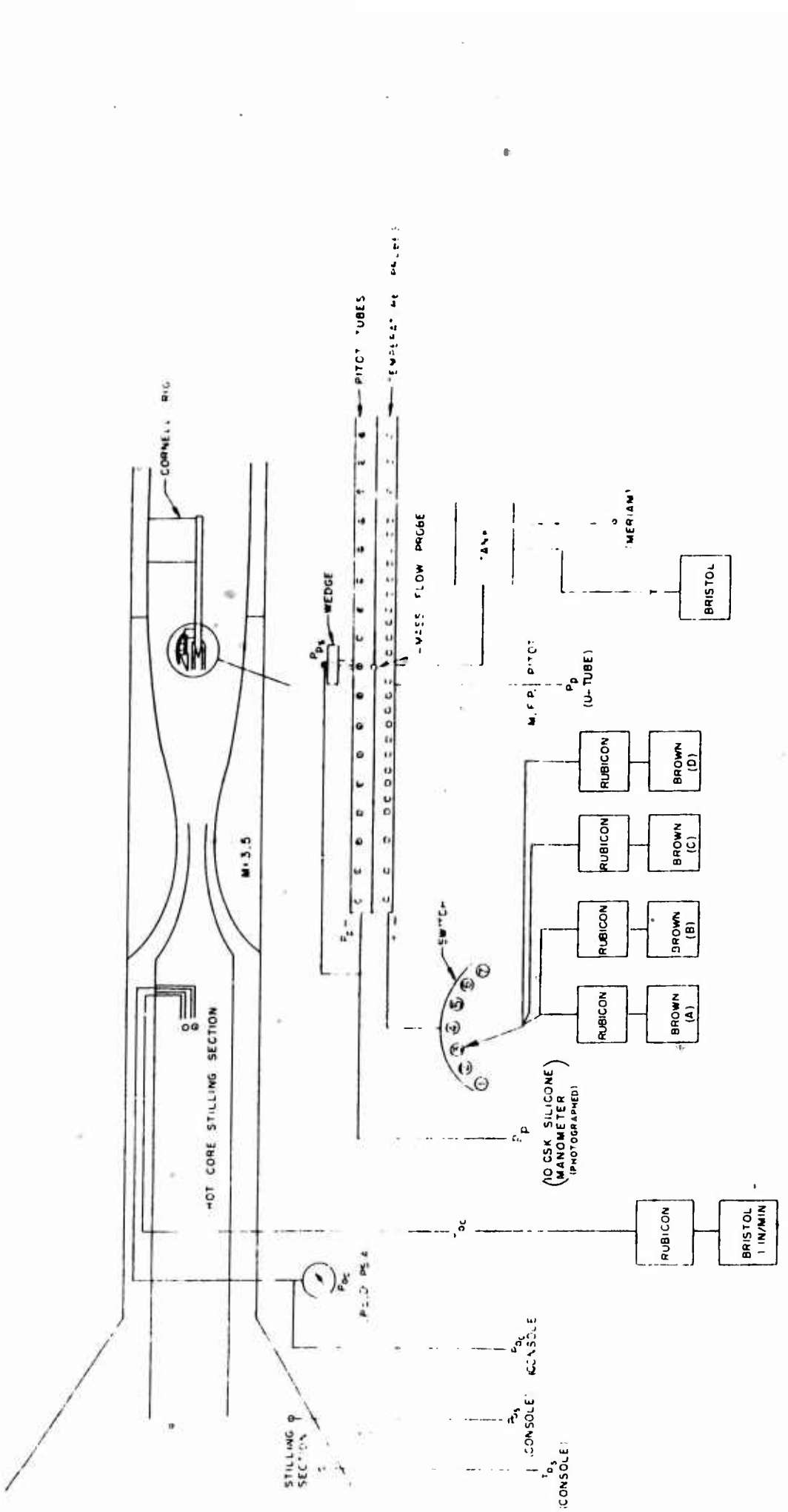

Figure 21. Instrumentation for the NSL heated core calibration - schematic diagram.

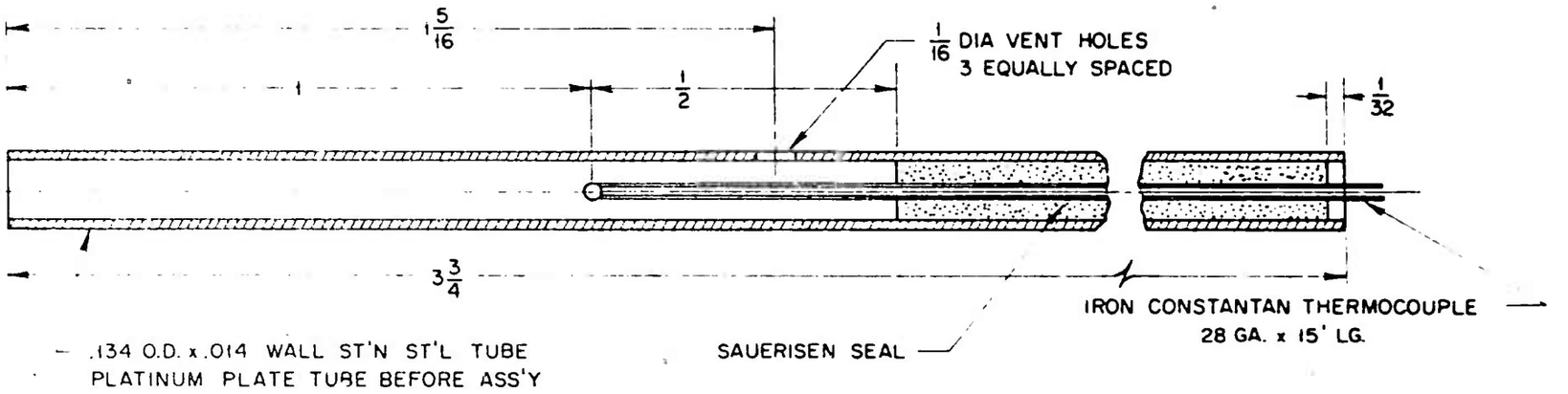

Figure 22. Detailed diagram of heated core calibration total temperature probe.

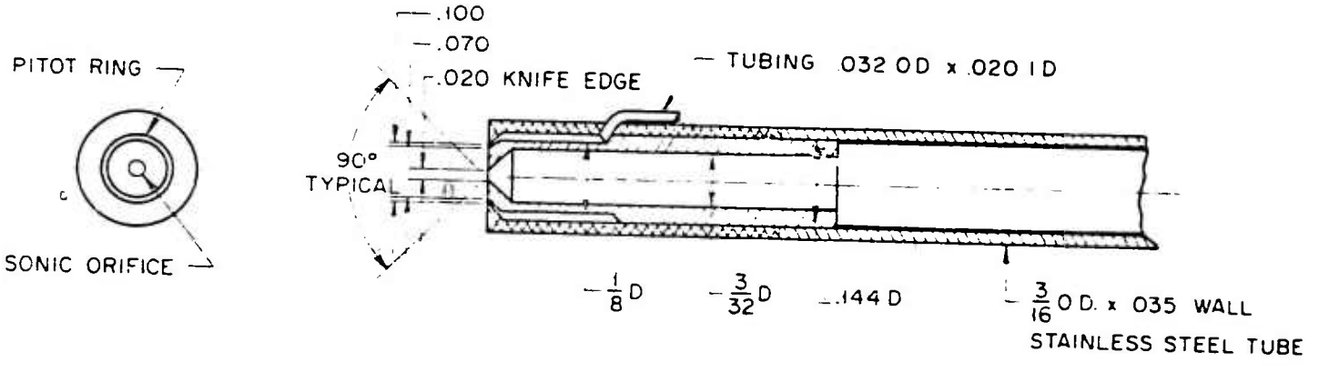

Figure 23. Detailed diagram of heated core calibration mass flow probe.

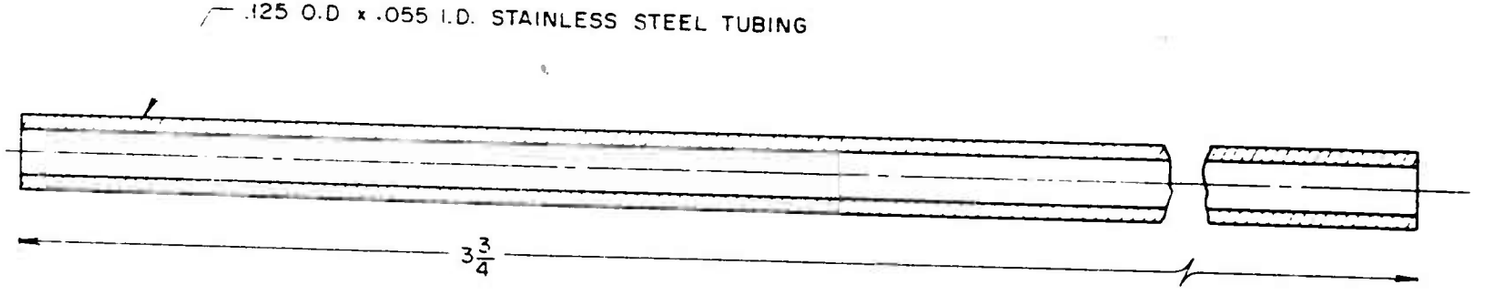

Figure 24. Detailed diagram of heated core calibration pitot probe.

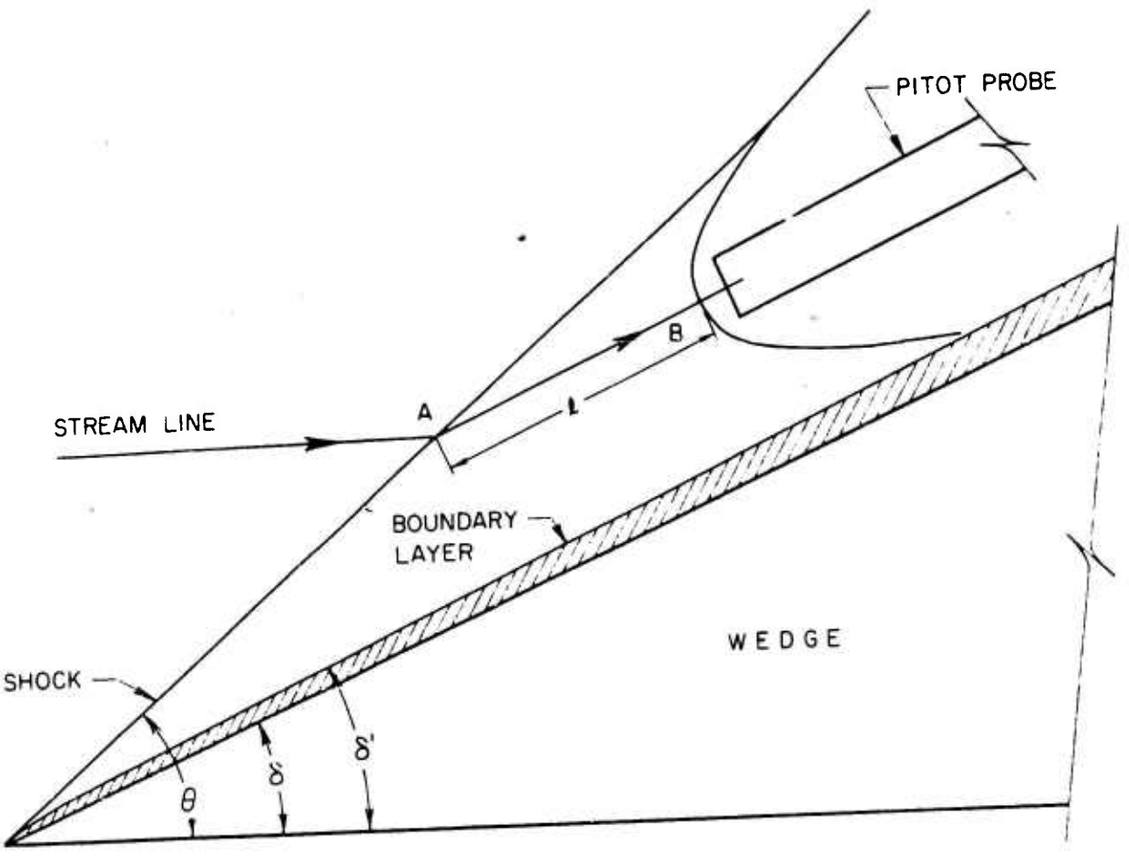

Figure 25. Sketch of wedge-pitot probe corrected for boundary layer.

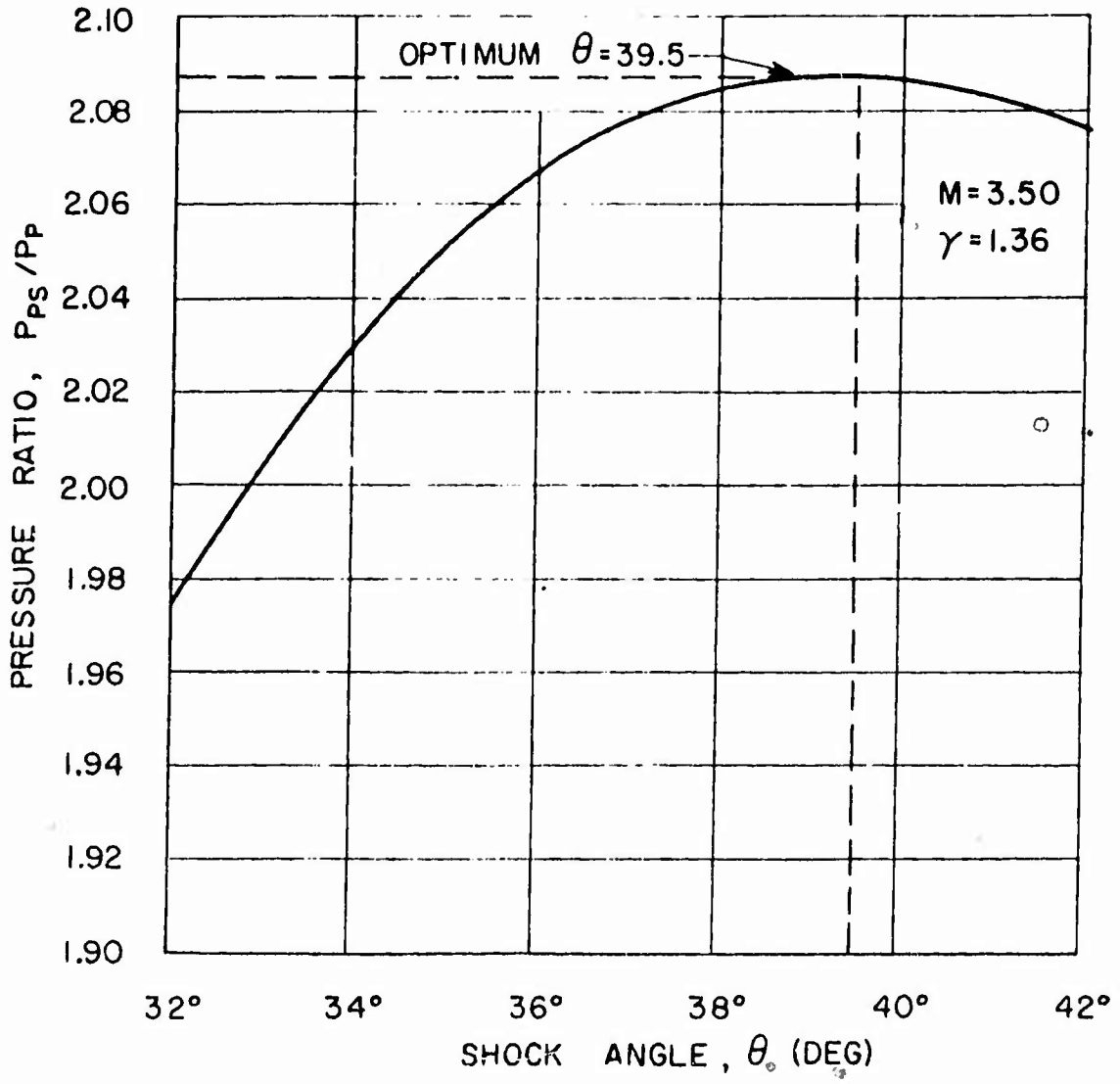

Figure 26. Optimum shock angle for wedge-pitot probe.

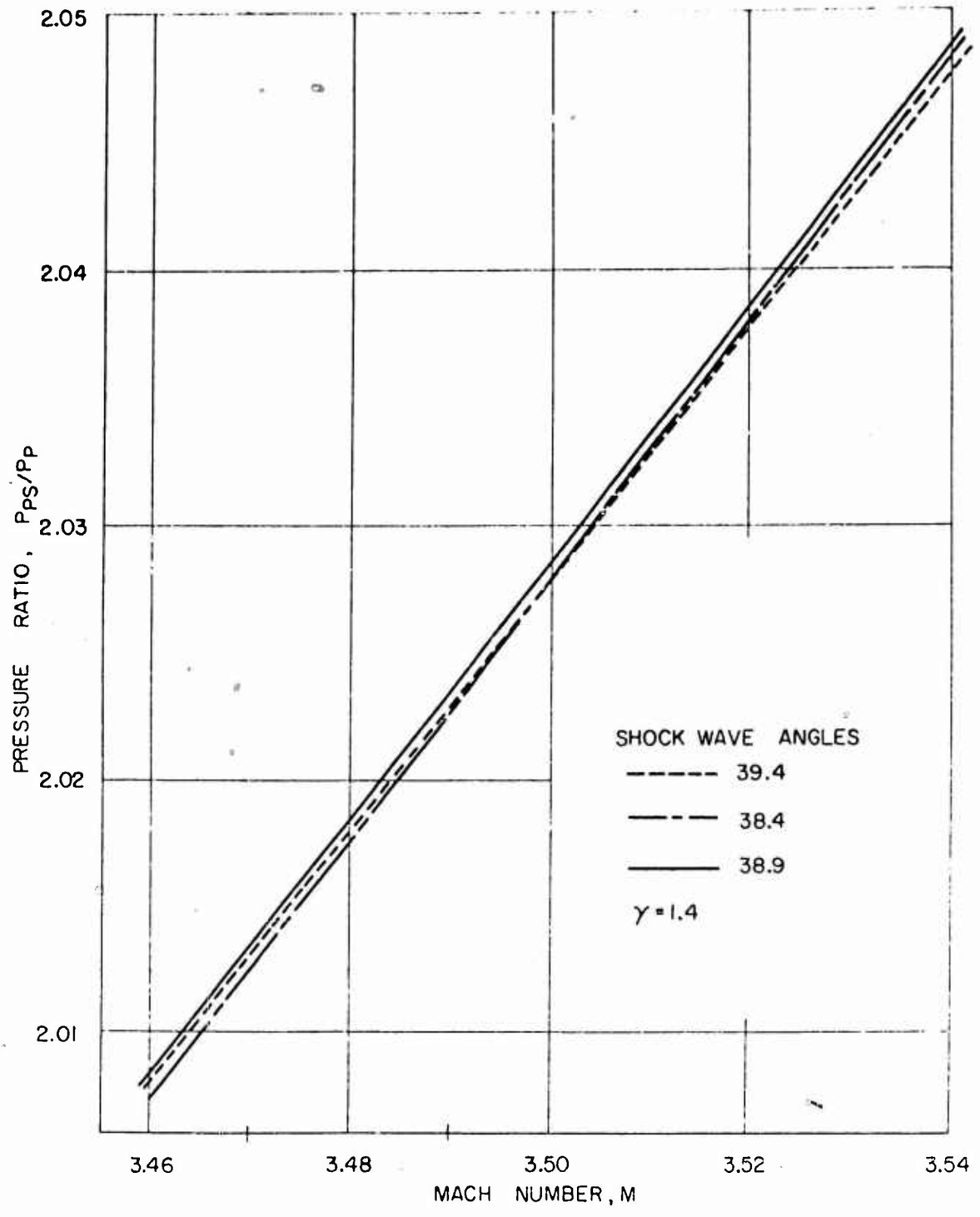

Figure 27. Pitot pressure behind and oblique shock over pitot pressure, p_{p_s}/p_p versus Mach number, for shock angles near the optimum.

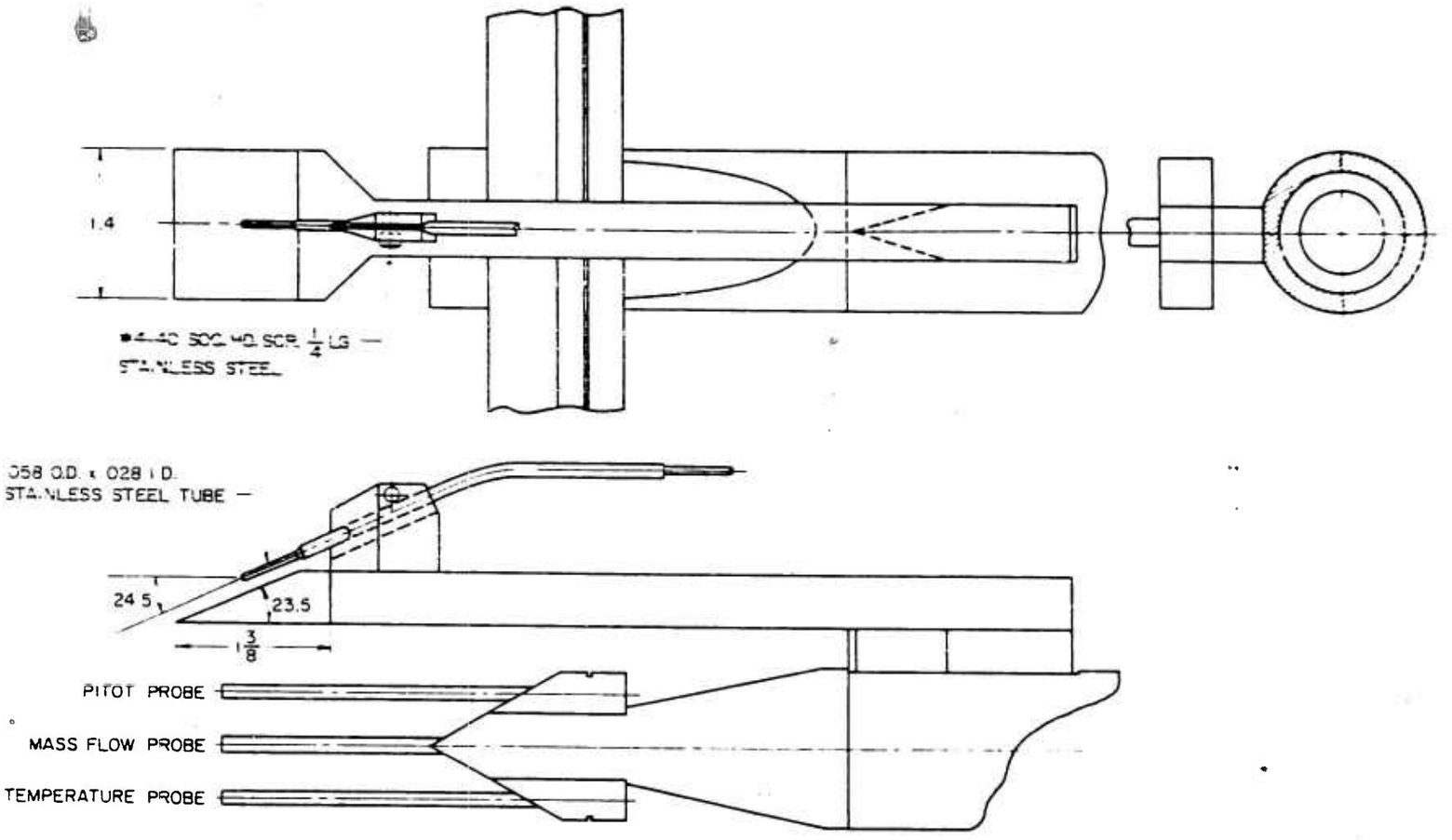

Figure 28. Wedge pitot probe assembly mounted on the calibration rake.

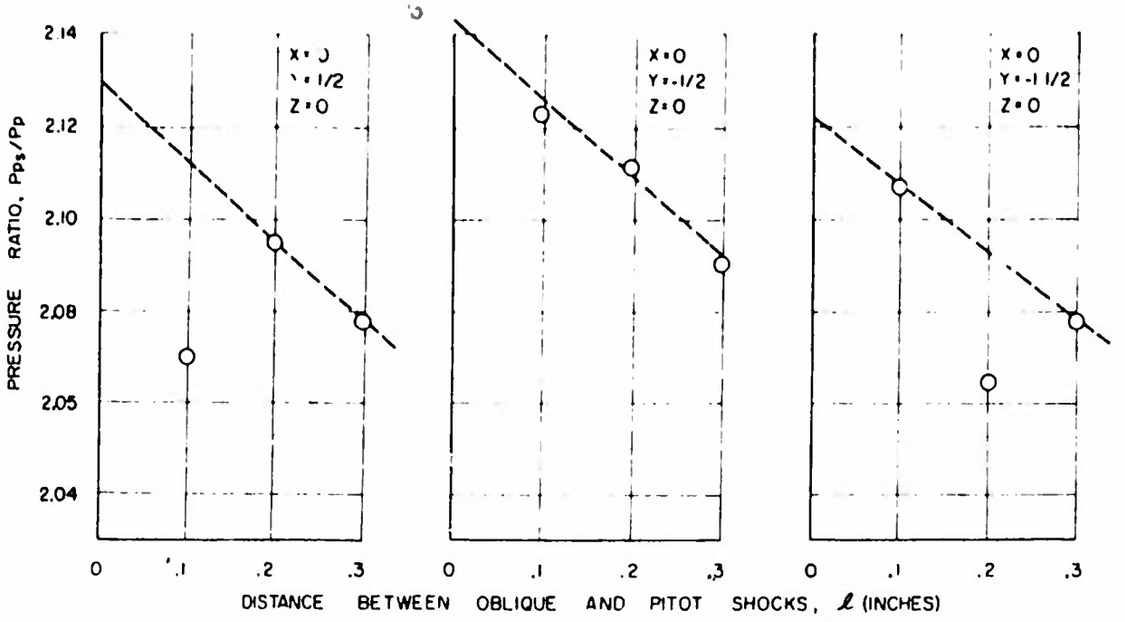

Figure 29.

Figure 30.

Figure 31.

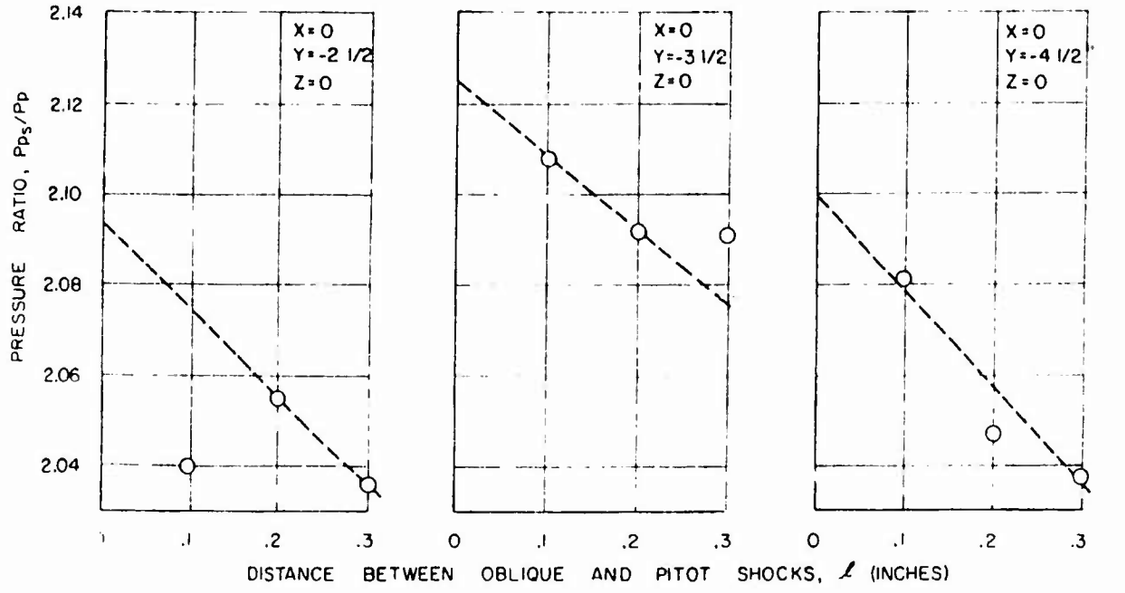

Figure 32.

Figure 33.

Figure 34.

Figures 29 - 34. Extrapolations to zero separation of oblique and pitot shocks for wedge-pitot probe data.

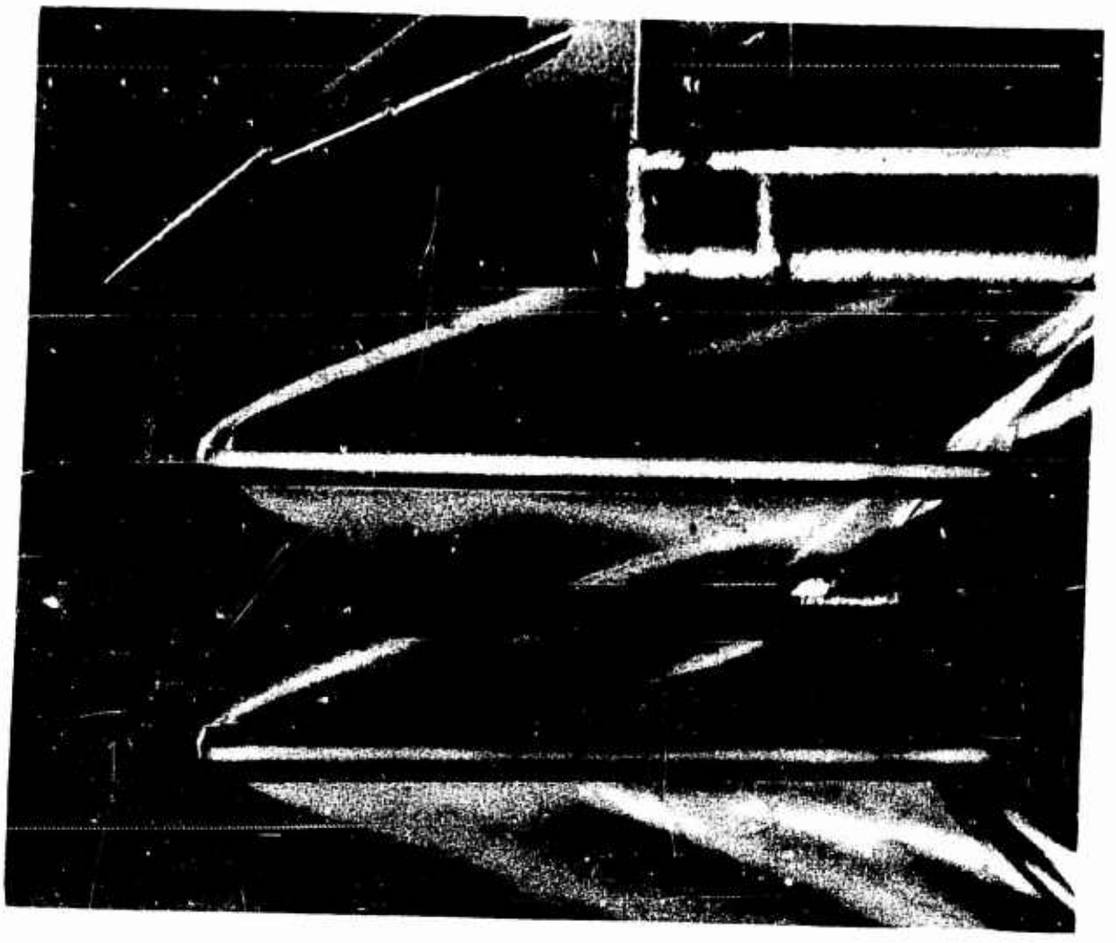

Figure 35. Enlarged schlieren photograph of calibration rake probes in Mach 3.5 flow.

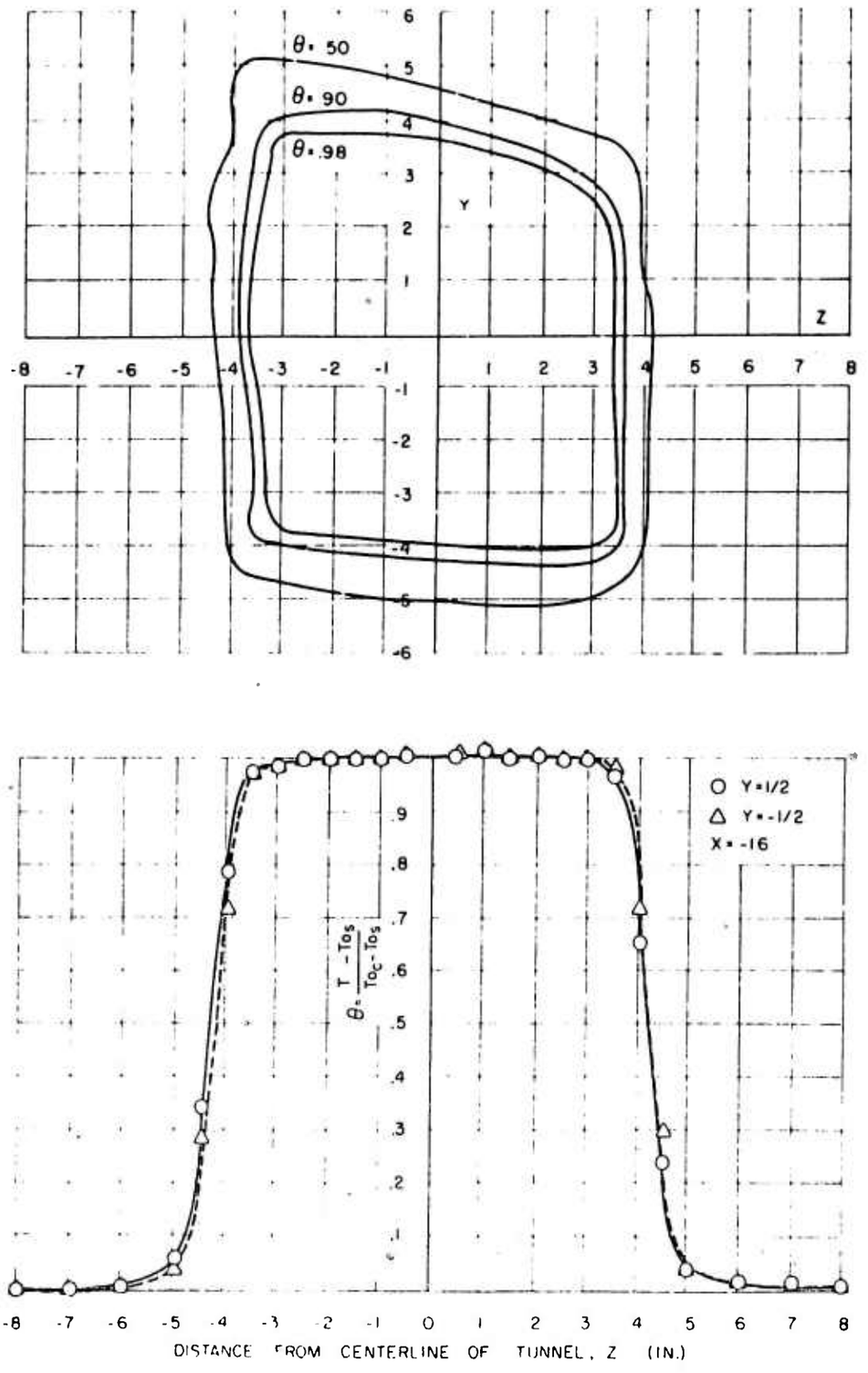

Figure 36. Isotherms and temperature distribution across the Mach 3.5 test section, sixteen inches upstream of the schlieren centerline.

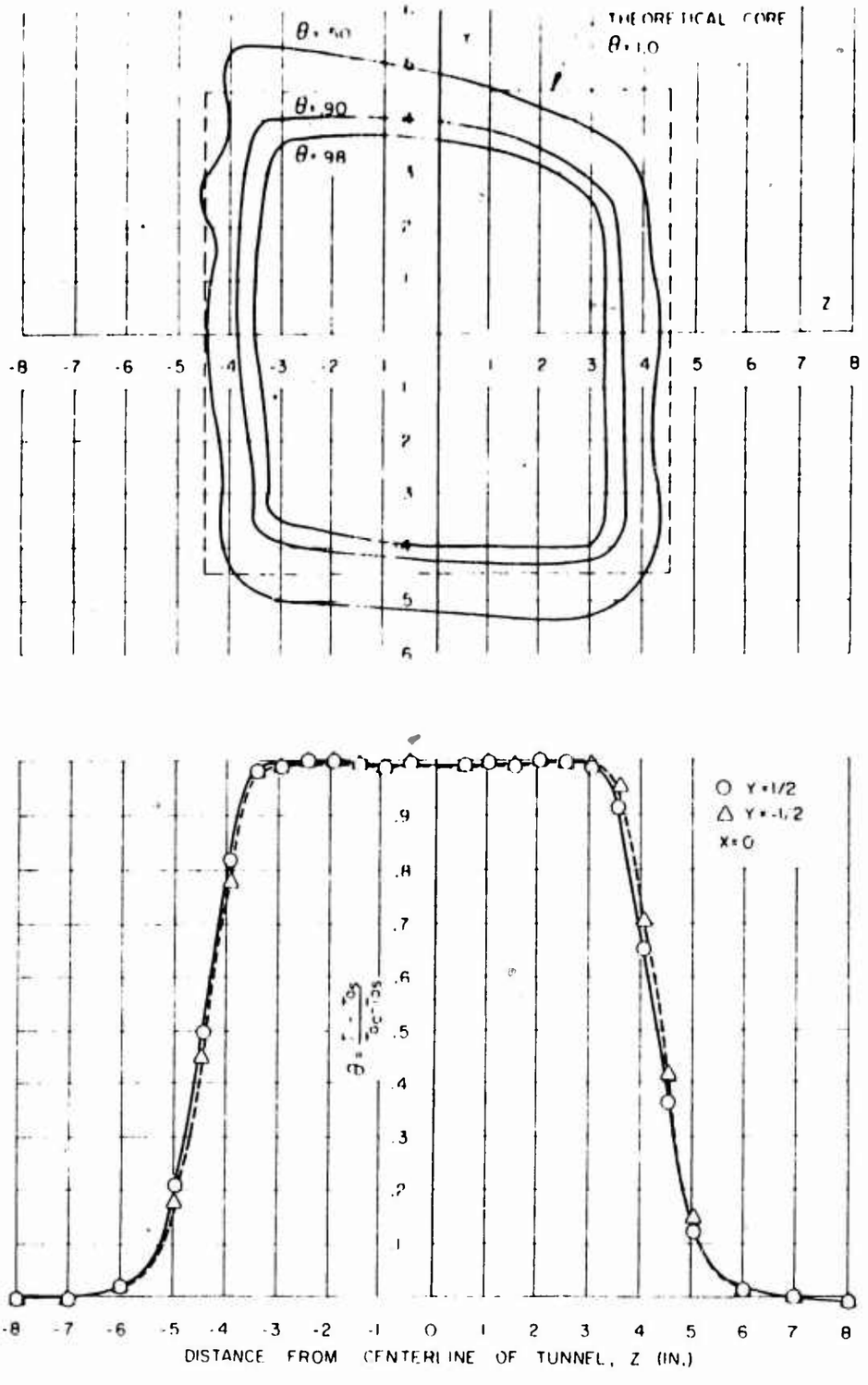

Figure 37. Isotherms and temperature distribution across the Mach 3.5 test section, at the schlieren centerline.

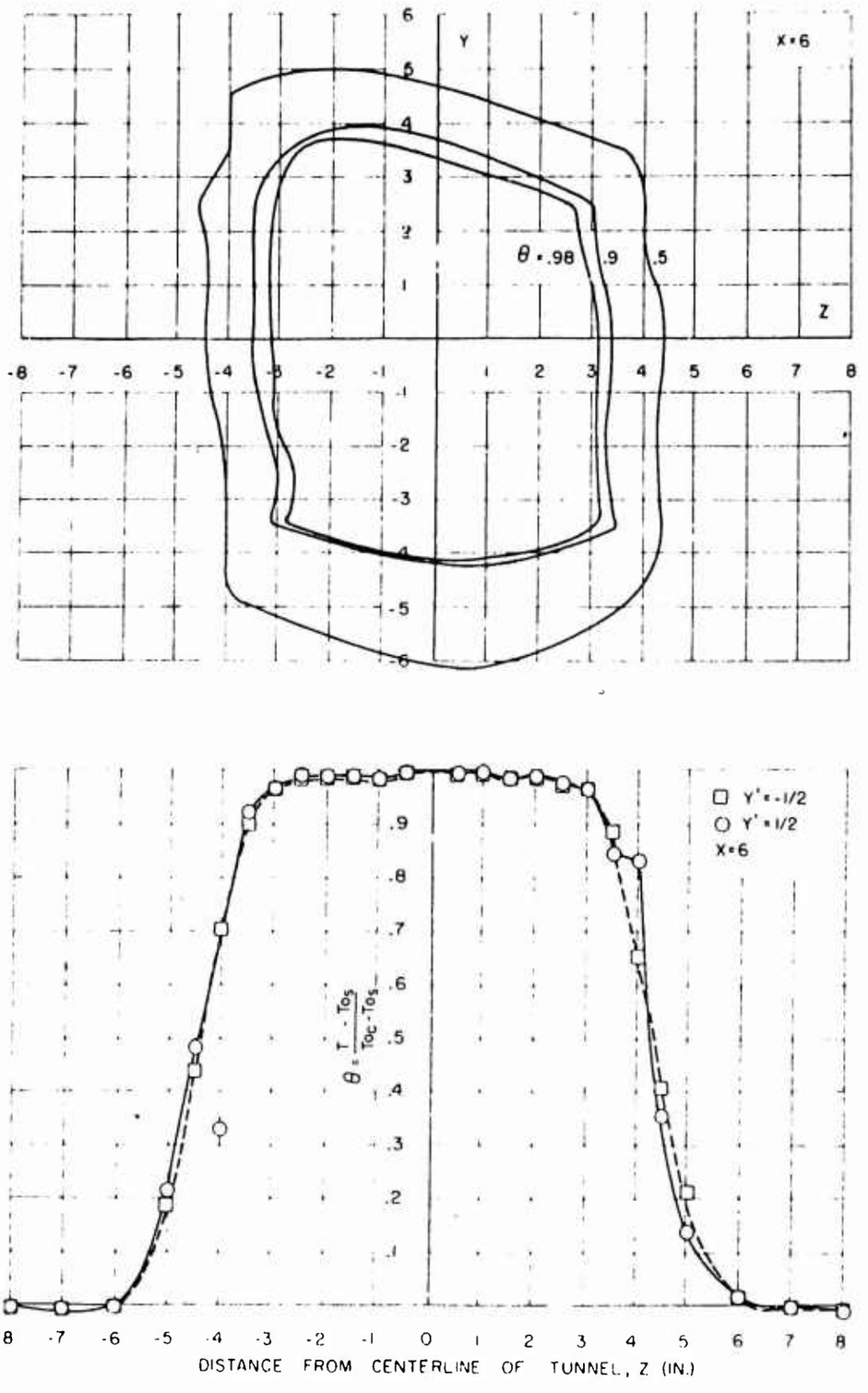

Figure 38. Isotherms and temperature distribution across the Mach 3.5 test section, six inches downstream of the schlieren centerline.

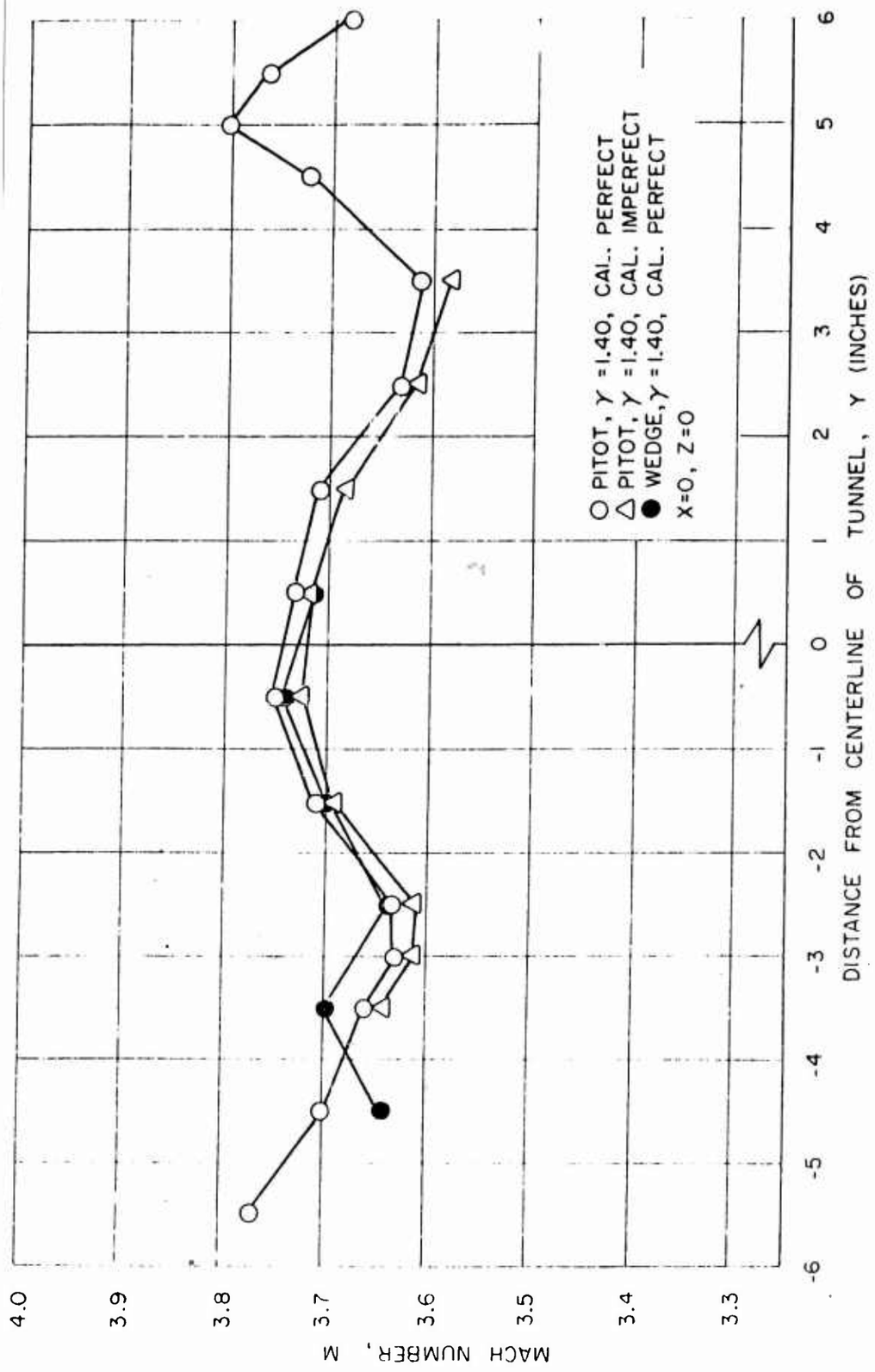

Figure 39. Comparison of pitot determined Mach numbers with wedge-pitot determined Mach numbers.

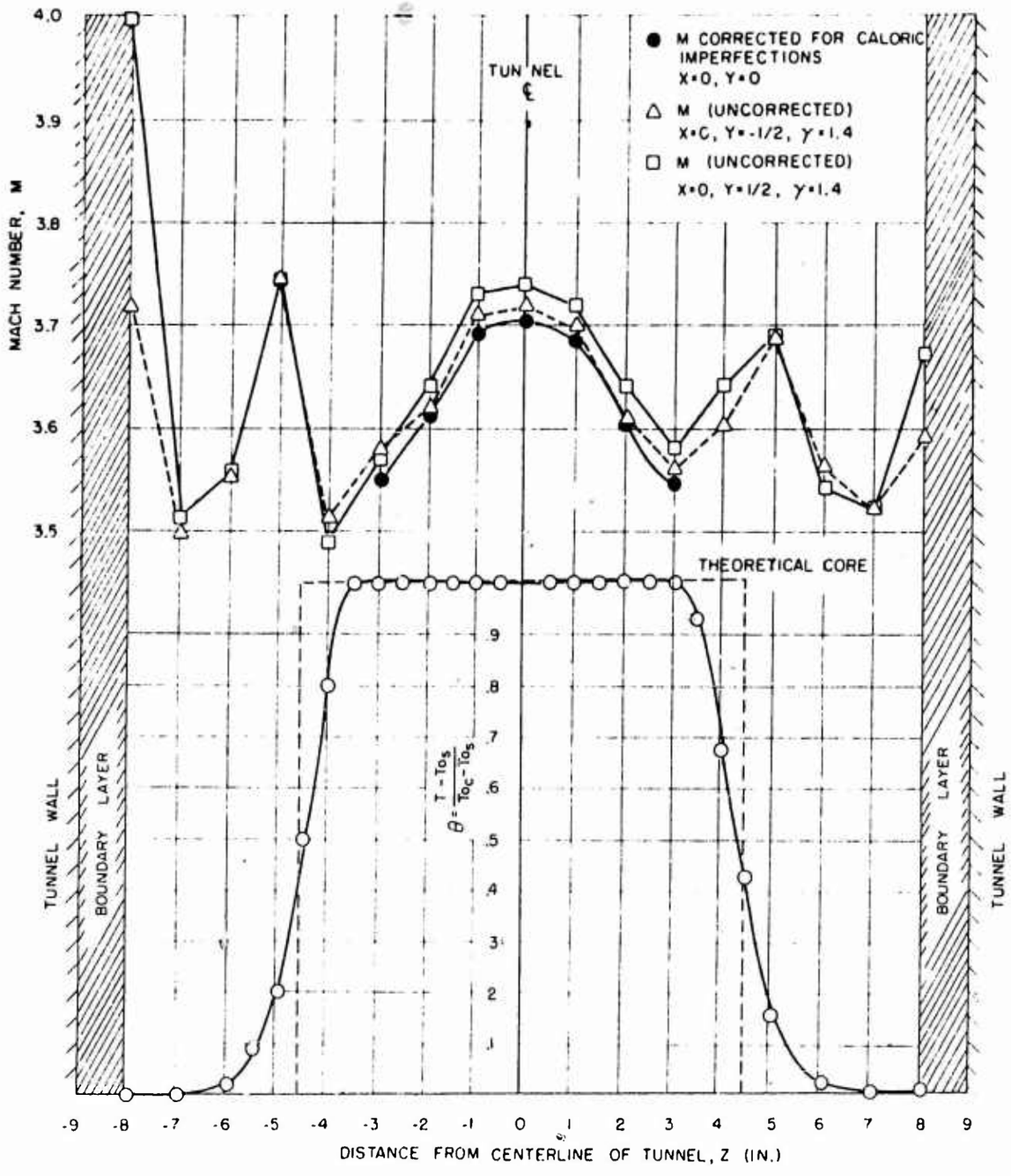

Figure 40. Mach number and temperature distribution in Mach 3.5 test section.

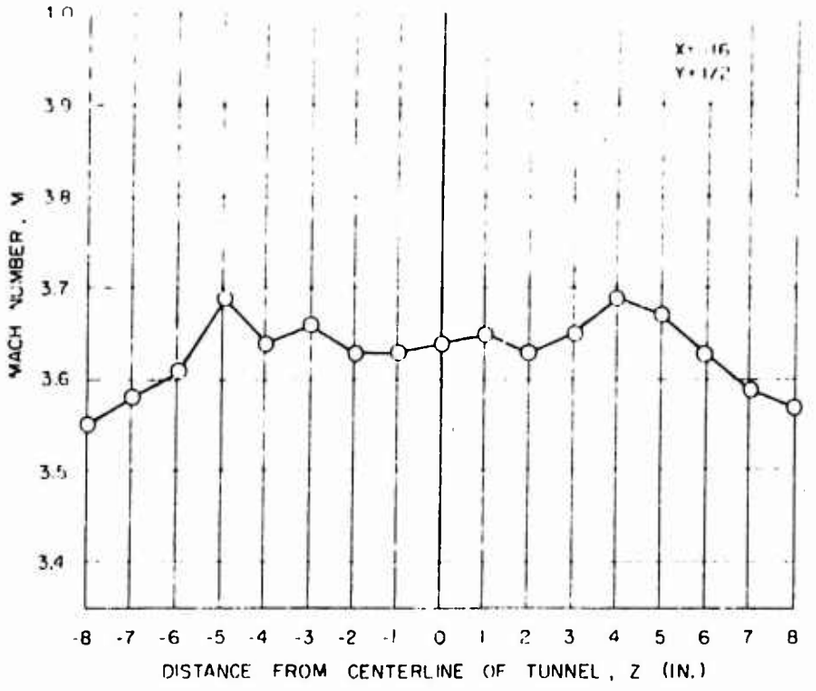

Figure 41. Mach number distribution in Mach 3.5 test section, sixteen inches in front of schlieren centerline.

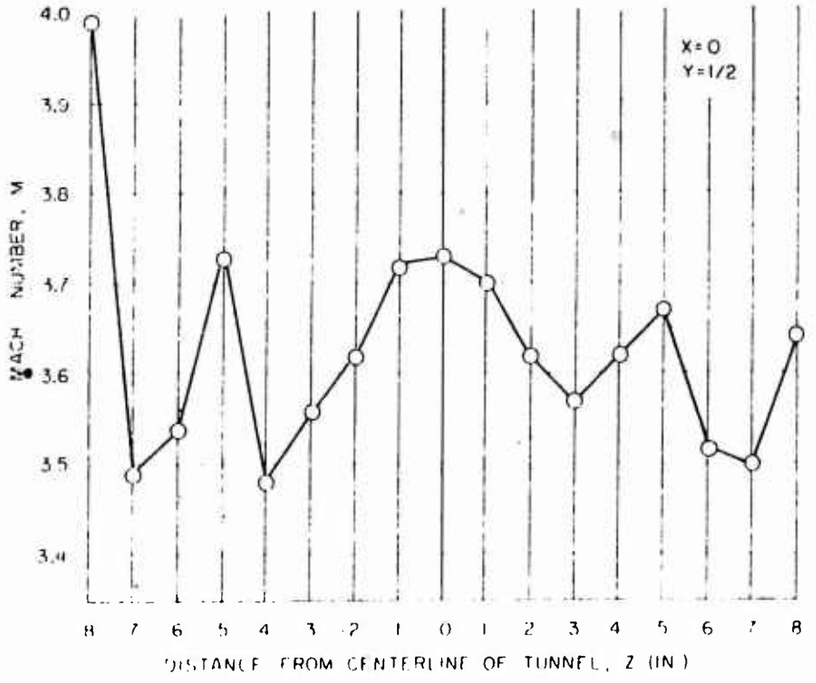

Figure 42. Mach number distribution in Mach 3.5 test section, at schlieren centerline.

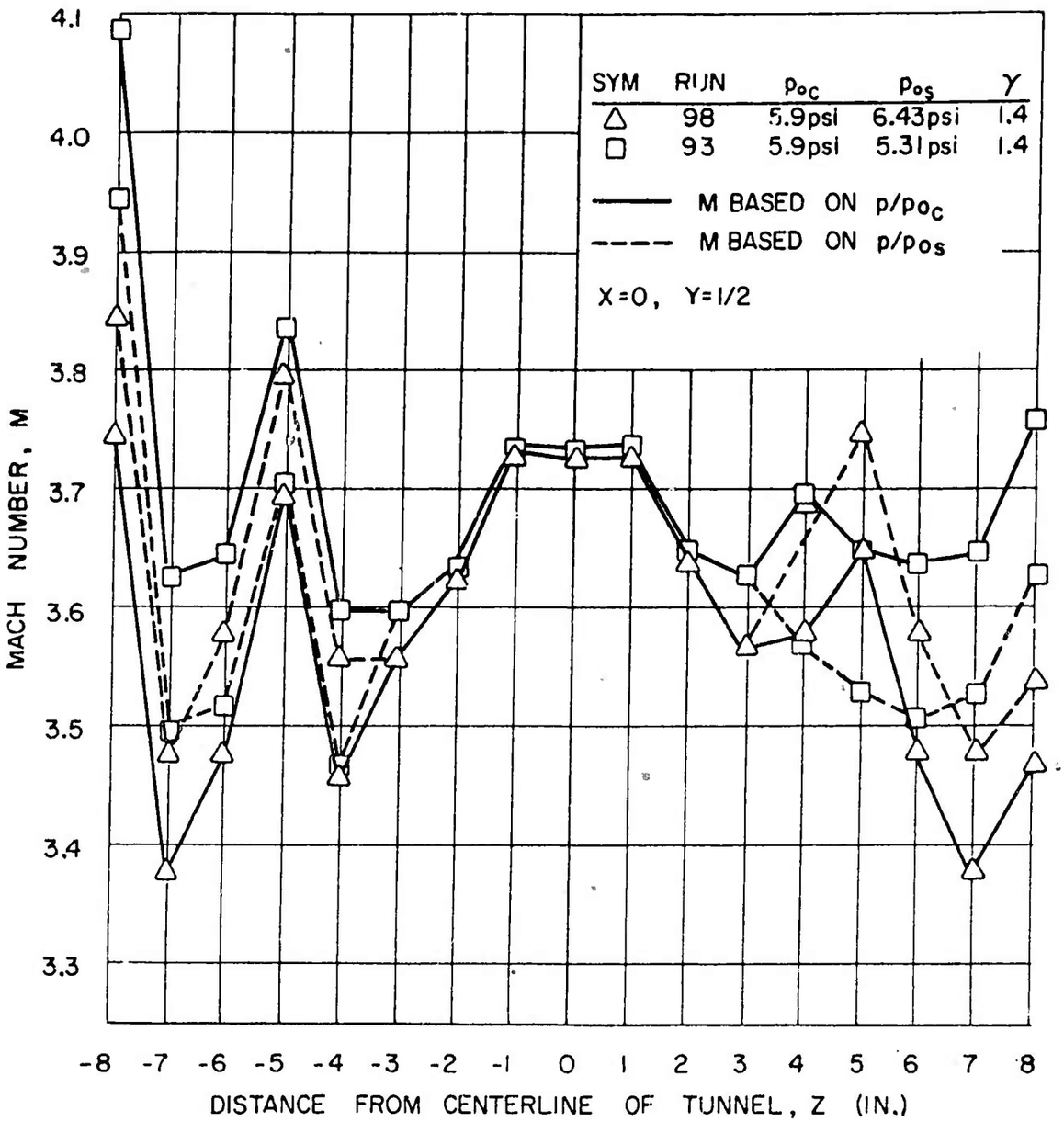

Figure 43. Effect of the variation of the ratio of core pressure to stream pressure on the Mach number distribution.

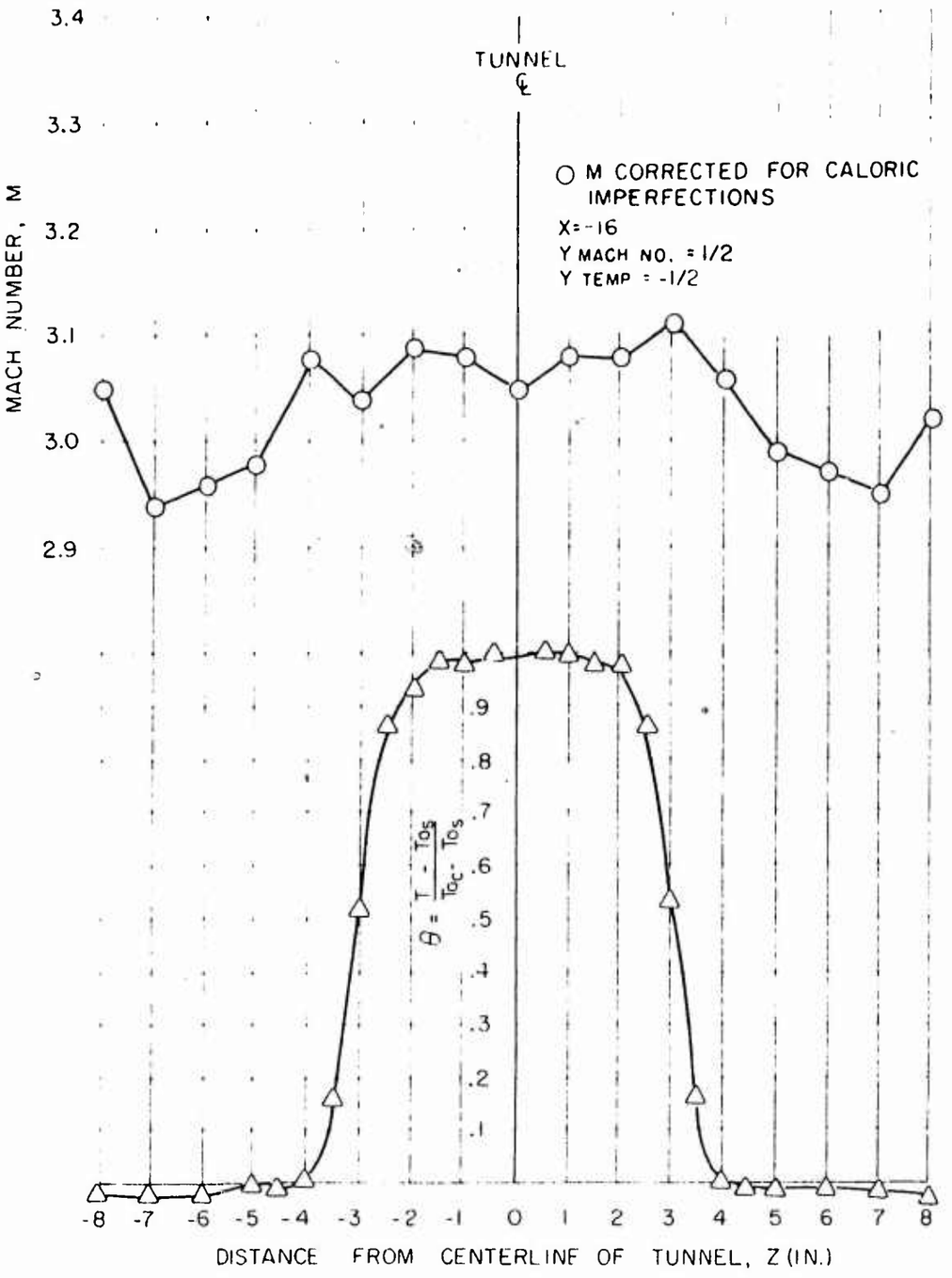

Figure 44. Mach number and temperature distributions sixteen inches in front of the schlieren centerline for the Mach 3.0 test section.

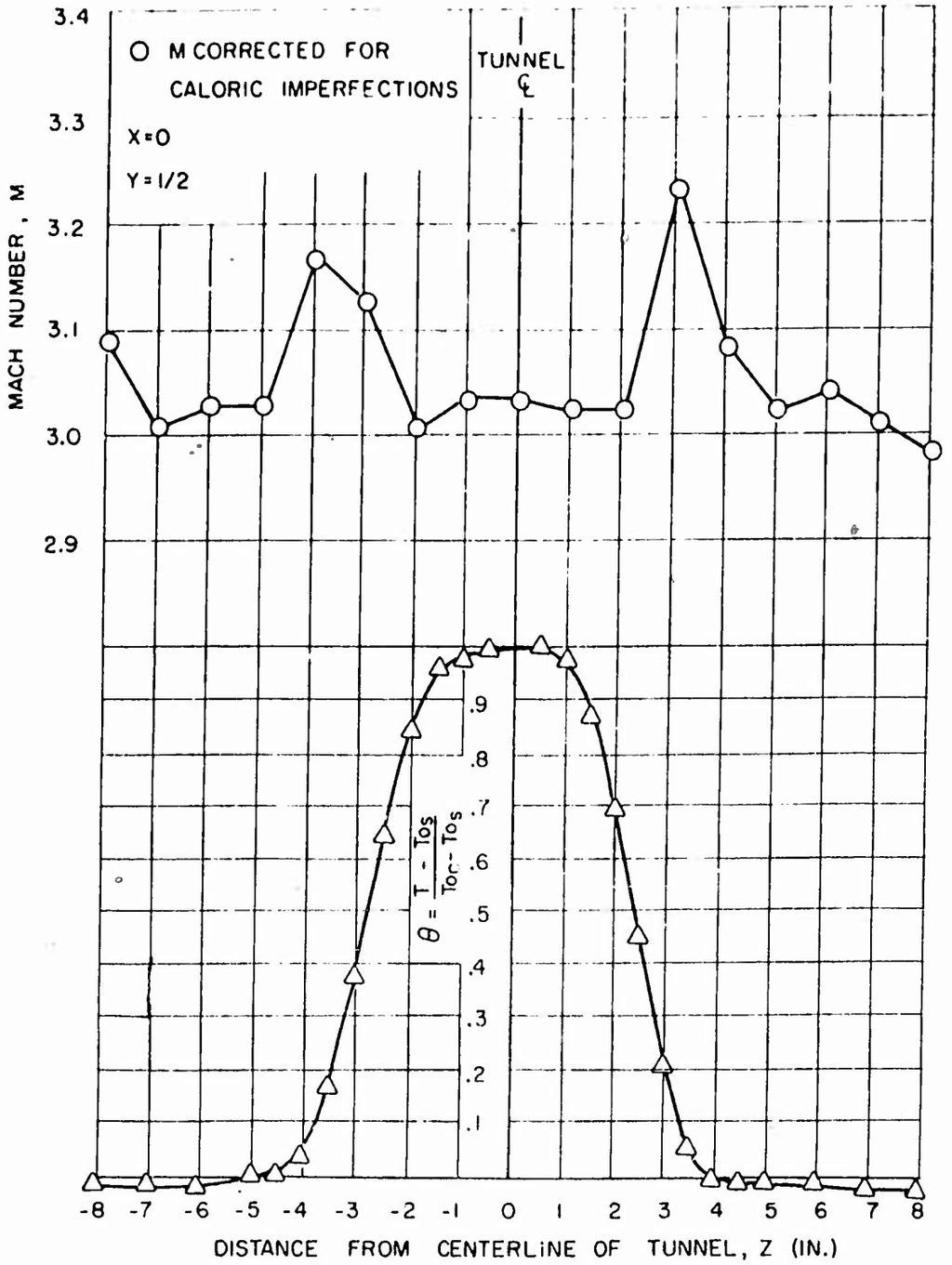

Figure 45. Mach number and temperature distributions at the schlieren centerline for the Mach 3.0 test section.

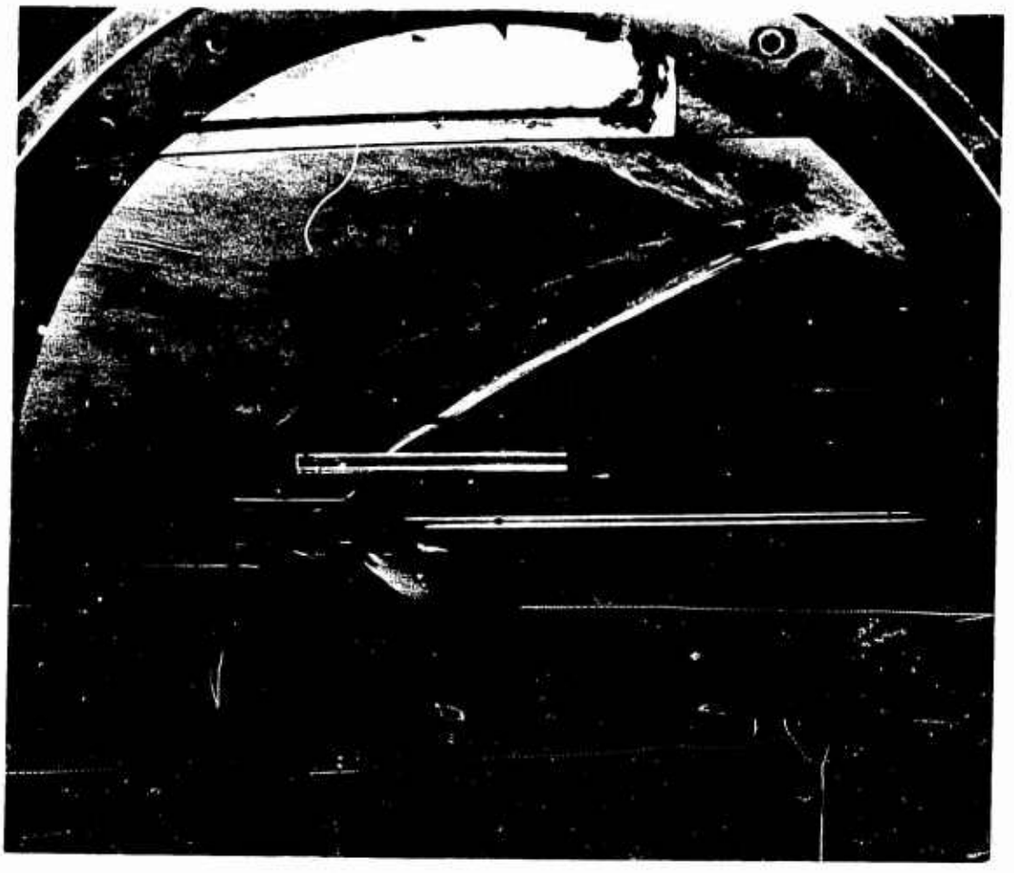

Figure 46. Schlieren photograph of calibration rake operating in Mach 3.5 test section.

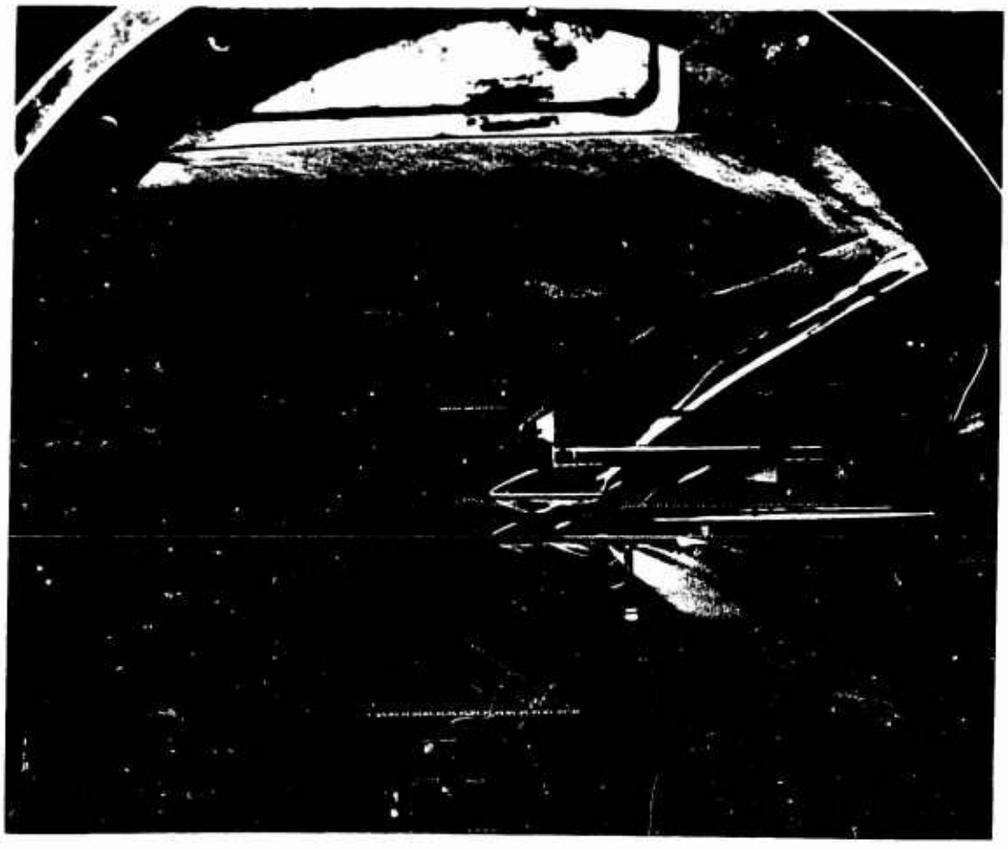

Figure 47. Schlieren photograph of calibration rake operating in Mach 3.0 test section.

APPENDIX A

ALLOWABLE COMPRESSOR INTAKE TEMPERATURE ESTIMATE

Due to the outlet temperature limit on the main compressors it was felt that the compressor efficiency should be found so as to be able to predict outlet temperatures for a given inlet temperature.

At M = 3.5 the compressors operate in series. Thus the critical compressor is the #1 compressor. A schematic diagram of series operation of the compressors is shown below.

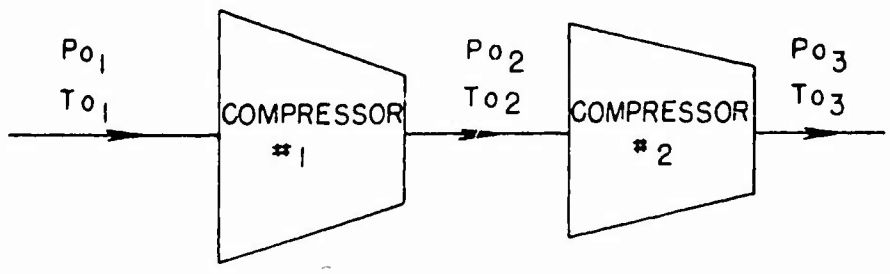

In order to obtain an indication of the efficiency, a thermocouple was installed at the outlet of the #1 compressor to obtain T_{o_2}. T_{o_1} was taken as T_o of the tunnel under operation. Measurements indicated that at M = 3.5 and T_{o_1} = 110°F a maximum T_{o_2} of 333°F would be obtained. From Reference 13 at M = 3.5, $p_{o_3} / p_{o_1} = 6.2$. In series operation

$$p_{o_2} / p_{o_1} = \sqrt{p_{o_3} / p_{o_1}} = 2.49 \qquad (A.1)$$

Compressor efficiency is given by:

$$\eta_c = \frac{\left[\left(\frac{p_{o_2}}{p_{o_1}}\right)^{\frac{\gamma-1}{\gamma}} - 1\right]}{T_{o_2} / T_{o_1} - 1} \qquad (A.2)$$

and for $T_{02}/T_{01} = {}^{793}/570$ and $p_{02}/p_{01} = 2.49$

$$\therefore \quad \eta_c \cong 77\%$$

Now, allowing T_{02} to be the limit of the compressor of 500°F and assuming $\eta_c = 0.77$ the maximum T_{01} from equation (A.2) was found to be 233°F.

It should be pointed out that the above investigation is not entirely conclusive and a more thorough investigation is now underway at NSL to determine the compressor efficiencies more accurately. However the above results are felt to be a good and sufficient approximation applicable to the hot core design problem at hand.

APPENDIX B

MECHANICAL DESIGN OF THE "HOT CORE" CIRCUIT

The following NSL report of the above title includes the work done on the revision of the NSL wind tunnel circuit in conjunction with obtaining an operational high temperature test section at NSL. Information included in this report upon the mechanical design of a high temperature wind tunnel circuit is apt to be of considerable value to one interested in the design and construction of a similar installation. For this reason the following report from Reference 12 is presented in whole:

Included are the design conditions considered and met in the construction of the addition to the S.W.T. known as the "Hot Core". References to specific parts can be followed on the attached sketch.

1) Proposed: to increase the range of wind tunnel operation in terms of stagnation temperature. Since the tunnel cannot withstand temperatures much greater than 200°F as it is now constructed, and to change its construction would be practically impossible, it was proposed to supply heated air to a section around the centerline of the tunnel. The tunnel walls would be insulated from this high temperature by the cooler air flowing around it.

2) Solution: supply air at a high temperature and at a controllable pressure to an auxiliary nozzle situated on the centerline of the existing S.W.T. nozzle.

3) Procedure: The H.W.T. heaters are able to supply air at 1000°F at a maximum flow of 1 #/sec. and 100 psia. Since this hot air source is available, it was decided to tap its outlet line--this point can be considered as the start of the "Hot Core". For this purpose two valves are supplied: one each to connect or disconnect the H.W.T. or the hot core to the H.W.T. heaters. (H-6 and H-10)

From the valve mentioned above (H-10), it is possible to pass

air at a pressure needed for testing in the tunnel. Accordingly, it would be possible to locate the p_0 control valve at this point. Three valid arguments are used against this proposal. The test facility is to operate at 5 psia; for air to be transported at such a low pressure using 1 #/sec. as design conditions shows extremely large velocity in even a 6-inch diameter pipe. Insulation would make the diameter of the unit much too large to handle. Finally, an expensive remote control valve would have to be purchased. Accordingly, a 2-1/2-inch line was chosen, giving a velocity of 160 ft/sec. at the design condition of 1000° F. 100 psia, and 1 #/sec. flow. p_0 control is attained by means of two hand-operated Globe valves (H-12 and H-12') located just before the hot core stilling section inside the main tunnel stilling section. They are reached by means of shafts through holes in the tunnel wall. Choice of the size of these valves was determined by use of Fisher Company Valve Sizing and Capacity Charts Bulletin AL-4 for design conditions of 1 #/sec. at 1000° F and a reduction of 100 psia to 5 psia.

Other valves (H-6, H-10, H-11) used are of the gate type specially constructed with a hinge in the gate so that it falls away from its seat when the stem is retracted. Also, gate and seat are of two different types of stainless steel. These two features prevent "galling" or seizing characteristics of stainless steel.

At 1000° F service, it is not permitted by any design codes to use steel under any stress. For this reason, and for its reputed resistance to scaling; chrome molybdenum steel was chosen as piping material (1-1/4 CR-1/2 Mo). Chrome-Mo fittings are practically impossible to obtain, so stainless-steel screwed fittings with litharge to prevent leaks have been used.

To further reduce complications, it is necessary to run the pipe from its origin to the point of use with as few bends as possible. This is to reduce the number of expansion joints used as they are expensive and involve long delivery time. Two pipe lengths were selected, one 40-feet long, the other 25-feet long; at 1-inch expansion for every

10-feet of pipe at 1000° F, 4 inches and 2.5 inches of expansion must be allowed. Therefore rockers and flexible joints have been provided. The rockers can be considered as point supports; a rough calculation which assumes the pipe to be equally supported on each rocker, with no end moments, shows that supports 5 feet apart give stresses of about 3200 psi. 7800 psi is allowed at 1000° F. Further factor of safety is provided by more redundant supports. The long lengths of small diameter tubing suggest buckling if any appreciable end loads are applied. Eulers buckling formula gives a critical end load of 2450 lbs at 1000° F for the 40-foot length. Loads of this size are not expected, but guides are supplied which restrict the motion of the pipe to that along the axis. (Flexible hoses provide expansion joints with practically no reaction).

Expansion in the 90-degree bend near the main tunnel stilling section is taken up by bending in the pipe itself, and in the pivot located there.

Heating of the lines without running the main tunnel is accomplished by passing the hot air into the test room through a bypass (H-11). Provision has also been made to pass cool air through the stilling section and nozzle using the pre-drying system as a source; thus allowing rapid shutdown of the system.

Insulation was designed and installed by the New England Insulation Company. It consists of 3 inches of "Kaylo 20" on the radius of the pipe. Flexible hoses and the stilling section are covered with a wool-like substance known as T.W.F. The wool is held in place by an asbestos jacket. The stilling section is covered on the outside by a skin of sheet metal to present a smooth surface to air flow by it.

Major alterations to the main tunnel consist of two openings cut in the stilling section between V-2 and the screen. The largest is an access hatch cut on the console side. The smaller on the top is to allow for the entrance of the 2-1/2-inch pipe carrying the hot air. In both cases, the piece cut out of the tunnel wall was replaced as nearly as possible to its original position to present a smooth surface to the flow of air past it.

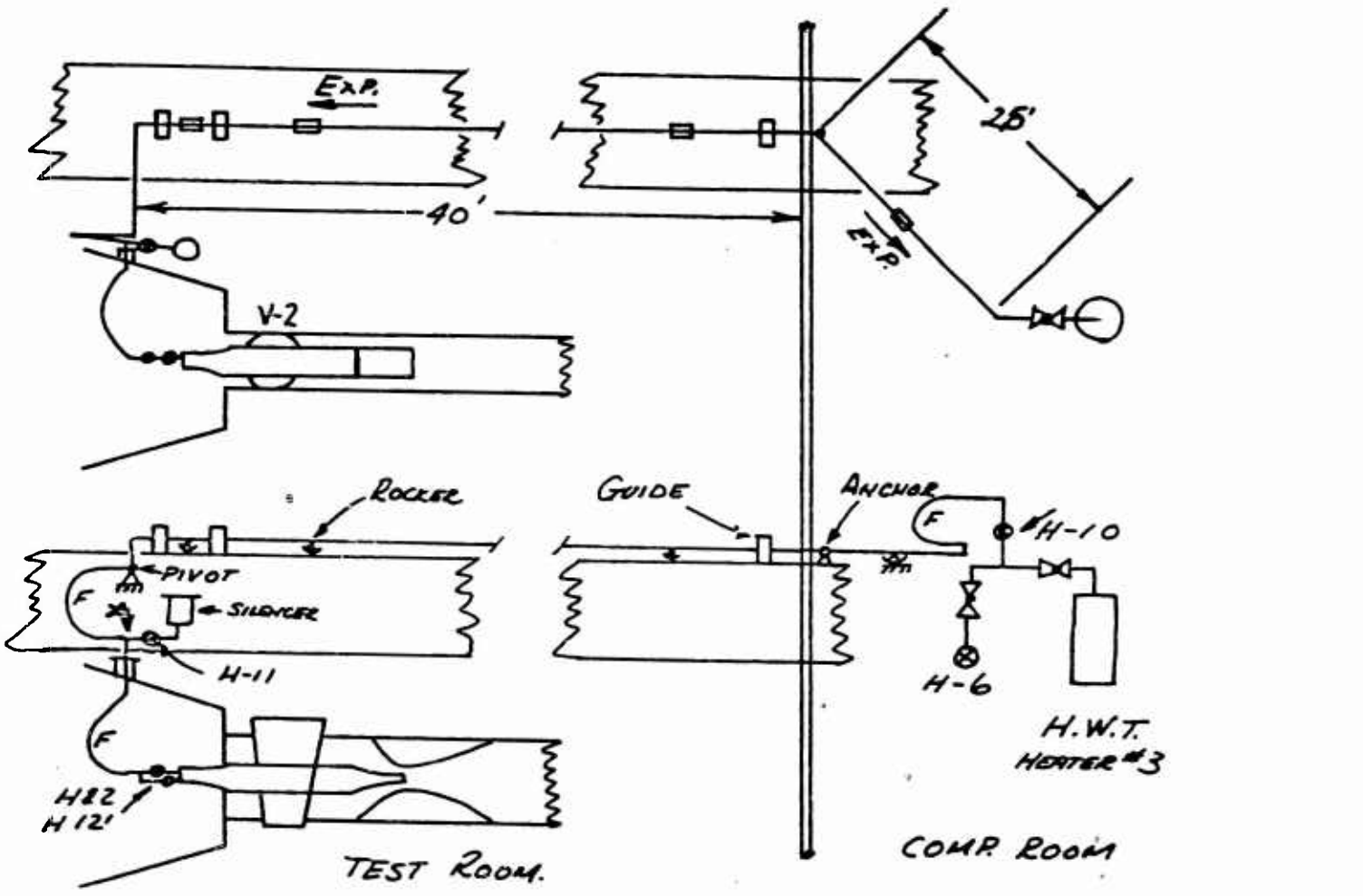
EXP.
40'
25'
EXP.
V-2
ROCKER
GUIDE
ANCHOR
F
H-10
PIVOT
SILENCER
H-11
H-6
H.W.T.
HEATER #3
F
H12
H 121
TEST ROOM.
COMP. ROOM
X PRE-DRYING AIR CAN BE BLOWN INTO HOT CORE FOR COOLING PURPOSES
F INDICATES FLEXIBLE HOSE
EXP. .. DIR. OF EXPANSION

Figure B.1

APPENDIX C

TEMPERATURE LOSS IN THE STILLING SECTION

Assume that the stilling section is a 10 foot insulated pipe with fully developed turbulent flow on both the outside and the inside.

The heat transfer rate from a fluid to the surface of a solid was defined by Newton as

$$q = hA\,(T_f - T_p) \qquad (C.1)$$

where q is the heat transfer rate, h the coefficient of heat transfer between a fluid and a solid surface, A the area normal to the direction of heat flow, T_f the temperature of the fluid, and T_p the temperature of the pipe.

W.H. McAdams, in Reference 13, has suggested the following empirical relation for the film coefficient h which has met with much success

$$\frac{hD}{k} = 0.023\,(Re)^{0.8}(Pr)^{0.4} \qquad (C.2)$$

where k is the thermal conductivity of the fluid.

First consider the flow inside of the pipe. For the problem at hand, i.e. operation of the hot core at a stagnation temperature of 1000°F, M = 3.5, ω_c = 1 #/sec and p_0 = 6 #/in²:

$D = 1$ ft.

$k = .0395$ Btu/(hr.)(ft.²)°F/ft

$Re = 5.14 \times 10^4$

$Pr = 0.665$

Using equation (C.2)

$h_1 = 4.1$ Btu/(hr.)(ft.²)(°F)

Secondly consider the flow outside of the pipe. As an approximation, consider this flow as being inside of the pipe and again use equation (C.2) in order to determine h. Such an approximation is conservative since the boundary layer for the fully developed pipe flow will not be as thick as for the fully developed turbulent flow on the outside of the pipe. Based on the

following flow properties outside of the pipe

T_f	$= 100°F$	k	$= .016\ ^{Btu}/(hr.)(ft.^2)\,°F/ft$
p_0	$= 6\ \#/in^2$	Re	$= 1.375 \times 10^5$
D	$= 1$ ft.	Pr	$= 0.696$

and using equation (C.2)

$$h_2 = 4.1\ ^{Btu}/(hr.)(ft.^2)(°F)$$

Equation (C.1) written so as to include the two heat transfer processes is

$$q = UA\ \Delta T_m \tag{C.3}$$

Where ΔT_m is the difference between the mean temperature of the fluid inside of the pipe and of the pipe itself, and the temperature of the fluid outside of the pipe and the pipe itself. U is the overall heat transfer coefficient which, allowing for insulation of thermal conductivity k, on the pipe is approximated by

$$1/U \cong 1/h_1 + 1/h_2 + 1/k_i \tag{C.4}$$

A reasonable value for the thermal conductivity of insulation is $k_i = .6\ ^{Btu}/(hr.)(ft.^2)(°F/ft.)$. Therefore $U \cong .465\ ^{Btu}/(hr.)(ft.^2)(°F/ft.)$. Using equation (C.3)

$$q_c \cong 13,150\ ^{Btu}/hr.$$

Now in order to find the heat loss due to radiation to the walls of the tunnel the temperature of the surface of the insulation must be known. Assume this temperature to be 170°F. The radiation equation is

$$q_r = A\sigma (T_1^4 - T_2^4) \frac{1}{1/\varepsilon_1 + 1/\varepsilon_2 - 1} \tag{C.5}$$

Assume the emissivity of the insulation is $\varepsilon_1 = 1$ to be conservative. The emissivity of steel (the tunnel wall) is about 0.6. T_1 is the temperature of the insulation and T_2 is the temperature of the tunnel wall, 100°F.

σ is the Stefan-Boltzmann constant. Thus we find

$$q_r = 2000 \ ^{Btu}/hr.$$

and if the above assumptions are valid the total heat loss is

$$q_T = q_c + q_r = 15,\ 500 \ ^{Btu}/hr.$$

A check may be made to see if the assumed insulation temperature of 170° F was correct. Since the total heat loss must pass through the one inch of insulation δ and the conductivity k_i is known for the insulation we may solve for ΔT and thus find the temperature of the insulation if we assume $T_p = 1000°F$. The conductivity equation is

$$qT = k A \Delta T/\delta \qquad (C.6)$$

thus we find

$$\Delta T = 825°F$$

or the temperature of the insulation is 175° F. This is in very close agreement with the original assumption so the conclusion is that $q_T = 15,000 \ ^{Btu}/hr.$ is the heat lost from the heated air in the stilling section. The heat loss is given by

$$q_T = \omega C_p \Delta T$$

Thus ΔT, the temperature drop is

$$\Delta T = \frac{15,500 \ ^{Btu}/hr.}{3000 \ ^{\#}/hr. \times .24 \ ^{Btu}/\#°F}$$

$$= 18°F$$

Such a temperature drop can be tolerated.

APPENDIX D

HEATED CORE NOZZLE COORDINATES

ξ	x	y	z
.5350	5.426	.849	4.472
.5300	5.375	.845	
.5250	5.324	.842	
.5200	5.274	.838	
.5150	5.233	.835	
.5100	5.173	.832	
.5050	5.122	.828	
.5000	5.071	.825	
.4950	5.021	.822	
.4900	4.970	.818	
.4850	4.920	.815	
.4800	4.869	.812	
.4750	4.818	.809	
.4700	4.768	.805	
.4650	4.717	.802	
.4600	4.666	.799	
.4550	4.616	.796	
.4500	4.565	.793	
.4450	4.575	.790	
.4400	4.464	.787	
.4350	4.413	.784	
.4300	4.363	.782	
.4250	4.312	.779	
.4200	4.261	.776	
.4150	4.211	.773	
.4100	4.160	.770	
.4050	4.109	.768	
.4000	4.059	.765	
.3950	4.008	.762	
.3900	3.957	.760	
.3850	3.907	.757	

HEATED CORE NOZZLE COORDINATES (Continued)

ξ	x	y	z
.3800	3.856	.755	4.472
.3750	3.805	.752	
.3700	3.755	.750	
.3650	3.704	.747	
.3600	3.653	.745	
.3550	3.603	.742	
.3500	3.552	.740	
.3450	3.501	.738	
.3400	3.451	.735	
.3350	3.400	.733	
.3300	3.349	.731	
.3250	3.298	.729	
.3200	3.248	.727	
.3150	3.197	.725	
.3100	3.146	.723	
.3050	3.096	.721	
.3000	3.045	.718	
.2950	2.994	.717	
.2900	2.944	.715	
.2850	2.893	.713	
.2800	2.842	.711	
.2750	2.791	.709	
.2700	2.741	.707	
.2650	2.690	.705	
.2600	2.639	.704	
.2550	2.588	.702	
.2500	2.538	.700	
.2450	2.487	.699	
.2400	2.436	.697	
.2350	2.386	.695	
.2300	2.335	.694	
.2250	2.284	.692	

HEATED CORE NOZZLE COORDINATES (Continued)

ξ	x	y	z
.2200	2.233	.691	4.472
.2150	2.103	.689	
.2100	2.132	.688	
.2050	2.081	.687	
.2000	2.030	.695	
.1950	1.900	.684	
.1900	1.929	.683	
.1850	1.878	.681	
.1800	1.827	.680	
.1750	1.777	.679	
.1700	1.726	.678	
.1650	1.675	.677	
.1600	1.624	.676	
.1550	1.574	.675	
.1500	1.523	.674	
.1450	1.472	.673	
.1400	1.421	.672	
.1350	1.371	.671	
.1300	1.320	.670	
.1250	1.269	.669	
.1200	1.218	.668	
.1150	1.168	.667	
.1100	1.117	.667	
.1050	1.066	.666	
.1000	1.015	.665	
.0950	.965	.665	
.0900	.914	.664	
.0850	.863	.663	
.0800	.812	.663	
.0750	.761	.662	
.0700	.711	.862	
.0650	.660	.661	

HEATED CORE NOZZLE COORDINATES (Continued)

ξ	x	y	z
.0600	.609	.661	4.472
.0550	.558	.661	
.0500	.508	.660	
.0450	.457	.660	
.0400	.406	.660	
.0350	.355	.659	
.0300	.305	.659	
.0250	.254	.659	
.0200	.203	.659	
.0150	.152	.659	
.0125	.127	.659	
-.015	-.152	.659	
-.02	-.203	.659	
-.04	-.406	.659	
-.06	-.609	.661	
-.03	-.812	.663	
-.12	-1.218	.668	
-.16	-1.624	.675	
-.20	-2.031	.684	
-.30	-3.045	.717	
-.40	-4.059	.763	
-.50	-5.072	.822	
-.60	-6.083	.893	
-.70	-7.093	.978	
-.80	-8.102	1.076	
-.90	-9.108	1.107	
-1.00	-10.112	1.310	
	-11.0	1.469	
	-12.0	1.665	
	-13.0	1.890	
	-14.0	2.157	

HEATED CORE NOZZLE COORDINATES (Concluded)

ξ	x	y	z
	-15.0	2.444	4.472
	-16.0	2.777	4.472
	-17.0	3.147	4.472
	-18.0	3.571	4.472
	-19.0	4.025	4.525
	-19.5		4.560
	-20.0	4.448	4.625
	-20.5		4.700
	-21.0	4.860	4.810
	-21.5		4.950
	-22.0	5.150	5.110
	-22.5		5.240
	-23.0	5.320	5.310
	-23.5		5.350
	-24.0	5.35	5.350
	-25.0	5.35	5.350
	-26.0	5.35	5.350

APPENDIX E

TEMPERATURE DATA

The temperature data from the heated core calibration tests is presented in tabulated form for future reference. The run numbers shown are the wind tunnel run numbers used in the tests. The temperatures, T, are the temperatures obtained after the application of the recovery factors explained in section 7.1.2. All temperatures are given in degrees Fahrenheit.

TEMPERATURE DATA

RUN 1

T_{0_B} = 100, T_{0_C} = 906, x = 0, y = -1/2

z	T	z	T
-8	93	8	91
-7	97	7	104
-6	122	6	119
-5	243	5	229
-4 1/2	463	4 1/2	455
-4	732	4	688
-3 1/2	887	3 1/2	880
-3	905	3	916
-2 1/2	907	2 1/2	916
-2	915	2	916
-1 1/2	905	1 1/2	915
-1	902	1	918
-1/2	915	1/2	916

RUN 2

T_{0_B} = 100, T_{0_C} = 906, x = 0, y = -1 1/2

z	T	z	T
-8	88	8	88
-7	96	7	99
-6	107	6	112
-5	200	5	236
-4 1/2	412	4 1/2	462
-4	677	4	706
-3 1/2	871	3 1/2	891
-3	913	3	922
-2 1/2	915	2 1/2	919
-2	921	2	921
-1 1/2	918	1 1/2	919
-1	913	1	924
-1/2	924	1/2	926

RUN 3

T_{0_B} = 100, T_{0_C} = 906, x = 0, y = -2 1/2

z	T	z	T
-8	87	8	85
-7	90	7	95
-6	95	6	101
-5	163	5	223
-4 1/2	361	4 1/2	470
-4	610	4	732
-3 1/2	835	3 1/2	901
-3	908	3	922
-2 1/2	913	2 1/2	921
-2	907	2	924
-1 1/2	913	1 1/2	921
-1	915	1	931
-1/2	927	1/2	932

RUN 4

T_{0_B} = 100, T_{0_C} = 906, x = 0, y = -3 1/2

z	T	z	T
-8	88	8	90
-7	94	7	99
-6	98	6	106
-5	163	5	248
-4 1/2	382	4 1/2	495
-4	650	4	727
-3 1/2	855	3 1/2	888
-3	904	3	918
-2 1/2	906	2 1/2	918
-2	914	2	920
-1 1/2	907	1 1/2	919
-1	908	1	926
-1/2	924	1/2	930

RUN 5

T_{0_B} = 73, T_{0_C} = 917, x = 0, y = -1/2

z	T	z	T
-8	69.5	8	68.1
-7	69.2	7	76.7
-6	88.3	6	89.0
-5	222	5	204
-4 1/2	452	4 1/2	428
-4	726	4	670
-3 1/2	899	3 1/2	880
-3	914	3	919
-2 1/2	923	2 1/2	921
-2	922	2	922
-1 1/2	920	1 1/2	919
-1	910	1	922
-1/2	918	1/2	905

RUN 6

T_{0_B} = 73, T_{0_C} = 910, x = 0, y = -4 1/2

z	T	z	T
-8	66	8	66
-7	67	7	68
-6	70	6	74
-5	113	5	124
-4 1/2	291	4 1/2	301
-4	540	4	534
-3 1/2	668	3 1/2	708
-3	637	3	719
-2 1/2	620	2 1/2	729
-2	623	2	742
-1 1/2	622	1 1/2	758
-1	662	1	779
-1/2	715	1/2	766

RUN 7

T_{0_B} = 73.5, T_{0_C} = 907, x = 0, y = -5 1/2

z	T	z	T
-8	67	8	65
-7	67	7	68
-6	74	6	72
-5	96	5	166
-4 1/2	217	4 1/2	300
-4	329	4	414
-3 1/2	316	3 1/2	407
-3	250	3	347
-2 1/2	211	2 1/2	356
-2	256	2	368
-1 1/2	266	1 1/2	384
-1	303	1	399
-1/2	343	1/2	388

RUN 8

T_{0_B} = 73.5, T_{0_C} = 909, x = 0, y = -6 1/2

z	T	z	T
-8	67	8	67
-7	68	7	69
-6	74	6	71
-5	96	5	131
-4 1/2	120	4 1/2	181
-4	117	4	197
-3 1/2	104	3 1/2	157
-3	86	3	124
-2 1/2	89	2 1/2	124
-2	88	2	123
-1 1/2	97	1 1/2	123
-1	91	1	125
-1/2	97	1/2	111

RUN 9

T_{0_B} = 74, T_{0_C} = 911, x = 0, y = 1/2

z	T	z	T
-8	67.1	8	69.1
-7	70.2	7	76.6
-6	90.5	6	88.5
-5	250	5	178
-4 1/2	491	4 1/2	381
-4	760	4	621
-3 1/2	898	3 1/2	845
-3	910	3	908
-2 1/2	913	2 1/2	914
-2	920	2	914
-1 1/2	907	1 1/2	906
-1	907	1	916
-1/2	912	1/2	910

RUN 10

T_{0_B} = 74, T_{0_C} = 912, x = 0, y = 1 1/2

z	T	z	T
-8	79.8	8	72.3
-7	714	7	76.6
-6	90.5	6	85.2
-5	204	5	138
-4 1/2	444	4 1/2	308
-4	744	4	533
-3 1/2	894	3 1/2	790
-3	908	3	902
-2 1/2	912	2 1/2	910
-2	918	2	910
-1 1/2	906	1 1/2	907
-1	907	1	916
-1/2	914	1/2	910

RUN 11

T_{0_B} = 74.0, T_{0_C} = 913, x = 0, y = 2 1/2

z	T	z	T
-8	79.7	8	72.3
-7	72.4	7	80.0
-6	86.2	6	80.9
-5	314	5	150
-4 1/2	573	4 1/2	332
-4	779	4	533
-3 1/2	883	3 1/2	742
-3	907	3	880
-2 1/2	911	2 1/2	907
-2	917	2	912
-1 1/2	907	1 1/2	907
-1	909	1	915
-1/2	919	1/2	912

RUN 12

T_{0_B} = 74.0, T_{0_C} = 914, x = 0, y = 3 1/2

z	T	z	T
-8	73.4	8	71.3
-7	70.3	7	81.0
-6	79.7	6	72.4
-5	147	5	90.5
-4 1/2	285	4 1/2	162
-4	505	4	330
-3 1/2	765	3 1/2	573
-3	892	3	774
-2 1/2	905	2 1/2	818
-2	907	2	824
-1 1/2	904	1 1/2	837
-1	905	1	867
-1/2	910	1/2	889

RUN 13

T_{0_H} = 74.5, T_{0_C} = 914, x = 0, y = 4

z	T	z	T
-8	72.4	8	72.4
-7	70.3	7	79.7
-6	72.4	6	74.5
-5	110	5	95.7
-4 1/2	259	4 1/2	202
-4	511	4	375
-3 1/2	761	3 1/2	219
-3	844	3	640
-2 1/2	838	2 1/2	613
-2	831	2	625
-1 1/2	833	1 1/2	656
-1	830	1	712
1/2	815	1/2	771

RUN 16

T_{0_H} = 76, T_{0_C} = 900, x = 0, y = 1/2

z	T	z	T
8	73.4	8	72.3
7	72.3	7	79.8
-6	85.1	6	87.2
5	226	5	202
4 1/2	452	4 1/2	417
4	842	4	659
3 1/2	880	3 1/2	862
3	899	3	903
2 1/2	906	2 1/2	903
2	906	2	906
1 1/2	900	1 1/2	900
1	940	1	905
1/2	903	1/2	904

RUN 14

T_{0_H} = 74.5, T_{0_C} = 916, x = 0, y = 4 1/2

z	T	z	T
-8	72.3	8	70.2
-7	70.2	7	78.7
-6	74.5	6	78.7
-5	150	5	117
-4 1/2	348	4 1/2	269
-4	573	4	404
-3 1/2	694	3 1/2	454
-3	703	3	428
-2 1/2	682	2 1/2	394
-2	668	2	417
-1 1/2	676	1 1/2	465
-1	666	1	533
-1/2	642	1/2	587

RUN 17

T_{0_H} = 76, T_{0_C} = 904, x = 0, y = -1 1/2

z	T	z	T
8	70.2	8	71.3
-7	71.3	7	77.6
-6	81.9	6	85.1
5	176	5	195
4 1/2	394	4 1/2	417
-4	658	4	660
-3 1/2	855	3 1/2	866
-3	899	3	905
-2 1/2	904	2 1/2	903
-2	904	2	908
-1 1/2	901	1 1/2	900
-1	898	1	908
-1/2	905	1/2	906

RUN 15

T_{0_H} = 74.5 T_{0_C} = 917, x = 0, y = 5

z	T	z	T
-8	72.3	8	70.2
-7	70.2	7	74.5
-6	78.7	6	78.7
-5	213	5	123
-4 1/4	432	4 1/2	265
-4	557	4	349
-3 1/2	544	3 1/2	313
-3	537	3	264
-2 1/2	521	2 1/2	249
-2	510	2	274
-1 1/2	520	1 1/2	317
-1	511	1	376
-1/2	485	1/2	423

RUN 18

T_{0_H} = 76.0, T_{0_C} = 905, x = 0, y = -2 1/2

z	T	z	T
8	69.1	8	70.2
-7	70.2	7	74.5
-6	72.3	6	79.8
-5	134	5	191
4 1/2	329	4 1/2	426
-4	574	4	685
3 1/2	815	3 1/2	878
3	894	3	904
2 1/2	905	2 1/2	903
2	905	2	904
-1 1/2	899	1 1/2	900
1	898	1	910
1/2	906	1/2	911

RUN 19

T_{0_B} = 76.5, T_{0_C} = 905, x = 0, y = -3 1/2

z	T	z	T
-8	69.1	8	70.2
-7	69.1	7	71.3
-6	71.3	6	77.6
-5	139	5	205
-4 1/2	348	4 1/2	437
-4	611	4	678
-3 1/2	830	3 1/2	865
-3	890	3	901
-2 1/2	900	2 1/2	899
-2	900	2	903
-1 1/2	895	1 1/2	898
-1	895	1	907
-1/2	905	1/2	909

RUN 20

T_{0_B} = 76.5, T_{0_C} = 905, x = 0, y = -4

z	T	z	T
-8	69.2	8	70.2
-7	69.2	7	73.4
-6	73.4	6	79.8
-5	142	5	168
-4 1/2	350	4 1/2	367
-4	614	4	610
-3 1/2	806	3 1/2	815
-3	836	3	866
-2 1/2	832	2 1/2	872
-2	832	2	882
-1 1/2	819	1 1/2	882
-1	835	1	897
-1/2	872	1/2	894

RUN 21

T_{0_B} = 76.5, T_{0_C} = 905, x = 0, y = -4 1/2

z	T	z	T
-8	69.2	8	69.2
-7	70.2	7	73.4
-6	75.5	6	80.9
-5	123	5	131
-4 1/2	305	4 1/2	306
-4	545	4	533
-3 1/2	669	3 1/2	705
-3	640	3	721
-2 1/2	624	2 1/2	731
-2	628	2	744
-1 1/2	628	1 1/2	759
-1	666	1	780
1/2	718	1/2	770

RUN 22

T_{0_B} = 76.5, T_{0_C} = 906, x = 0, y = 5 1/2

z	T	z	T
-8	70.2	8	70.2
-7	71.3	7	74.5
-6	80.8	6	77.6
-5	104	5	169
-4 1/2	224	4 1/2	299
-4	326	4	403
-3 1/2	310	3 1/2	401
-3	246	3	340
-2 1/2	241	2 1/2	349
-2	255	2	362
-1 1/2	264	1 1/2	378
-1	301	1	398
-1/2	338	1/2	388

RUN 23

T_{0_B} = 76.5, T_{0_C} = 907, x = 0, y = -6 1/2

z	T	z	T
-8	70.2	8	70.2
-7	72.3	7	74.5
-6	79.8	6	75.5
-5	98.9	5	128
-4 1/2	117	4 1/2	164
-4	115	4	181
-3 1/2	98.9	3 1/2	150
-3	90.4	3	117
-2 1/2	91.5	2 1/2	122
-2	91.5	2	123
-1 1/2	91.5	1 1/2	121
-1	91.5	1	126
-1/2	100	1/2	114

RUN 24

T_{0_B} = 76.5, T_{0_C} = 907, x = 0, y = 4

z	T	z	T
-8	78	8	79
-7	72	7	85
-6	78	6	80
-5	113	5	97
-4 1/2	260	4 1/2	196
-4	510	4	369
-3 1/2	752	3 1/2	565
-3	839	3	658
-2 1/2	838	2 1/2	633
-2	828	2	641
-1 1/2	834	1 1/2	668
-1	828	1	727
-1/2	822	1/2	781

RUN 32

T_{0_B} = 75, T_{0_C} = 900, x = 0, y = 1/2

z	T	z	T
-8	70	8	70
-7	70	7	79
-6	87	6	89
-5	230	5	194
-4 1/2	460	4 1/2	512
-4	729	4	644
-3 1/2	886	3 1/2	856
-3	902	3	905
-2 1/2	912	2 1/2	906
-2	907	2	910
-1 1/2	905	1 1/2	904
-1	897	1	907
-1/2	904	1/2	906

RUN 33

T_{0_B} = 75, T_{0_C} = 903, x = -2 y = -1/2

z	T	z	T
-8	69	8	70
-7	70	7	80
-6	88	6	89
-5	218	5	186
-4 1/2	469	4 1/2	402
-4	750	4	657
-3 1/2	894	3 1/2	869
-3	905	3	908
-2 1/2	913	2 1/2	907
-2	908	2	912
-1 1/2	906	1 1/2	905
-1	899	1	910
-1/2	906	1/2	909

RUN 34

T_{0_B} = 75, T_{0_C} = 908, x = -2, y = 1/2

z	T	z	T
-8	64	8	73
-7	72	7	85
-6	91	6	94
-5	233	5	174
-4 1/2	500	4 1/2	372
-4	770	4	623
-3 1/2	900	3 1/2	855
-3	907	3	913
-2 1/2	917	2 1/2	913
-2	915	2	918
-1 1/2	911	1 1/2	908
-1	903	1	917
-1/2	912	1/2	916

RUN 35

T_{0_B} = 75.5, T_{0_C} = 913, x = -2, y = 1 1/2

z	T	z	T
-8	72	8	79
-7	723	7	86
-6	90	6	95
-5	206	5	145
-4 1/2	461	4 1/2	314
-4	754	4	548
-3 1/2	903	3 1/2	808
-3	922	3	911
-2 1/2	920	2 1/2	916
-2	918	2	920
-1 1/2	915	1 1/2	914
-1	911	1	920
-1/2	917	1/2	920

RUN 36

T_{0_B} = 75.5, T_{0_C} = 915, x = -2, y = 2 1/2

z	T	z	T
-8	77	8	78
-7	73	7	83
-6	87	6	86
-5	313	5	156
-4 1/2	578	4 1/2	348
-4	773	4	206
-3 1/2	887	3 1/2	760
-3	910	3	891
-2 1/2	920	2 1/2	915
-2	917	2	921
-1 1/2	916	1 1/2	915
-1	912	1	923
-1/2	920	1/2	924

RUN 37

T_{0_B} = 75.5, T_{0_C} = 917, x = -2, y = 3

z	T	z	T
-8	79	8	78
-7	81	7	87
-6	83	6	83
-5	259	5	121
-4 1/2	439	4 1/2	238
-4	614	4	406
-3 1/2	823	3 1/2	650
-3	905	3	851
-2 1/2	919	2 1/2	908
-2	918	2	917
-1 1/2	917	1 1/2	911
-1	912	1	920
-1/2	922	1/2	925

RUN 38

T_{0_B} = 75.5, T_{0_C} = 918, x = 2, y = 3 1/2

z	T	z	T
-8	77	8	80
-7	73	7	91
-6	81	6	83
-5	157	5	98
-4 1/2	284	4 1/2	161
-4	517	4	338
3 1/2	789	3 1/2	597
3	894	3	784
-2 1/2	908	2 1/2	805
-2	904	2	802
-1 1/2	904	1 1/2	819
-1	899	1	856
-1/2	903	1/2	884

RUN 39

T_{0_B} = 75.5, T_{0_C} = 919, x = -2, y = 3 3/4

z	T	z	T
-8	78	8	80
-7	723	7	85
-6	80	6	81
-5	113	5	94
-4 1/2	249	4 1/2	166
-4	511	4	349
-3 1/2	783	3 1/2	587
-3	877	3	729
2 1/2	881	2 1/2	710
-2	870	2	713
-1 1/2	871	1 1/2	736
-1	865	1	783
-1/2	863	1/2	830

RUN 40

T_{0_B} = 75.5, T_{0_C} = 920, x = -2, y = 4

z	T	z	T
-8	77	8	80
-7	77	7	87
-6	79	6	85
-5	114	5	102
-4 1/2	263	4 1/2	204
-4	520	4	388
-3 1/2	767	3 1/2	558
-3	834	3	647
-2 1/2	830	2 1/2	607
-2	812	2	615
-1 1/2	820	1 1/2	647
-1	808	1	713
-1/2	802	1/2	766

RUN 41

T_{0_B} = 75.5, T_{0_C} = 920, x = -2, y = 4 1/2

z	T	z	T
-8	78	8	77
-7	78	7	81
-6	80	6	80
-5	142	5	114
-4 1/2	345	4 1/2	262
-4	574	4	412
-3 1/2	695	3 1/2	467
-3	700	3	440
-2 1/2	687	2 1/2	405
-2	666	2	430
-1 1/2	682	1 1/2	480
-1	670	1	550
-1/2	660	1/2	609

RUN 42

T_{0_B} = 76, T_{0_C} = 923, x = -2, y = 5

z	T	z	T
-8	73	8	83
-7	84	7	87
-6	85	6	86
-5	206	5	125
-4 1/2	437	4 1/2	289
-4	550	4	354
-3 1/2	520	3 1/2	307
-3	502	3	260
-2 1/2	501	2 1/2	242
-2	470	2	265
-1 1/2	483	1 1/2	306
-1	478	1	362
-1/2	461	1/2	407

RUN 43

T_{0_B} = 76.5, T_{0_C} = 930, x = -2, y = 1 1/2

z	T	z	T
-8	72	8	75
-7	77	7	83
-6	84	6	86
-5	171	5	542
-4 1/2	410	4 1/2	434
-4	689	4	693
-3 1/2	885	3 1/2	897
-3	923	3	931
2 1/2	934	2 1/2	930
-2	930	2	936
-1 1/2	928	1 1/2	925
-1	922	1	936
-1/2	925	1/2	930

RUN 44

T_{0_B} = 76.5, T_{0_C} = 915, x = -2, y = -2 1/2

z	T	z	T
-8	72	8	75
-7	74	7	80
-6	78	6	81
-5	136	5	191
-4 1/2	328	4 1/2	432
-4	579	4	713
-3 1/2	826	3 1/2	890
-3	905	3	913
-2 1/2	920	2 1/2	910
-2	918	2	917
-1 1/2	916	1 1/2	910
-1	913	1	922
-1/2	923	1/2	918

RUN 45

T_{0_B} = 76.5, T_{0_C} = 906, x = -2, y = -3 1/2

z	T	z	T
-8	72	8	76
-7	75	7	78
-6	76	6	82
-5	129	5	213
-4 1/2	335	4 1/2	464
-4	609	4	716
-3 1/2	833	3 1/2	883
-3	892	3	906
-2 1/2	905	2 1/2	903
-2	903	2	911
-1 1/2	900	1 1/2	903
-1	898	1	913
-1/2	906	1/2	913

RUN 46

T_{0_B} = 76.5, T_{0_C} = 905, x = -2, y = -4 1/2

z	T	z	T
-8	72	8	75
-7	75	7	78
-6	78	6	85
-5	122	5	136
-4 1/2	315	4 1/2	308
-4	567	4	542
-3 1/2	709	3 1/2	727
-3	681	3	745
-2 1/2	675	2 1/2	762
-2	685	2	779
-1 1/2	682	1 1/2	790
-1	720	1	819
-1/2	770	1/2	815

RUN 47

T_{0_B} = 76.5, T_{0_C} = 906, x = -2, y = -4 1/4

z	T	z	T
-8	72	8	74
-7	74	7	76
-6	77	6	82
-5	130	5	206
-4 1/2	346	4 1/2	424
-4	627	4	670
-3 1/2	840	3 1/2	856
-3	894	3	896
-2 1/2	894	2 1/2	896
-2	890	2	903
-1 1/2	886	1 1/2	897
-1	894	1	905
-1/2	899	1/2	907

RUN 48

T_{0_B} = 76.5, T_{0_C} = 906, x = -2 y = -4

z	T	z	T
-8	72	8	74
-7	74	7	77
-6	78	6	85
-5	137	5	173
-4 1/2	349	4 1/2	381
-4	632	4	621
-3 1/2	832	3 1/2	840
-3	861	3	871
-2 1/2	864	2 1/2	881
-2	862	2	891
-1 1/2	856	1 1/2	889
-1	864	1	900
-1/2	887	1/2	901

RUN 49

T_{0_B} = 76.5, T_{0_C} = 908, x = -2 y = 5

z	T	z	T
-8	74	8	74
-7	76	7	78
-6	80	6	84
-5	109	5	139
-4 1/2	272	4 1/2	282
-4	458	4	464
-3 1/2	496	3 1/2	568
-3	438	3	534
-2 1/2	438	2 1/2	548
-2	458	2	569
-1 1/2	472	1 1/2	597
-1	514	1	626
-1/2	567	1/2	623

RUN 50

T_{0_B} = 76.5, T_{0_C} = 910, x = -2, y = -5 1/2

z	T	z	T
8	75	8	74
7	76	7	78
6	84	6	80
5	109	5	157
-4 1/2	335	4 1/2	281
-4	335	4	396
-3 1/2	315	3 1/2	396
-3	256	3	333
-2 1/2	260	2 1/2	348
-2	277	2	369
-1 1/2	287	1 1/2	389
-1	327	1	417
-1/2	368	1/2	414

RUN 51

T_{0_B} = 77, T_{0_C} = 910, x = -2, y = -6

z	T	z	T
-8	74	8	76
-7	77	7	79
-6	84	6	80
-5	109	5	153
-4 1/2	162	4 1/2	230
-4	199	4	273
-3 1/2	178	3 1/2	238
-3	136	3	187
-2 1/2	140	2 1/2	198
-2	146	2	206
-1 1/2	151	1 1/2	216
-1	170	1	223
-1/2	190	1/2	221

RUN 52

T_{0_B} = 77, T_{0_C} = 910, x = -2, y = -6 1/2

z	T	z	T
-8	74	8	74
-7	77	7	78
-6	82	6	79
-5	101	5	128
-4 1/2	112	4 1/2	134
-4	109	4	153
-3 1/2	98	3 1/2	131
-3	90	3	109
-2 1/2	94	2 1/2	114
-2	85	2	115
-1 1/2	94	1 1/2	115
-1	98	1	121
-1/2	103	1/2	113

RUN 53

T_{0_B} = 77, T_{0_C} = 910, x = -6, y = -6 1/2

z	T	z	T
-8	70	8	723
-7	73	7	734
-6	81	6	79
-5	915	5	107
-4 1/2	112	4 1/2	128
-4	103	4	159
-3 1/2	947	3 1/2	128
-3	89	3	104
-2 1/2	90	2 1/2	113
-2	90	2	115
-1 1/2	91	1 1/2	115
-1	98	1	121
-1/2	100	1/2	107

RUN 54

T_{0_B} = 77, T_{0_C} = 910, x = -6, y = -5 1/2

z	T	z	T
-8	70	8	72
-7	73	7	74
-6	80	6	82
-5	95	5	133
-4 1/2	204	4 1/2	256
-4	343	4	400
-3 1/2	344	3 1/2	430
-3	282	3	361
-2 1/2	285	2 1/2	381
-2	300	2	399
-1 1/2	315	1 1/2	421
-1	358	1	455
-1/2	391	1/2	436

RUN 55

T_{0_B} = 77, T_{0_C} = 912, x = -6, y = -4 1/2

z	T	z	T
-8	70	8	76
-7	72	7	77
-6	76	6	83
-5	103	5	110
-4 1/2	281	4 1/2	256
-4	553	4	500
-3 1/2	724	3 1/2	723
-3	711	3	748
-2 1/2	700	2 1/2	765
-2	705	2	776
-1 1/2	706	1 1/2	805
-1	741	1	834
-1/2	774	1/2	807

RUN 56

T_{0_B} = 78, T_{0_C} = 900, x = -6, y = -1 1/2

z	T	z	T
-8	67	8	73
-7	69	7	76
-6	71	6	77
-5	111	5	166
-4 1/2	315	4 1/2	420
-4	603	4	705
-3 1/2	843	3 1/2	885
-3	893	3	905
-2 1/2	903	2 1/2	904
-2	904	2	911
-1 1/2	903	1 1/2	904
-1	896	1	906
-1/2	902	1/2	905

RUN 59

T_{0_B} = 78, T_{0_C} = 897, x = -6, y = 1/2

z	T	z	T
8	68	8	72
7	71	7	81
6	88	6	86
5	195	5	172
4 1/2	456	4 1/2	404
4	751	4	687
3 1/2	888	3 1/2	900
3	894	3	902
2 1/2	902	2 1/2	899
2	902	2	905
-1 1/2	899	1 1/2	900
-1	895	1	905
1/2	902	1/2	905

RUN 57

T_{0_B} = 78, T_{0_C} = 899, x = -6 y = -2 1/2

z	T	z	T
-8	67	8	73
-7	70	7	81
-6	73	6	82
-5	117	5	152
-4 1/2	315	4 1/2	395
-4	590	4	697
-3 1/2	834	3 1/2	880
-3	891	3	902
-2 1/2	903	2 1/2	901
-2	905	2	910
-1 1/2	899	1 1/2	898
-1	893	1	904
-1/2	901	1/2	903

RUN 60

T_{0_B} = 78, T_{0_C} = 895, x = -6, y = 1/2

z	T	z	T
8	71	8	74
7	72	7	81
-6	88	6	90
-5	220	5	148
-4 1/2	500	4 1/2	359
-4	767	4	632
3 1/2	891	3 1/2	863
-3	927	3	899
-2 1/2	901	2 1/2	897
-2	900	2	903
-1 1/2	889	1 1/2	898
-1	891	1	903
-1/2	900	1/2	903

RUN 58

T_{0_B} = 78, T_{0_C} = 898, x = -6, y = -1 1/2

z	T	z	T
-8	67	8	71
-7	71	7	83
-6	79	6	84
-5	119	5	139
-4 1/2	395	4 1/2	383
-4	685	4	690
-3 1/2	870	3 1/2	880
-3	891	3	900
-2 1/2	901	2 1/2	899
-2	882	2	905
-1 1/2	898	1 1/2	898
-1	894	1	904
-1/2	922	1/2	904

RUN 61

T_{0_B} = 78, T_{0_C} = 895, x = -6, y = 1 1/2

z	T	z	T
-8	72	8	77
-7	73	7	82
-6	87	6	88
-5	184	5	189
-4 1/2	447	4 1/2	284
-4	748	4	536
3 1/2	747	3 1/2	817
3	893	3	897
2 1/2	902	2 1/2	932
-2	902	2	905
-1 1/2	897	1 1/2	899
-1	888	1	904
1/2	866	1/2	904

RUN 62

T_{0_B} = 78, T_{0_C} = 895, x = -6, y = 2 1/2

z	T	z	T
8	71	8	74
7	73	7	82
6	79	6	82
5	273	5	130
4 1/2	551	4 1/2	323
4	897	4	543
3 1/2	869	3 1/2	762
3	890	3	880
2 1/2	901	2 1/2	896
2	902	2	905
1 1/2	898	1 1/2	899
1	890	1	903
1/2	900	1/2	904

RUN 63

T_{0_B} = 78, T_{0_C} = 896, x = -6, y = 3 1/2

z	T	z	T
-8	76	8	79
-7	72	7	85
-6	76	6	81
-5	112	5	91
-4 1/2	221	4 1/2	133
-4	455	4	306
-3 1/2	757	3 1/2	593
-3	877	3	796
2 1/2	843	2 1/2	815
2	890	2	810
-1 1/2	888	1 1/2	820
-1	875	1	850
-1/2	879	1/2	870

RUN 64

T_{0_B} = 78, T_{0_C} = 901, x = -6, y = 4 1/2

z	T	z	T
-8	74	8	78
-7	73	7	84
-6	79	6	82
-5	114	5	103
-4 1/2	307	4 1/2	249
-4	558	4	417
-3 1/2	685	3 1/2	467
-3	681	3	421
-2 1/2	667	2 1/2	390
-2	642	2	417
-1 1/2	658	1 1/2	473
-1	648	1	541
-1/2	632	1/2	588

RUN 65

T_{0_B} = 77.5, T_{0_C} = 904, x = -16, y = 4 1/2

z	T	z	T
8	71.3	8	78.7
7	71.3	7	81.9
6	75.5	6	80.8
5	86.2	5	89.4
4 1/2	192	4 1/2	157
4	510	4	394
3 1/2	613	3 1/2	396
3	554	3	323
2 1/2	555	2 1/2	297
2	522	2	323
1 1/2	541	1 1/2	356
-1	538	1	419
-1/2	524	1/2	471

RUN 66

T_{0_B} = 77, T_{0_C} = 904, x = -16, y = 3 1/2

z	T	z	T
-8	71.3	8	74.5
-7	71.3	7	84.0
-6	75.5	6	76.6
-5	85.1	5	84.0
-4 1/2	131	4 1/2	88.3
-4	322	4	237
-3 1/2	708	3 1/2	571
-3	888	3	822
-2 1/2	903	2 1/2	812
-2	898	2	812
-1 1/2	901	1 1/2	819
-1	896	1	860
-1/2	900	1/2	890

RUN 67

T_{0_B} = 77, T_{0_C} = 904, x = -16, y = 2 1/2

z	T	z	T
-8	73.4	8	75.5
-7	73.4	7	85.1
-6	80.8	6	80.8
-5	131	5	90.4
-4 1/2	429	4 1/2	211
-4	721	4	503
-3 1/2	870	3 1/2	776
-3	899	3	894
-2 1/2	910	2 1/2	906
-2	913	2	915
-1 1/2	913	1 1/2	912
-1	907	1	920
-1/2	918	1/2	922

RUN 68

T_{0_B} = 77, T_{0_C} = 904, x = -16, y = 1 1/2

z	T	z	T
-8	73.4	8	74.5
-7	73.4	7	83.0
-6	87.2	6	85.1
-5	122	5	96.8
-4 1/2	333	4 1/2	197
-4	704	4	499
-3 1/2	889	3 1/2	898
-3	896	3	902
-2 1/2	910	2 1/2	903
-2	911	2	915
-1 1/2	910	1 1/2	911
-1	906	1	921
-1/2	915	1/2	919

RUN 69

T_{0_B} = 77, T_{0_C} = 904, x = -16, y = 1/2

z	T	z	T
-8	69.1	8	72.3
-7	73.4	7	81.9
-6	86.2	6	87.2
-5	126	5	104
-4 1/2	365	4 1/2	272
-4	733	4	615
-3 1/2	888	3 1/2	879
-3	894	3	902
-2 1/2	905	2 1/2	902
-2	906	2	912
-1 1/2	904	1 1/2	906
-1	905	1	914
-1/2	910	1/2	913

RUN 70

T_{0_B} = 77, T_{0_C} = 904, x = -16, y = 1/2

z	T	z	T
-8	66.0	8	69.1
-7	74.5	7	79.8
-6	83.0	6	85.1
-5	112	5	110
-4 1/2	313	4 1/2	318
-4	676	4	670
-3 1/2	885	3 1/2	891
-3	894	3	904
-2 1/2	908	2 1/2	904
-2	910	2	915
-1 1/2	910	1 1/2	912
-1	907	1	919
-1/2	917	1/2	919

RUN 71

T_{0_B} = 77, T_{0_C} = 904, x = -16, y = 1 1/2

z	T	z	T
8	64.9	8	68.1
7	72.3	7	75.5
6	73.4	6	79.8
5	91.5	5	72.3
4 1/2	239	4 1/2	319
4	589	4	674
3 1/2	863	3 1/2	895
3	900	3	911
2 1/2	912	2 1/2	911
2	913	2	919
-1 1/2	913	1 1/2	916
-1	911	1	923
-1/2	922	1/2	924

RUN 72

T_{0_B} = 77, T_{0_C} = 905, x = -16, y = -2 1/2

z	T	z	T
-8	66.0	8	69.1
-7	70.2	7	71.3
-6	69.1	6	73.4
-5	79.8	5	93.6
-4 1/2	168	4 1/2	290
-4	473	4	662
-3 1/2	802	3 1/2	900
-3	902	3	912
-2 1/2	912	2 1/2	913
-2	915	2	921
-1 1/2	915	1 1/2	918
-1	912	1	926
-1/2	922	1/2	926

RUN 73

T_{0_B} = 77, T_{0_C} = 907, x = -16, y = 3 1/2

z	T	z	T
-8	66.0	8	68.1
-7	68.1	7	69.2
-6	68.1	6	73.4
-5	111	5	90.4
-4 1/2	136	4 1/2	308
-4	472	4	655
-3 1/2	817	3 1/2	917
-3	902	3	914
-2 1/2	916	2 1/2	916
-2	917	2	924
-1 1/2	917	1 1/2	920
-1	914	1	928
-1/2	924	1/2	928

RUN 74

T_{0_B} = 77, T_{0_C} = 907, x = -16, y = -4 1/2

z	T	z	T
8	66.0	8	66.0
7	69.2	7	69.2
-6	70.2	6	79.8
5	75.5	5	88.3
-4 1/2	114	4 1/2	158
-4	352	4	390
-3 1/2	649	3 1/2	729
3	679	3	716
-2 1/2	664	2 1/2	724
-2	665	2	734
-1 1/2	650	1 1/2	756
-1	679	1	786
1/2	735	1/2	784

RUN 75

T_{0_B} = 77, T_{0_C} = 908, x = -16, y = -5 1/2

z	T	z	T
-8	67.0	8	68.1
-7	71.3	7	71.3
-6	74.5	6	78.7
-5	75.5	5	107
-4 1/2	117	4 1/2	190
-4	211	4	347
-3 1/2	267	3 1/2	337
-3	184	3	242
-2 1/2	188	2 1/2	248
-2	196	2	253
-1 1/2	188	1 1/2	269
-1	217	1	285
-1/2	249	1/2	285

RUN 76

T_{0_B} = 76.5, T_{0_C} = 910, x = -16, y = -6 1/2

z	T	z	T
-8	67.0	8	67.0
-7	72.4	7	71.3
-6	75.5	6	75.5
-5	74.5	5	83.0
-4 1/2	86.2	4 1/2	74.5
-4	74.5	4	75.5
-3 1/2	72.4	3 1/2	74.5
3	76.6	3	76.6
-2 1/2	79.8	2 1/2	76.6
-2	75.5	2	76.6
-1 1/2	76.6	1 1/2	76.6
-1	75.5	1	77.7
-1/2	75.0	1/2	75.8

RUN 77

T_{0_B} = 76.5, T_{0_C} = 906, x = -16, y = -1/2

z	T	z	T
8	68.1	8	68.1
-7	69.2	7	76.6
-6	76.6	6	79.8
5	101	5	99.0
4 1/2	246	4 1/2	240
-4	584	4	583
-3 1/2	864	3 1/2	871
3	896	3	908
2 1/2	911	2 1/2	911
-2	912	2	916
-1 1/2	911	1 1/2	914
-1	909	1	921
1/2	920	1/2	921

RUN 78

T_{0_B} = 78, T_{0_C} = 104, x = 0, y = -1/2

z	T	z	T
-8	65	8	66
-7	67	7	62
-6	62	6	64
-5	66	5	66
-4 1/2	71	4 1/2	57.5
-4	58.5	4	56
-3 1/2	57.5	3 1/2	58.5
-3	59.5	3	59.5
-2 1/2	59.5	2 1/2	59.5
-2	58.5	2	58.5
-1 1/2	59.5	1 1/2	56
-1	59.5	1	64
-1/2	58	1/2	57

RUN 79

T_{0_B} = 77, T_{0_C} = 800, x = 0, y = -1/2

z	T	z	T
-8	69	8	69
-7	68	7	73
-6	78	6	81
-5	170	5	187
-4 1/2	361	4 1/2	385
-4	605	4	606
-3 1/2	760	3 1/2	764
-3	782	3	790
-2 1/2	790	2 1/2	788
-2	787	2	793
1 1/2	786	1 1/2	787
-1	782	1	793
1/2	788	1/2	790

RUN 80

T_{0_S} = 77, T_{0_C} = 906, x = 0, y = 1/2

z	T	z	T
-8	68	8	71
-7	67	7	78
-6	80	6	85
-5	196	5	211
-4 1/2	415	4 1/2	435
-4	675	4	670
-3 1/2	858	3 1/2	859
-3	884	3	892
-2 1/2	897	2 1/2	896
-2	892	2	897
-1 1/2	891	1 1/2	888
-1	883	1	896
-1/2	890	1/2	891

RUN 81

T_{0_S} = 77, T_{0_C} = 913, x = 6, y = 1/2

z	T	z	T
-8	67	8	67
-7	68	7	77
-6	80	6	84
-5	232	5	256
-4 1/2	440	4 1/2	417
-4	662	4	622
-3 1/2	827	3 1/2	816
-3	878	3	886
-2 1/2	898	2 1/2	888
-2	897	2	900
-1 1/2	900	1 1/2	896
-1	894	1	904
-1/2	907	1/2	905

RUN 82

T_{0_S} = 77, T_{0_C} = 915, x = 6, y = 1/2

z	T	z	T
-8	70	8	64
-7	68	7	74
-6	85	6	96
-5	255	5	193
-4 1/2	479	4 1/2	373
-4	351	4	574
-3 1/2	849	3 1/2	784
-3	884	3	883
-2 1/2	904	2 1/2	896
-2	904	2	904
-1 1/2	904	1 1/2	900
-1	901	1	911
-1/2	909	1/2	912

RUN 83

T_{0_S} = 77, T_{0_C} = 918, x = 6, y = 1 1/2

z	T	z	T
-8	70	8	70
-7	69	7	76
-6	81	6	91
-5	234	5	161
-4 1/2	457	4 1/2	297
-4	691	4	500
-3 1/2	849	3 1/2	724
-3	886	3	865
-2 1/2	904	2 1/2	893
-2	904	2	901
-1 1/2	905	1 1/2	900
-1	898	1	911
-1/2	907	1/2	911

RUN 84

T_{0_S} = 76.5, T_{0_S} = 919, x = 6, y = 2 1/2

z	T	z	T
-8	71	8	73
-7	69	7	81
-6	80	6	85
-5	331	5	174
-4 1/2	552	4 1/2	335
-4	728	4	499
-3 1/2	844	3 1/2	682
-3	886	3	830
-2 1/2	906	2 1/2	885
-2	905	2	903
-1 1/2	905	1 1/2	903
-1	898	1	912
-1/2	907	1/2	910

RUN 85

T_{0_S} = 76.5, T_{0_C} = 921, x = 6, y = 3 1/2

z	T	z	T
-8	70	8	74
-7	66	7	86
-6	71	6	80
-5	167	5	101
-4 1/2	301	4 1/2	187
-4	478	4	331
-3 1/2	700	3 1/2	538
-3	855	3	719
-2 1/2	897	2 1/2	776
-2	887	2	783
-1 1/2	889	1 1/2	784
-1	879	1	815
-1/2	876	1/2	847

RUN 86

T_{0_H} = 76.5, T_{0_C} = 924, x = 6, y = 4 1/2

z	T	z	T
8	68	8	76
7	67	7	84
6	69	6	77
5	135	5	135
-4 1/2	327	4 1/2	263
-4	510	4	368
3 1/2	636	3 1/2	417
-3	653	3	401
-2 1/2	632	2 1/2	359
-2	598	2	372
-1 1/2	613	1 1/2	413
-1	596	1	473
-1/2	578	1/2	525

RUN 89

T_{0_H} = 77, T_{0_C} = 928, x = 6, y = 5 1/2

z	T	z	T
8	59	8	68
7	64	7	67
6	62	6	74
5	128	5	234
-4 1/2	301	4 1/2	451
-4	511	4	679
3 1/2	739	3 1/2	854
3	868	3	903
2 1/2	909	2 1/2	905
-2	906	2	915
-1 1/2	908	1 1/2	906
-1	904	1	919
-1/2	918	1/2	916

RUN 87

T_{0_H} = 76.5, T_{0_C} = 925, x = 6, y = -1 1/2

z	T	z	T
-8	60.6	8	63.9
-7	65	7	79.7
-6	71.3	6	79.7
-5	188	5	213
-4 1/2	353	4 1/2	413
-4	604	4	626
-3 1/2	798	3 1/2	820
-3	897	3	898
-2 1/2	908	2 1/2	898
-2	908	2	909
-1 1/2	908	1 1/2	903
-1	903	1	918
-1/2	918	1/2	914

RUN 90

T_{0_H} = 77, T_{0_C} = 929, x = 6, y = -4 1/2

z	T	z	T
-8	62	8	66
-7	63	7	63
-6	63	6	75
-5	117	5	159
-4 1/2	287	4 1/2	344
-4	517	4	531
-3 1/2	691	3 1/2	691
-3	686	3	725
-2 1/2	658	2 1/2	732
-2	646	2	745
-1 1/2	676	1 1/2	758
-1	666	1	772
-1/2	722	1/2	773

RUN 88

T_{0_H} = 77, T_{0_C} = 926, x = 6, y = -2 1/2

z	T	z	T
-8	62	8	69
-7	64	7	76
-6	64	6	74
-5	132	5	196
-4 1/2	303	4 1/2	405
-4	504	4	634
-3 1/2	721	3 1/2	817
-3	862	3	902
-2 1/2	908	2 1/2	902
-2	906	2	915
-1 1/2	910	1 1/2	905
-1	906	1	920
-1/2	918	1/2	915

RUN 91

T_{0_H} = 77, T_{0_C} = 924, x = 6, y = 5 1/2

z	T	z	T
-8	63	8	67
-7	64	7	65
-6	68	6	73
-5	97	5	157
-4 1/2	223	4 1/2	279
-4	349	4	388
-3 1/2	353	3 1/2	419
-3	283	3	372
-2 1/2	264	2 1/2	368
-2	271	2	384
-1 1/2	284	1 1/2	400
-1	316	1	421
-1/2	362	1/2	11

RUN 92

T_{0_B} = 77, T_{0_C} = 923, x = 0, y = -1/2

z	T	z	T
8	76	8	66
7	94	7	65
6	104	6	74
-5	170	5	135
-4 1/2	264	4 1/2	176
-4	295	4	195
-3 1/2	257	3 1/2	139
-3	175	3	133
-2 1/2	171	2 1/2	128
-2	172	2	126
-1 1/2	170	1 1/2	126
-1	191	1	131
-1/2	107	1/2	119

RUN 95

T_{0_B} = 77, T_{0_C} = 926, x = 0, y = -1/2

z	T	z	T
8	66	8	85
7	66	7	74
6	80	6	87
-5	206	5	209
-4 1/2	426	4 1/2	438
-4	692	4	676
-3 1/2	871	3 1/2	869
-3	897	3	904
-2 1/2	907	2 1/2	903
-2	906	2	909
-1 1/2	903	1 1/2	902
-1	896	1	908
1/2	901	1/2	904

RUN 93

T_{0_B} = 77, T_{0_C} = 924, x = 0, y = -1/2

z	T	z	T
-8	65.9	8	63.8
-7	64.9	7	72.3
-6	77.6	6	85.1
-5	209	5	265
-4 1/2	422	4 1/2	452
-4	686	4	686
-3 1/2	869	3 1/2	869
-3	894	3	903
-2 1/2	905	2 1/2	903
-2	903	2	908
-1 1/2	902	1 1/2	901
-1	896	1	907
-1/2	902	1/2	905

RUN 96

T_{0_B} = 77, T_{0_C} = 928, x = 0, y = 1/2

z	T	z	T
-8	66	8	67
-7	67	7	74
-6	80	6	87
-5	206	5	211
-4 1/2	425	4 1/2	436
-4	696	4	675
-3 1/2	873	3 1/2	871
-3	899	3	906
-2 1/2	909	2 1/2	905
-2	907	2	912
-1 1/2	905	1 1/2	903
-1	898	1	911
-1/2	903	1/2	906

RUN 94

T_{0_B} = 77, T_{0_C} = 925, x = 0, y = -1/2

z	T	z	T
-8	66	8	67
-7	67	7	74
-6	80	6	86
-5	208	5	213
-4 1/2	426	4 1/2	439
-4	690	4	676
-3 1/2	869	3 1/2	868
-3	895	3	903
-2 1/2	906	2 1/2	902
-2	903	2	908
-1 1/2	902	1 1/2	900
-1	895	1	907
-1/2	900	1/2	902

RUN 97

T_{0_B} = 77, T_{0_C} = 925, x = 0, y = -1/2

z	T	z	T
8	66	8	66
-7	67	7	78
-6	79	6	87
-5	206	5	211
-4 1/2	423	4 1/2	437
-4	693	4	676
-3 1/2	870	3 1/2	868
-3	896	3	904
-2 1/2	907	2 1/2	902
-2	904	2	907
-1 1/2	902	1 1/2	900
-1	895	1	907
-1/2	900	1/2	903

[illegible]

T_{0_B} = 77.5, T_{0_C} = 908, x = 0, y = -1/2

z	T	z	T
8	67	8	65
7	67	7	71
6	80	6	85
-5	207	5	211
4 1/2	423	4 1/2	431
4	688	4	666
-3 1/2	856	3 1/2	851
-3	880	3	887
-2 1/2	890	2 1/2	886
-2	887	2	889
-1 1/2	886	1 1/2	883
-1	878	1	889
-1/2	886	1/2	887

RUN 101

T_{0_B} = 76.5, T_{0_C} = 917, x = 13.9, y = -1/2

z	T	z	T

Unable to obtain data due to unsteady conditions.

1 1/2	902		
-1	919		
-1/2	934	1/2	936

RUN 99

T_{0_B} = 76.5, T_{0_C} = 914, x = 13.9, y = -1/2

z	T	z	T

Unable to obtain data due to unsteady conditions.

-2	807	2	528
-1 1/2	905	1 1/2	682
-1	918	1	829
-1/2	937	1/2	915

RUN 102

T_{0_B} = 76.5, T_{0_C} = 917, x = 8, y = -1/2

z	T	z	T
-8	61	8	63
-7	59	7	55
-6	61	6	78
-5	171	5	167
-4 1/2	384	4 1/2	383
-4	626	4	594
-3 1/2	811	3 1/2	796
-3	870	3	879
-2 1/2	888	2 1/2	886
-2	893	2	898
-1 1/2	901	1 1/2	896
-1	895	1	907
-1/2	902	1/2	905

RUN 100

T_{0_B} = 76.5, T_{0_C} = 914, x = 13.9, y = -2 1/2

z	T	z	T

Unable to obtain data due to unsteady conditions.

-2	888	2	909
-1 1/2	901	1 1/2	909
-1	917	1	924
-1/2	931	1/2	937

RUN 103

T_{0_B} = 77.5, T_{0_C} = 805, x = 0, y = -1/2

z	T	z	T
-8	62	8	62
-7	67	7	70
-6	72	6	74
-5	185	5	181
-4 1/2	394	4 1/2	386
-4	638	4	594
-3 1/2	764	3 1/2	758
-3	773	3	785
-2 1/2	783	2 1/2	783
-2	779	2	784
-1 1/2	779	1 1/2	782
-1	771	1	784
-1/2	777	1/2	786

RUN 104

T_{0_H} = 77.5, T_{0_C} = 810, x = 0, y = 2 1/2

z	T	z	T
8	67	8	70
7	71	7	70
6	75	6	75
5	265	5	138
4 1/2	492	4 1/2	302
4	662	4	465
3 1/2	759	3 1/2	643
3	781	3	757
2 1/2	769	2 1/2	775
2	787	2	780
1 1/2	787	1 1/2	774
1	783	1	781
1/2	790	1/2	790

RUN 107

T_{0_H} = 74, T_{0_C} = 797, x = 0, y = 1/2

z	T	z	T
8	57	8	57
7	57	7	61
6	56	6	67
5	71	5	69
4 1/2	67	4 1/2	67
4	84	4	80
3 1/2	166	3 1/2	151
3	317	3	301
2 1/2	498	2 1/2	472
2	656	2	638
1 1/2	764	1 1/2	744
1	786	1	813
-1/2	800	1/2	780

RUN 105

T_{0_H} = 77.5, T_{0_C} = 800, x = 0, y = 3 1/2

z	T	z	T
8	57	8	61
7	62	7	56
6	59	6	66
5	113	5	197
4 1/2	292	4 1/2	80
4	519	4	635
3 1/2	704	3 1/2	755
3	756	3	768
2 1/2	768	2 1/2	765
2	766	2	771
1 1/2	767	1 1/2	765
1	764	1	774
1/2	771	1/2	777

RUN 108

T_{0_H} = 73, T_{0_C} = 804, x = 0, y = 1/2

z	T	z	T
8	61.1	8	60
7	60	7	62.2
6	58.9	6	69
5	74.7	5	71.3
4 1/2	75.8	4 1/2	69
4	101	4	736
3 1/2	197	3 1/2	117
3	352	3	234
2 1/2	547	2 1/2	411
2	695	2	584
1 1/2	783	1 1/2	715
1	795	1	793
1/2	808	1/2	813

RUN 106

T_{0_H} = 77.5, T_{0_C} = 802, x = 16, y = 1/2

z	T	z	T
8	56	8	59
7	61	7	65
6	65	6	70
5	98	5	101
4 1/2	280	4 1/2	396
4	603	4	608
3 1/2	757	3 1/2	764
3	763	3	772
2 1/2	773	2 1/2	771
2	774	2	781
1 1/2	779	1 1/2	774
1	773	1	787
1/2	782	1/2	786

RUN 109

T_{0_H} = 73.5, T_{0_C} = 806, x = 0, y = 1 1/2

z	T	z	T
8	61	8	62
7	58	7	62
6	58	6	69
5	80	5	87
4 1/2	107	4 1/2	137
4	153	4	175
3 1/2	257	3 1/2	212
3	404	3	294
2 1/2	594	2 1/2	447
2	729	2	598
1 1/2	756	1 1/2	724
1	795	1	793
1/2	806	1/2	812

RUN 110

T_{0_B} = 73.5, T_{0_C} = 808, x = 0, y = 2 1/2

z	T	z	T
8	59	8	61
7	57	7	66
6	58	6	69
5	171	5	153
4 1/2	268	4 1/2	272
4	356	4	350
-3 1/2	462	3 1/2	419
-3	586	3	500
-2 1/2	707	2 1/2	608
-2	756	2	348
-1 1/2	776	1 1/2	723
-1	770	1	731
-1/2	771	1/2	744

RUN 111

T_{0_B} = 73.5, T_{0_C} = 809, x = 0, y = 3 1/2

z	T	z	T
-8	58	8	59
-7	57	7	66
-6	58	6	64
-5	201	5	120
-4 1/2	340	4 1/2	214
-4	446	4	299
-3 1/2	508	3 1/2	371
-3	529	3	417
-2 1/2	519	2 1/2	401
-2	491	2	381
-1 1/2	507	1 1/2	364
-1	508	1	376
-1/2	504	1/2	430

RUN 112

T_{0_B} = 73.5, T_{0_C} = 810, x = -16, y = -1/2

z	T	z	T
-8	55.5	8	56.6
-7	56.6	7	65.6
-6	56.6	6	69
-5	70.2	5	69
-4 1/2	66.8	4 1/2	69
-4	80.4	4	80.4
-3 1/2	192.5	3 1/2	198
-3	458	3	470
-2 1/2	713	2 1/2	713
-2	766	2	799
-1 1/2	805	1 1/2	798
-1	798	1	810
-1/2	810	1/2	818

RUN 113

T_{0_B} = 73.5, T_{0_C} = 812, x = -16, y = 2 1/2

z	T	z	T
-3	664	3	611
-2 1/2	751	2 1/2	716
-2	735	2	714
-1 1/2	740	1 1/2	673
-1	741	1	676
1/2	746	1/2	711

APPENDIX F

PRESSURE AND MACH NUMBER DATA

A complete table of pitot pressure to core stagnation pressure ratios, $^{P}p/p_{0_c}$, and Mach numbers computed on the Bendix G-15 computer from pressure data taken in the calibration tests of the NSL Heated Core Installation is presented in this appendix. The Mach number was computed from the ratio $^{P}p/p_{0_c}$ divided by 0.98, the correction factor for this ratio which accounts for caloric imperfections at T_{0_c} = 900°F and M = 3.5 (Reference 10). All runs were conducted with the Mach 3.5 nozzle blocks, with the exception of runs 107-113 which were conducted with the Mach 3.0 nozzle blocks.

The following summary of core stagnation pressures and ratios of cold stream stagnation pressure to core stagnation pressure, $^{p_{0_s}}/p_{0_c}$, for each wind tunnel run is presented for use in conjunction with the table.

Run	p_{0_c}	$^{p_{0_s}}/p_{0_c}$
1-4	5.90	1.00
5-31	5.95	1.00
32-42	5.90	1.00
43-45	5.95	1.00
46-76	5.90	1.00
77	5.60	1.05
78	5.20	1.00
79	5.65	1.00
80-92	5.90	1.00
93	5.90	0.90
94	5.90	0.96
95	5.90	0.98
96	5.90	1.02
97	5.90	1.04
98	5.90	1.06
99-102	5.90	1.00
103-113	5.65	1.00

The following table employs the "floating decimal" system, based upon the prefix 50 representing the decimal point as it stands (i.e. a prefix 51 indicates the decimal point should be shifted one place to the right, etc.) Based upon the accuracies stated in section 7.2.2 the data should be considered valid to three significant figures only.

PRESSURE AND MACH NUMBER DATA

Run	x	y	z	P_p P_{o_1}	M	Run	x	y	z	P_p P_{o_1}	M
1	0	1/2	8	50.18152	51.36615	5	0	1 1/2	8	50.18653	51.36424
			7	50.21473	51.34670				7	50.20810	51.35032
			6	50.20328	51.35304				6	50.20641	51.35239
			5	50.17865	51.36796				5	50.20157	51.35401
			4	50.18896	51.36144				4	50.18709	51.36262
			3	50.19583	51.35708				3	50.19646	51.35698
			2	50.18782	51.36216				2	50.18823	51.36190
			1	50.17407	51.37086				1	50.17375	51.37107
			0	50.17064	51.37304				0	50.17091	51.37287
			-1	50.17293	51.37159				-1	50.17261	51.37179
			-2	50.18782	51.36216				-2	50.18794	51.36208
			-3	50.19870	51.35567				-3	50.19873	51.35565
			-4	50.21301	51.34762				-4	50.21179	51.34829
			-5	50.17121	51.37268				-5	50.17034	51.37323
			-6	50.20041	51.35468				-6	50.20157	51.35401
			-7	50.21358	51.34732				-7	50.21009	51.34923
			-8	50.15747	51.38272				-8	50.13627	51.39964
2	0	-1/2	8	49.80166	51.46408	6	0	-3 1/2	8	50.211	51.349
			7	50.27485	51.31825				7	50.209	51.350
			6	50.27371	51.31878				6	50.1985	51.356
			5	50.18953	51.36107				5	50.174	51.371
			4	50.19297	51.35890				4	50.1824	51.366
			3	50.19812	51.35601				3	50.1805	51.367
			2	50.18839	51.36180				2	50.1715	51.373
			1	50.17465	51.37050				1	50.1685	51.375
			0	50.17293	51.37159				0	50.1865	51.363
			-1	50.17407	51.37086				-1	50.1715	51.373
			-2	50.19068	51.36033				-2	50.1775	51.369
			-3	50.19812	51.35601				-3	50.1875	51.362
			-4	50.21072	51.34887				-4	50.1835	51.365
			-5	50.17865	51.36796				-5	50.1835	51.365
			-6	50.26054	51.32441				-6	50.205	51.352
			-7	50.27027	51.32019				-7	50.2075	51.3505
			-8	49.84746	51.45720				-8	50.2085	51.350
3	0	-1 1/2	8	49.58406	51.50173	7	0	4 1/2	8	50.21576	51.34614
			7	50.25710	51.32595				7	50.21463	51.34675
			6	50.31494	51.30249				6	50.20498	51.35207
			5	50.21416	51.34701				5	50.13230	51.40310
			4	50.19812	51.35601				4	50.18056	51.36676
			3	50.19755	51.35634				3	50.17602	51.36963
			2	50.18667	51.36289				2	50.17204	51.37215
			1	50.17522	51.37014				1	50.18056	51.36676
			0	50.17808	51.36833				0	50.17886	51.36783
			-1	50.17579	51.36978				-1	50.16466	51.37750
			-2	50.18782	51.36216				-2	50.16239	51.37912
			-3	50.20099	51.35435				-3	50.17318	51.37143
			-4	50.20958	51.34951				-4	50.18170	51.36604
			-5	50.21015	51.34919				-5	50.18794	51.36208
			-6	50.30577	51.30592				-6	50.21065	51.34891
			-7	50.25481	51.32676				-7	50.22258	51.34254
			-8	49.52108	51.51948				-8	50.21917	51.34433
4	0	-2 1/2	8	49.66995	51.48649	8	0	5 1/2	8	50.22258	51.34254
			7	50.27600	51.31777				7	50.22087	51.34343
			6	50.31265	51.30334				6	50.20952	51.34954
			5	50.21473	51.34670				5	50.19021	51.36064
			4	50.19755	51.35634				4	50.17829	51.36819
			3	50.19068	51.36035				3	50.16296	51.37872
			2	50.18209	51.36579				2	50.16012	51.38077
			1	50.17694	51.36905				1	50.16864	51.37472
			0	50.19182	51.35962				0	50.16637	51.37630
			-1	50.17636	51.36941				1	50.16523	51.37710
			-2	50.18782	51.36216				-2	50.15955	51.38118
			-3	50.19641	51.35702				-3	50.16296	51.37872
			-4	50.19125	51.35999				4	50.17886	51.36783
			-5	50.22332	51.34215				-5	50.19532	51.35741
			-6	50.30749	51.30527				-6	50.21236	51.34798
			-7	50.26054	51.32441				-7	50.22258	51.34254
			-8	49.56116	51.50877				-8	50.22428	51.34166

Run	x	y	z	P_p/P_{o_c}	M	Run	x	y	z	P_p/P_{o_c}	M
9	0	1 1/2	8	50.19816	51.35598	14	0		8	50.21633	51.34584
			7	50.21406	51.34706				7	50.21463	51.34675
			6	50.20469	51.35223				6	50.20327	51.35304
			5	50.18397	51.36460				5	50.18567	51.36352
			4	50.18170	51.36604				4	50.17375	51.37107
			3	50.19759	51.35632				3	50.16523	51.37710
			2	50.18084	51.36658				2	50.15955	51.38118
			1	50.17431	51.37071				1	50.16466	51.37750
			0	50.17829	51.36819				0	50.16409	51.37791
			-1	50.17431	51.37071				-1	50.16637	51.37630
			-2	50.18567	51.36352				-2	50.15671	51.38328
			-3	50.19759	51.35632				-3	50.16353	51.37831
			-4	50.21207	51.34813				-4	50.17772	51.36855
			-5	50.17545	51.36999				-5	50.18453	51.36424
			-6	50.19986	51.35499				-6	50.20214	51.35368
			-7	50.21349	51.34776				-7	50.21917	51.34433
			8	50.18964	51.36100				8	50.21917	51.34433
10	0	2 1/2	8	50.21179	51.34829	14	0	5 1/2	8	50.22087	51.34343
			7	50.21463	51.34675				7	50.21974	51.34403
			6	50.20498	51.35207				6	50.20498	51.35207
			5	50.18425	51.36442				5	50.19532	51.35741
			4	50.18397	51.36460				4	50.17999	51.36712
			3	50.19305	51.35885				3	50.18056	51.36676
			2	50.18737	51.36244				2	50.17204	51.37215
			1	50.17375	51.37107				1	50.17375	51.37107
			0	50.19021	51.36064				0	50.17034	51.37323
			-1	50.17545	51.36999				-1	50.17204	51.37215
			-2	50.18453	51.36424				-2	50.16069	51.38036
			-3	50.19305	51.35885				-3	50.16523	51.37710
			-4	50.19674	51.35682				-4	50.17659	51.36927
			-5	50.19021	51.36064				-5	50.19248	51.35920
			-6	50.19561	51.35723				-6	50.20668	51.35112
			-7	50.21463	51.34675				-7	50.22258	51.34254
			-8	50.20923	51.34969				-8	50.22428	51.34166
11	0	3 1/2	8	50.26800	51.32116	15	0	6	8	50.22201	51.34283
			7	50.21179	51.34829				7	50.224	51.343
			6	50.20412	51.35256				6	50.21	51.349
			5	50.19362	51.35849				5	50.201	51.354
			4	50.17318	51.37143				4	50.188	51.362
			3	50.18964	51.36100				3	50.188	51.362
			2	50.18198	51.36586				2	50.1815	51.366
			1	50.17744	51.36873				1	50.187	51.363
			0	50.19419	51.35813				0	50.1815	51.366
			-1	50.18113	51.36640				1	50.181	51.366
			-2	50.18397	51.36460				2	50.1685	51.375
			-3	50.19362	51.35849				3	50.173	51.372
			-4	50.17602	51.36963				4	50.1775	51.369
			-5	50.19447	51.35795				5	50.1925	51.359
			-6	50.20384	51.35272				6	50.211	51.349
			-7	50.20753	51.35064				7	50.224	51.341
			-8	50.21122	51.34860				8	50.226	51.341
12	0	4 1/2	8	50.21747	51.34523	16	0	1/2	8	50.18453	51.36424
			7	50.21236	51.34798				7	50.20838	51.35017
			6	50.20668	51.35112				6	50.20554	51.35175
			5	50.18737	51.36244				5	50.18113	51.36640
			4	50.17829	51.36819				4	50.18908	51.36136
			3	50.16466	51.37750				3	50.19816	51.35598
			2	50.16012	51.38077				2	50.19021	51.36064
			1	50.17148	51.37251				1	50.17545	51.36999
			0	50.17659	51.36927				0	50.17261	51.37179
			-1	50.17545	51.36999				1	50.17431	51.37071
			-2	50.16750	51.37551				2	50.19021	51.36064
			-3	50.17602	51.36963				3	50.20043	51.35467
			-4	50.18113	51.36640				4	50.21406	51.34706
			-5	50.16340	51.36500				5	50.172	51.372
			-6	50.21009	51.34923				6	50.2025	51.353
			-7	50.218	51.345				7	50.2105	51.349
			-8	50.1933	51.363				8	50.1405	51.406

Run	x	y	z	P_0	M
17	0	1/2	8	50.19419	51.35813
			7	50.20668	51.35112
			6	50.19930	51.35532
			5	50.17772	51.36855
			4	50.19192	51.35956
			3	50.19816	51.35598
			2	50.18908	51.36136
			1	50.17431	51.37071
			0	50.17261	51.37179
			-1	50.17375	51.37107
			-2	50.19078	51.36028
			-3	50.19930	51.35532
			-4	50.21122	51.34860
			-5	50.17148	51.37251
			-6	50.20214	51.35368
			-7	50.21292	51.34767
			-8	50.17602	51.36963
18	0	-1 1/2	6	50.207	51.351
			7	50.209	51.35
			6	50.201	51.354
			5	50.1765	51.369
			4	50.19362	51.35849
			3	50.19703	51.35665
			2	50.18624	51.36316
			1	50.17431	51.37071
			0	50.17659	51.36927
			-1	50.17545	51.36999
			-2	50.18737	51.36244
			-3	50.20	51.355
			-4	50.207	51.351
			-5	50.177	51.369
			-6	50.199	51.356
			-7	50.21	51.349
			-8	50.193	51.359
19	0	-2 1/2	8	50.20952	51.34954
			7	50.21179	51.34829
			6	50.20157	51.35401
			5	50.17715	51.36891
			4	50.19505	51.35885
			3	50.19078	51.36028
			2	50.18170	51.36604
			1	50.17715	51.36891
			0	50.18964	51.36100
			-1	50.17602	51.36963
			-2	50.18737	51.36244
			-3	50.19703	51.35665
			-4	50.18908	51.36136
			-5	50.19248	51.35920
			-6	50.19135	51.35992
			-7	50.21179	51.34829
			-8	50.20554	51.35175
20	0	-3	8	50.21065	51.34891
			7	50.21020	51.34916
			6	50.20100	51.35434
			5	50.17488	51.37035
			4	50.18851	51.36172
			3	50.18567	51.36352
			2	50.17886	51.36783
			1	50.17488	51.37035
			0	50.19021	51.36064
			-1	50.17488	51.37035
			-2	50.18397	51.36460
			-3	50.19248	51.35920
			-4	50.18453	51.36424
			-5	50.20100	51.35434
			-6	50.19703	51.35665
			-7	50.21009	51.34923
			-8	50.20838	51.35017

Run	x	y	z	P_0	M
21	0	3 1/2	8	50.21236	51.34798
			7	50.21065	51.34891
			6	50.20100	51.35434
			5	50.17602	51.36963
			4	50.18397	51.36460
			3	50.18170	51.36604
			2	50.17318	51.37143
			1	50.17034	51.37323
			0	50.18681	51.36280
			-1	50.17318	51.37143
			-2	50.17886	51.36783
			-3	50.18908	51.36136
			-4	50.18567	51.36352
			-5	50.18397	51.36460
			-6	50.20725	51.35080
			-7	50.20895	51.34985
			-8	50.21009	51.34923
22	0	4 1/2	8	50.21747	51.34523
			7	50.21520	51.34645
			6	50.20611	51.35143
			5	50.18510	51.36388
			4	50.18226	51.36568
			3	50.17659	51.36927
			2	50.17261	51.37179
			1	50.18056	51.36676
			0	50.17886	51.36783
			-1	50.16580	51.37670
			-2	50.16353	51.37831
			-3	50.17375	51.37107
			-4	50.18283	51.36532
			-5	50.18908	51.36136
			-6	50.212	51.348
			-7	50.2235	51.342
			8	50.22	51.344
23	0	-5 1/2	8	50.22428	51.34166
			7	50.22258	51.34254
			6	50.21179	51.34829
			5	50.19192	51.35956
			4	50.17942	51.36747
			3	50.16409	51.37791
			2	50.16182	51.37953
			1	50.16977	51.37394
			0	50.16864	51.37472
			-1	50.16750	51.37551
			-2	50.16182	51.37953
			-3	50.16637	51.37630
			-4	50.18113	51.36640
			-5	50.19759	51.35632
			-6	50.21406	51.34706
			-7	50.22428	51.34166
			-8	50.22598	51.34078
24	0	5	8	50.21917	51.34433
			7	50.21633	51.34584
			6	50.20	51.35
			5	50.1885	51.36
			4	50.1865	51.369
			3	50.167	51.37
			2	50.162	51.38
			1	50.1675	51.375
			0	50.167	51.37
			-1	50.1675	51.375
			-2	50.18	51.365
			-3	50.1865	51.37
			-4	50.1806	51.362
			-5	50.182	51.363
			-6	50.205	51.352
			-7	50.222	51.343
			-8	50.222	51.343

Run	x	y	z	P_p/P_{o_1}	M	Run	x	y	z	P_p/P_{o_1}	M
25	0	1/2	8	50.18453	51.36424	29	0	1 1/2	8	50.21065	51.34891
			7	50.20781	51.35048				7	50.20895	51.34985
			6	50.20611	51.35143				6	50.19872	51.35565
			5	50.18113	51.36640				5	50.17488	51.37035
			4	50.19021	51.36064				4	50.18170	51.36604
			3	50.19930	51.35532				3	50.18113	51.36640
			2	50.22031	51.34373				2	50.17204	51.37215
			1	50.17659	51.36927				1	50.16920	51.37433
			0	50.17375	51.37107				0	50.18453	51.36424
			-1	50.17602	51.36963				-1	50.17091	51.37287
			-2	50.19192	51.35956				-2	50.17772	51.36855
			-3	50.20157	51.35401				-3	50.18737	51.36244
			-4	50.21576	51.34614				-4	50.18397	51.36460
			-5	50.17261	51.37179				-5	50.18170	51.36604
			-6	50.20327	51.35304				-6	50.20611	51.35143
			-7	50.21065	51.34891				-7	50.20725	51.35080
			-8	50.14025	51.39628				-8	50.20895	51.34985
26	0	-1/2	8	50.19986	51.35499	30	0	-4 1/2	8	50.21747	51.34523
			7	50.21292	51.34767				7	50.21576	51.34614
			6	50.20554	51.35175				6	50.20668	51.35112
			5	50.18453	51.36424				5	50.18510	51.36388
			4	50.19873	51.35565				4	50.18113	51.36640
			3	50.20554	51.35175				3	50.17602	51.36963
			2	50.19646	51.35698				2	50.17204	51.37215
			1	50.18170	51.36604				1	50.18056	51.36676
			0	50.17999	51.36712				0	50.17942	51.36747
			-1	50.18113	51.36640				-1	50.16750	51.37551
			-2	50.19192	51.35956				-2	50.16796	51.37872
			-3	50.19930	51.35532				-3	50.17261	51.37179
			-4	50.21236	51.34798				-4	50.18283	51.36532
			-5	50.17204	51.37215				-5	50.18794	51.36208
			-6	50.20214	51.35368				-6	50.23166	51.33790
			-7	50.21236	51.34798				-7	50.22371	51.34195
			-8	50.17659	51.36927				-8	50.22087	51.34343
27	0	-1 1/2	8	50.20668	51.35112	31	0	-5 1/2	8	50.22371	51.34195
			7	50.20838	51.35017				7	50.22258	51.34254
			6	50.20100	51.35434				6	50.21122	51.34860
			5	50.17829	51.36819				5	50.19135	51.35992
			4	50.19362	51.35849				4	50.17886	51.36783
			3	50.19816	51.35598				3	50.16409	51.37791
			2	50.18794	51.36208				2	50.16182	51.37953
			1	50.17545	51.36999				1	50.17091	51.37287
			0	50.17829	51.36819				0	50.16920	51.37433
			-1	50.17659	51.36927				-1	50.16750	51.37551
			-2	50.18794	51.36208				-2	50.16182	51.37953
			-3	50.20100	51.35434				-3	50.16523	51.37710
			-4	50.20838	51.35017				-4	50.18113	51.36640
			-5	50.17829	51.36819				-5	50.19703	51.35665
			-6	50.19986	51.35499				-6	50.21292	51.34767
			-7	50.21122	51.34860				-7	50.22371	51.34195
			-8	50.19476	51.35777				-8	50.22542	51.34107
28	0	-2 1/2	8	50.20952	51.34954	33	-2	1/2	8	50.19240	51.35926
			7	50.21179	51.34829				7	50.20041	51.35469
			6	50.20157	51.35401				6	50.19812	51.35601
			5	50.17886	51.36783				5	50.17980	51.36724
			4	50.19192	51.35956				4	50.18896	51.36144
			3	50.19192	51.35956				3	50.19812	51.35601
			2	50.18283	51.36532				2	50.18782	51.36216
			1	50.17715	51.36891				1	50.17350	51.37123
			0	50.19078	51.36028				0	50.15919	51.38145
			-1	50.17715	51.36891				-1	50.17121	51.37268
			-2	50.18851	51.36172				-2	50.18553	51.36361
			-3	50.19759	51.35632				-3	50.20041	51.35468
			-4	50.19021	51.36064				-4	50.19641	51.35702
			-5	50.19192	51.35956				-5	50.18553	51.36361
			-6	50.19078	51.36028				-6	50.19526	51.35745
			7	50.21122	51.34860				-7	50.20213	51.35369
			8	50.20554	51.35175				-8	50.13972	51.39672

Run	x	y	z	P_p/P_{p_1}	M	Run	x	y	z	P_p/P_{p_1}	M
34	-2	1/2	8	50.21015	51.34919	38	2	4 1/2	8	50.21759	51.34516
			7	50.20499	51.35206				7	50.20557	51.35174
			6	50.20385	51.35271				6	50.20041	51.35468
			5	50.18724	51.36252				5	50.18667	51.36289
			4	50.18667	51.36289				4	50.17923	51.36760
			3	50.19870	51.35567				3	50.16606	51.37652
			2	50.19182	51.35962				2	50.16205	51.37937
			1	50.18157	51.36611				1	50.16205	51.37937
			0	50.16377	51.37814				0	50.17636	51.36941
			-1	50.18095	51.36651				1	50.16663	51.37612
			-2	50.18953	51.36107				-2	50.17007	51.37374
			-3	50.20213	51.35369				-3	50.17577	51.36978
			-4	50.20041	51.35468				-4	50.18724	51.36500
			-5	50.19411	51.35817				-5	50.18438	51.36434
			-6	50.25825	51.32543				-6	50.20385	51.35271
			-7	50.20671	51.35110				-7	50.21587	51.34608
			-8	50.20671	51.35110				-8	50.22103	51.34335
35	-2	2 1/2	8	50.21702	51.34547	39	-2	5	8	50.21645	51.34577
			7	50.20786	51.35046				7	50.21015	51.34919
			6	50.20499	51.35206				6	50.20270	51.35336
			5	50.18610	51.36325				5	50.18667	51.36289
			4	50.18724	51.36252				4	50.17636	51.36941
			3	50.17007	51.37374				3	50.16606	51.37652
			2	50.18953	51.36107				2	50.16319	51.37855
			1	50.18381	51.36500				1	50.16090	51.38020
			0	50.17178	51.37231				0	50.17350	51.37123
			-1	50.18495	51.36397				-1	50.16377	51.37814
			-2	50.18782	51.36216				-2	50.16720	51.37572
			-3	50.19984	51.35501				-3	50.17121	51.37268
			-4	50.19984	51.35501				-4	50.18209	51.36579
			-5	50.19125	51.35999				-5	50.18381	51.36500
			-6	50.20270	51.35336				-6	50.20499	51.35206
			-7	50.20385	51.35271				-7	50.21301	51.34762
			-8	50.21129	51.34856				-8	50.21988	51.34395
36	-2	3 1/2	8	50.21645	51.34577	40	-2	4 3/4	8	50.21931	51.34425
			7	50.20614	51.35142				7	50.20958	51.34951
			6	50.20156	51.35402				6	50.20499	51.35206
			5	50.19068	51.36035				5	50.18839	51.36180
			4	50.16606	51.37652				4	50.17694	51.36905
			3	50.18896	51.36144				3	50.17121	51.37268
			2	50.17980	51.36724				2	50.16720	51.37572
			1	50.17923	51.36760				1	50.16319	51.37855
			0	50.18953	51.36107				0	50.17350	51.37123
			-1	50.18324	51.36500				-1	50.16319	51.37855
			-2	50.18667	51.36289				-2	50.16663	51.37612
			-3	50.19297	51.35890				-3	50.17007	51.37374
			-4	50.17407	51.37086				-4	50.18037	51.36687
			-5	50.18209	51.36579				-5	50.18610	51.36325
			-6	50.22446	51.34156				-6	50.20900	51.34982
			-7	50.20843	51.35014				-7	50.21187	51.34825
			-8	50.21301	51.34762				-8	50.22275	51.34245
37	-2	4	8	50.21587	51.34608	41	-2	5 1/2	8	50.22275	51.34245
			7	50.20728	51.35078				7	50.21244	51.34794
			6	50.20270	51.35336				6	50.21187	51.34825
			5	50.18896	51.36144				5	50.19526	51.35745
			4	50.17636	51.36941				4	50.18095	51.36651
			3	50.17350	51.37123				3	50.18553	51.36361
			2	50.15976	51.38103				2	50.17808	51.36833
			1	50.16033	51.38061				1	50.17064	51.37304
			0	50.17980	51.36724				0	50.17694	51.36905
			-1	50.17007	51.37374				-1	50.16606	51.37652
			-2	50.17522	51.37014				-2	50.16777	51.37532
			-3	50.18381	51.36500				-3	50.17064	51.37304
			-4	50.17751	51.36869				4	50.17808	51.36833
			-5	50.18553	51.36361				-5	50.19125	51.35999
			-6	50.20213	51.35369				-6	50.21187	51.34825
			-7	50.22046	51.34365				-7	50.21702	51.34547
			-8	50.22103	51.34335				8	50.22504	51.34127

Run	x	y	z	P_p/P_{p_c}	M	Run	x	y	z	P_p/P_{p_c}	M
42	-2	6	8	50.22618	51.34068	46	2	-3 1/2	8	50.21587	51.34608
			7	50.21759	51.34516				7	50.20786	51.35046
			6	50.21015	51.34919				6	50.20385	51.35271
			5	50.20328	51.35304				5	50.17636	51.36941
			4	50.19240	51.35926				4	50.18553	51.36361
			3	50.19469	51.35781				3	50.18381	51.36500
			2	50.19011	51.36071				2	50.17751	51.36869
			1	50.18610	51.36325				1	50.17121	51.37268
			0	50.19125	51.35999				0	50.16548	51.37692
			-1	50.17751	51.36869				-1	50.17064	51.37304
			-2	50.17923	51.36760				-2	50.17751	51.36869
			-3	50.18266	51.36542				-3	50.18782	51.36216
			-4	50.18209	51.36579				-4	50.18381	51.36500
			-5	50.19927	51.35534				-5	50.18209	51.36579
			-6	50.21072	51.34887				-6	50.20614	51.35142
			-7	50.21988	51.34395				-7	50.21358	51.34732
			-8	50.22867	51.33951				-8	50.21473	51.34670
43	-2	-1/2	8	50.20441	51.35239	47	-2	-2 3/4	8	50.21187	51.34825
			7	50.20100	51.35434				7	50.20328	51.35304
			6	50.19986	51.35499				6	50.19812	51.35601
			5	50.17602	51.36963				5	50.17293	51.37159
			4	50.19419	51.35813				4	50.18667	51.36289
			3	50.20043	51.35467				3	50.18553	51.36361
			2	50.18908	51.36136				2	50.17579	51.36978
			1	50.17488	51.37035				1	50.17465	51.37050
			0	50.16239	51.37912				0	50.15690	51.38315
			-1	50.17602	51.36963				-1	50.17407	51.37086
			-2	50.19192	51.35956				-2	50.17808	51.36833
			-3	50.20498	51.35207				-3	50.18782	51.36216
			-4	50.19873	51.35565				-4	50.17923	51.36760
			-5	50.18737	51.36244				-5	50.17865	51.36796
			-6	50.19930	51.35532				-6	50.20786	51.35046
			-7	50.20327	51.35304				-7	50.19469	51.35781
			-8	50.19192	51.35956				-8	50.20843	51.35014
44	-2	-1 1/2	8	50.21009	51.34923	48	-2	-3	8	50.21358	51.34732
			7	50.20214	51.35368				7	50.20499	51.35206
			6	50.20117	51.35401				6	50.20099	51.35435
			5	50.18056	51.36676				5	50.17522	51.37014
			4	50.19873	51.35565				4	50.18839	51.36180
			3	50.20100	51.35434				3	50.18495	51.36397
			2	50.19021	51.36064				2	50.18209	51.36579
			1	50.18453	51.36424				1	50.17236	51.37195
			0	50.16466	51.37750				0	50.15804	51.38230
			-1	50.18397	51.36460				-1	50.17178	51.37231
			-2	50.19305	51.35885				-2	50.17751	51.36869
			-3	50.20270	51.35336				-3	50.18839	51.36180
			-4	50.19816	51.35598				-4	50.18095	51.36651
			-5	50.19759	51.35632				-5	50.18037	51.36687
			-6	50.18908	51.36136				-6	50.21530	51.34639
			-7	50.20157	51.35401				-7	50.19984	51.35501
			-8	50.20441	51.35239				-8	50.21015	51.34919
45	-2	-2 1/2	8	50.21453	51.34675	49	-2	-4	8	50.21702	51.34547
			7	50.20498	51.35207				7	50.20614	51.35142
			6	50.20043	51.35467				6	50.20499	51.35206
			5	50.17545	51.36999				5	50.17808	51.36833
			4	50.18841	51.36172				4	50.18206	51.36542
			3	50.18964	51.36100				3	50.18381	51.36500
			2	50.18283	51.36532				2	50.17923	51.36760
			1	50.18170	51.36604				1	50.17579	51.36978
			0	50.16182	51.37953				0	50.17865	51.36796
			-1	50.18170	51.36604				-1	50.17522	51.37014
			-2	50.18453	51.36424				-2	50.18037	51.36687
			-3	50.19305	51.35885				-3	50.18896	51.36144
			-4	50.18397	51.36460				-4	50.18839	51.36180
			-5	50.17829	51.36819				-5	50.18495	51.36397
			-6	50.20556	51.35207				-6	50.20557	51.35174
			7	50.19816	51.35598				7	50.21931	51.34425
			8	50.21009	51.34923				8	50.21988	51.34395

50	-2	-4 1/2	8	50.21611	51.[illegible]				1/2	8	50.20213	51.[illegible]9
			7	50.21[illegible]6	51.[illegible]96					7	50.20156	51.[illegible]402
			6	50.20619	51.[illegible]29					6	50.20961	51.[illegible]668
			5	50.19326	51.[illegible]80					5	50.18[illegible]3	51.[illegible]961
			4	50.18037	51.[illegible]8					4	50.19[illegible]83	51.[illegible]708
			3	50.17900	51.[illegible]77					3	50.19[illegible]83	51.[illegible]708
			2	50.17930	51.[illegible]726					2	50.18096	51.[illegible]146
			1	50.17867	51.[illegible]79					1	50.18037	51.36687
			0	50.18610	51.[illegible]42					0	50.18093	51.36651
			1	50.17007	51.[illegible]26					1	50.17980	51.36724
			2	50.17064	51.[illegible]306					2	50.19041	51.36107
			3	50.17751	51.[illegible]69					3	50.19641	51.35702
			4	50.18067	51.[illegible]289					4	50.20385	51.35271
			5	50.18890	51.[illegible]144					5	50.18438	51.36434
			6	50.20843	51.[illegible]014					6	50.22790	51.33980
			7	50.22103	51.[illegible]37					7	50.19011	51.36071
			8	50.22103	51.[illegible]37					8	50.17178	51.37231
51	-2	-5	8	50.21988	51.34395	62	6		1/2	8	50.21244	51.34794
			7	50.21587	51.34608					7	50.20328	51.35304
			6	50.20786	51.35046					6	50.20156	51.35402
			5	50.19068	51.36035					5	50.19641	51.35702
			4	50.18095	51.36651					4	50.17293	51.37159
			3	50.17064	51.37304					3	50.19011	51.36071
			2	50.16949	51.37413					2	50.18381	51.6500
			1	50.16949	51.37413					1	50.17808	51.6833
			0	50.17522	51.37014					0	50.17007	51.37374
			1	50.16319	51.37855					-1	50.17178	51.37231
			-2	50.16319	51.37855					2	50.19182	51.35962
			-3	50.16663	51.37612					3	50.19469	51.35781
			-4	50.18095	51.36651					4	50.17579	51.36978
			-5	50.19297	51.35890					5	50.19011	51.36071
			6	50.21072	51.34887					6	50.20499	51.35206
			7	50.22046	51.34365					7	50.20900	51.34982
			8	50.22275	51.34245					8	50.21645	51.34577
52	-2	-5 1/2	8	50.22389	51.34186	65	16	-5 1/2		8	50.21473	51.34670
			7	50.22046	51.34365					7	50.21816	51.34486
			6	50.21244	51.34794					6	50.23191	51.33778
			5	50.19297	51.35890					5	50.23878	51.33437
			4	50.18266	51.36542					4	50.23763	51.33494
			3	50.16777	51.37532					3	50.23882	51.32518
			2	50.16663	51.37612					2	50.23992	51.33382
			1	50.16663	51.37612					1	50.24470	51.33052
			0	50.17121	51.37268					0	50.24622	51.33079
			1	50.16319	51.37855					1	50.23821	51.33466
			2	50.16548	51.37692					2	50.23019	51.33864
			3	50.16892	51.37453					3	50.21988	51.34395
			4	50.17980	51.36724					4	50.22389	51.34186
			5	50.19870	51.35567					5	50.24279	51.33243
			6	50.21358	51.34732					6	50.23363	51.33692
			7	50.22504	51.34127					7	50.22160	51.34305
			8	50.22504	51.34127					8	50.21874	51.34455
56	-6	-2 1/2	8	50.20786	51.35046	66	16	4 1/2		8	50.19411	51.35817
			7	50.20385	51.35271					7	50.19755	51.35634
			6	50.19927	51.3554					6	50.19755	51.35634
			5	50.17751	51.36869					5	50.21358	51.34732
			4	50.19011	51.36071					4	50.18667	51.6289
			3	50.19125	51.35999					3	50.20728	51.35078
			2	50.19240	51.35926					2	50.21129	51.34856
			1	50.17121	51.37268					1	50.22160	51.34305
			0	50.17121	51.37268					0	50.22561	51.34097
			1	50.17064	51.37304					1	50.22561	51.34097
			2	50.19068	51.36035					2	50.22160	51.34305
			3	50.18896	51.36144					3	50.19469	51.35781
			4	50.18381	51.36500					4	50.19354	51.35853
			5	50.18595	51.36397					5	50.21416	51.34701
			6	50.20270	51.35336					6	50.20557	51.35174
			7	50.22477	51.34035					7	50.20213	51.35369
			8	50.22900	51.33782					8	50.19812	51.35601

Run	x	y	z	P_p/P_{0_c}	M	Run	x	y	z	P_p/P_{0_c}	M
67	16	3 1/2	8	50.19469	51.35781	71	-16	1 2	8	50.19812	51.35601
			7	50.19698	51.35668				7	50.19411	51.35817
			6	50.19812	51.35601				6	50.18896	51.36144
			5	50.20385	51.35271				5	50.18209	51.36579
			4	50.18610	51.36325				4	50.18209	51.36579
			3	50.20328	51.35304				3	50.18839	51.36180
			2	50.21129	51.34856				2	50.19984	51.35501
			1	50.22046	51.34365				1	50.20328	51.35304
			0	50.21816	51.34486				0	50.20385	51.35271
			-1	50.21931	51.34425				-1	50.20328	51.35304
			2	50.21473	51.34670				-2	50.19641	51.35702
			3	50.20614	51.35142				3	50.18495	51.36397
			-4	50.21759	51.34516				4	50.18782	51.36216
			5	50.19297	51.35890				5	50.17923	51.36760
			-6	50.20328	51.35304				6	50.19011	51.36071
			-7	50.21702	51.34547				7	50.19641	51.35702
			-8	50.19870	51.35567				-8	50.20156	51.35402
68	-16	2 1/2	8	50.193	51.359	72	-16	-1 1/2	8	50.20156	51.35402
			7	50.1945	51.358				7	50.20270	51.35336
			6	50.196	51.357				6	50.19297	51.35890
			5	50.203	51.353				5	50.19297	51.35890
			4	50.1845	51.364				4	50.18953	51.36107
			3	50.2015	51.354				3	50.20099	51.35435
			2	50.209	51.350				2	50.21072	51.34887
			1	50.218	51.345				1	50.21416	51.34701
			0	50.216	51.346				0	50.21301	51.34762
			-1	50.217	51.346				-1	50.21530	51.34639
			-2	50.212	51.348				-2	50.20671	51.35110
			-3	50.204	51.353				-3	50.19870	51.35567
			-4	50.1925	51.359				-4	50.19182	51.35962
			-5	50.1915	51.360				-5	50.19411	51.35817
			-6	50.2015	51.354				-6	50.18953	51.36107
			-7	50.198	51.356				-7	50.20213	51.35369
			-8	50.1965	51.357				-8	50.20499	51.35206
69	-16	1 1/2	8	50.19927	51.35534	73	-16	-2 1/2	8	50.19755	51.35634
			7	50.19927	51.35534				7	50.20614	51.35142
			6	50.18495	51.36397				6	50.20900	51.34982
			5	50.19469	51.35781				5	50.20385	51.5271
			4	50.18037	51.36687				4	50.19354	51.3585
			3	50.18953	51.36107				3	50.20786	51.3504
			2	50.20213	51.3569				2	50.21759	51.34516
			1	50.20728	51.35078				1	50.22103	51.4335
			0	50.20499	51.35206				0	50.21988	51.34395
			-1	50.20557	51.35174				-1	50.22046	51.465
			-2	50.20156	51.35402				-2	50.2150	51.4639
			-3	50.18953	51.36107				-3	50.20385	51.35271
			-4	50.18724	51.36252				-4	50.19125	51.35999
			-5	50.18724	51.36252				5	50.20900	51.34982
			-6	50.19011	51.36071				-6	50.20156	51.35402
			-7	50.20156	51.35402				7	50.20385	51.35271
			-8	50.20099	51.35435				-8	50.20270	51.35336
70	-16	1/2	8	50.19698	51.35668	74	16	3 1/2	8	50.19870	51.35567
			7	50.19354	51.35853				7	50.20213	51.35369
			6	50.18610	51.36325				6	50.21129	51.34856
			5	50.18037	51.36687				5	50.21072	51.34887
			4	50.17694	51.36905				4	50.19641	51.35702
			3	50.18266	51.36542				3	50.21358	51.34732
			2	50.18724	51.36252				2	50.22160	51.34305
			1	50.18381	51.36500				1	50.22733	51.34009
			0	50.18495	51.36397				0	50.22618	51.34068
			1	50.18667	51.36289				1	50.22561	51.34097
			2	50.18610	51.36325				2	50.21988	51.34345
			3	50.18152	51.36615				3	50.20900	51.34982
			4	50.18495	51.36397				4	50.20270	51.35336
			5	50.17636	51.36941				5	50.22046	51.34365
			6	50.19011	51.36071				6	50.20270	51.35336
			7	50.19469	51.35781				7	50.20270	51.35336
			8	50.20041	51.35468				8	50.19927	51.35534

Run	x	y	z	P_p P_{o_c}	M	Run	x	y	z	P_p P_{o_c}	M
75	16	4 1/2	8	50.21072	51.34887	79	0	1/2	8	50.21115	51.34864
			7	50.21301	51.34762				7	50.21115	51.34864
			6	50.22561	51.34097				6	50.20934	51.34963
			5	50.22217	51.34275				5	50.18225	51.36568
			4	50.20442	51.35239				4	50.19486	51.35770
			3	50.20499	51.35206				3	50.19848	51.35580
			2	50.21645	51.34577				2	50.19004	51.36076
			1	50.22618	51.34068				1	50.17616	51.36954
			0	50.22561	51.34097				0	50.16952	51.37411
			-1	50.21759	51.34516				-1	50.17616	51.36954
			-2	50.20900	51.34982				-2	50.19183	51.35961
			-3	50.20213	51.35369				-3	50.20089	51.35440
			-4	50.21072	51.34887				-4	50.21417	51.34700
			-5	50.22618	51.34068				-5	50.17918	51.36763
			-6	50.21587	51.34608				-6	50.20451	51.35233
			-7	50.21244	51.34794				-7	50.21417	51.34700
			-8	50.20900	51.34982				-8	50.15022	51.38824
76	-16	5 1/2	8	50.21988	51.34395	80	0	1/2	8	50.25767	51.32569
			7	50.22160	51.34305				7	50.21129	51.34856
			6	50.23935	51.33410				6	50.20557	51.35174
			5	50.23534	51.33606				5	50.17980	51.36724
			4	50.22446	51.34156				4	50.19125	51.35999
			3	50.19755	51.35634				3	50.19812	51.35601
			2	50.21072	51.34887				2	50.18953	51.36107
			1	50.21702	51.34547				1	50.17522	51.37014
			0	50.21874	51.34455				0	50.17407	51.37086
			-1	50.21587	51.34608				-1	50.17522	51.37014
			-2	50.20958	51.34951				-2	50.19125	51.35999
			-3	50.19870	51.35567				-3	50.20041	51.35468
			-4	50.21645	51.34577				-4	50.21015	51.34919
			-5	50.23534	51.33606				-5	50.17121	51.37268
			-6	50.23763	51.33494				-6	50.20442	51.35239
			-7	50.22046	51.34365				-7	50.21416	51.34701
			-8	50.21816	51.34486				-8	50.15002	51.38838
77	-16	1/2	8	50.20391	51.35268	81	6	1/2	8	50.14602	51.39156
			7	50.19788	51.35615				7	50.21645	51.34577
			6	50.19245	51.35923				6	50.21587	51.34608
			5	50.19426	51.35808				5	50.18266	51.36542
			4	50.17978	51.36725				4	50.18266	51.36542
			3	50.19667	51.35686				3	50.18782	51.36216
			2	50.19969	51.35510				2	50.18495	51.36397
			1	50.20150	51.35405				1	50.17865	51.36796
			0	50.20331	51.35302				0	50.19068	51.36035
			-1	50.20210	51.35371				1	50.19182	51.35962
			-2	50.19788	51.35615				2	50.19354	51.35853
			-3	50.19064	51.36037				-3	50.19526	51.35745
			-4	50.18581	51.36343				-4	50.18152	51.36615
			-5	50.18943	51.36114				-5	50.18610	51.36325
			-6	50.20150	51.35405				6	50.18324	51.36500
			-7	50.20089	51.35440				7	50.21416	51.34701
									8	50.14029	51.39624
78	0	1/2	8	50.172	51.372	82	6	1 1/2	8	50.17007	51.37374
			7	50.1885	51.362				7	50.21358	51.34732
			6	50.1752	51.370				6	50.21244	51.34794
			5	50.1663	51.376				5	50.18438	51.36434
			4	50.1645	51.378				4	50.17751	51.36869
			3	50.164	51.379				3	50.18495	51.36397
			2	50.155	51.385				2	50.17751	51.36869
			1	50.1445	51.393				1	50.19011	51.36071
			0	50.144	51.393				0	50.19011	51.36071
			-1	50.1452	51.392				1	50.19068	51.36035
			-2	50.158	51.382				2	50.20156	51.35402
			3	50.167	51.376				3	50.18495	51.36397
			-4	50.1835	51.365				4	50.18324	51.36500
			5	50.1605	51.380				5	50.18152	51.36615
			-6	50.176	51.369				6	50.21072	51.34887
			7	50.191	51.360				7	50.21473	51.34670
			8	50.120	51.400				8	50.16568	51.37692

Run	x	y	z	P_0, P	M	Run	x	y	z	P_0, P_{0_1}	M
83	6	2 1/2	8	50.19[illegible]	51.3[illegible]	87	[illegible]	1 1/2	8	50.18491	51.37733
			7	50.21416	51.34701				7	50.21874	51.34455
			[illegible]	50.20[illegible]	51.3[illegible]				[illegible]	50.21416	51.34701
			5	50.18[illegible]	51.36361				5	50.18037	51.36687
			4	50.17751	51.36869				4	50.18381	51.36500
			3	50.18266	51.36542				3	50.18266	51.36542
			2	50.19011	51.36071				2	50.17865	51.36796
			1	50.19126	51.35[illegible]				1	50.19125	51.35999
			0	50.19297	51.35890				0	50.19870	51.35667
			1	50.19297	51.35890				1	50.22503	51.34335
			2	50.20270	51.35336				2	50.21988	51.34395
			3	50.19240	51.35926				3	50.19698	51.35668
			4	50.18209	51.36579				4	50.18495	51.36397
			5	50.18839	51.36180				5	50.18438	51.36434
			6	50.20786	51.35046				6	50.21187	51.34825
			7	50.21473	51.34670				7	50.21645	51.34577
			8	50.18896	51.36144				8	50.14487	51.39248
84	6	3 1/2	8	50.21587	51.34608	88	6	1 1/2	8	50.19755	51.35634
			7	50.21587	51.34608				7	50.21816	51.34486
			6	50.21416	51.34701				6	50.21129	51.34856
			5	50.19411	51.35817				5	50.18266	51.36542
			4	50.18610	51.36325				4	50.18495	51.36397
			3	50.19125	51.35999				3	50.18610	51.36325
			2	50.19698	51.35668				2	50.18495	51.36397
			1	50.20156	51.35402				1	50.19354	51.35853
			0	50.17007	51.37374				0	50.19583	51.35708
			1	50.18553	51.36361				1	50.19641	51.35702
			-2	50.21129	51.34856				-2	50.19583	51.35708
			-3	50.21759	51.34516				-3	50.18610	51.36325
			4	50.20900	51.34982				4	50.18324	51.36500
									5	50.18839	51.36180
									6	50.21244	51.34794
									7	50.21816	51.34486
85	6	4 1/2	8	50.21816	51.34486	89	6	-2 1/2	8	50.22561	51.34097
			7	50.21874	51.34455				7	50.24794	51.32997
			6	50.21931	51.34425				6	50.20786	51.35046
			5	50.19583	51.35708				5	50.18381	51.36500
			4	50.17980	51.36724				4	50.18667	51.36289
			3	50.17236	51.37195				3	50.18896	51.36144
			2	50.17064	51.37304				2	50.20270	51.35336
			1	50.17121	51.37268				1	50.25252	51.32782
			0	50.16949	51.37413				0	50.19469	51.35781
			-1	50.17579	51.36978				1	50.20099	51.35435
			2	50.17980	51.36724				2	50.19240	51.35926
			-3	50.18896	51.36144				3	50.19011	51.36071
			4	50.18324	51.36500				-4	50.17636	51.36941
			5	50.18953	51.36107				5	50.19068	51.36035
			-6	50.21473	51.34670				6	50.21530	51.34639
			7	50.22103	51.34335				7	50.25767	51.32569
			-8	50.21759	51.34516				8	50.17522	51.37014
86	6	5 1/2	8	50.22217	51.34275	90	6	-3 1/2	8	50.21816	51.34486
			7	50.21759	51.34516				7	50.27886	51.31657
			6	50.21187	51.34825				6	50.21129	51.34856
			5	50.20385	51.35271				5	50.18553	51.36361
			4	50.18324	51.36500				4	50.19125	51.35999
			3	50.19698	51.35668				3	50.19240	51.35926
			2	50.19125	51.35999				2	50.19927	51.35534
			1	50.18152	51.36615				1	50.19469	51.35781
			0	50.17522	51.37014				0	50.19125	51.35999
			1	50.17579	51.36978				1	50.19812	51.35601
			2	50.18037	51.36687				2	50.20328	51.35304
			3	50.17808	51.36833				3	50.20156	51.35402
			4	50.18667	51.36289				4	50.17636	51.36941
			5	50.20156	51.35402				5	50.19125	51.35999
			6	50.21187	51.34825				6	50.21759	51.34516
			7	50.21416	51.34701				7	50.29031	51.31192
			8	50.22046	51.34365				8	50.1[illegible]	51.38103

Run	x	y	z	P_p/P_{o_c}	M	Run	x	y	z	P_p/P_{o_c}	M
91	6	4 1/2	8	50.27085	51.31994	95	0	1/2	8	50.19297	51.35890
			7	50.25939	51.32492				7	50.20557	51.35174
			6	50.20958	51.34951				6	50.20156	51.35402
			5	50.18667	51.36289				5	50.17751	51.36869
			4	50.17980	51.36724				4	50.18839	51.36180
			3	50.18782	51.36216				3	50.19641	51.35702
			2	50.18610	51.36325				2	50.18839	51.36180
			1	50.18553	51.36361				1	50.17407	51.37086
			0	50.18324	51.36500				0	50.17236	51.37195
			-1	50.18266	51.36542				1	50.17407	51.37086
			-2	50.18324	51.36500				2	50.19011	51.36071
			-3	50.19068	51.36035				3	50.19870	51.35567
			-4	50.18896	51.36144				4	50.20671	51.35110
			-5	50.18839	51.36180				-5	50.16835	51.37492
			-6	50.21301	51.34762				-6	49.12597	51.72835
			-7	50.28516	51.31399				7	50.43089	51.26543
			-8	50.18782	51.36216						
92	6	-5 1/2	8	50.25939	51.32492	96	0	1/2	8	50.20099	51.35435
			7	50.21931	51.34425				7	50.21530	51.34639
			6	50.20728	51.35078				6	50.20728	51.35078
			5	50.19297	51.35890				5	50.18152	51.36615
			4	50.17579	51.36978				4	50.19182	51.35962
			3	50.16835	51.37492				3	50.19670	51.35567
			2	50.16777	51.37532				2	50.18953	51.36107
			1	50.16606	51.37652				1	50.17522	51.37014
			0	50.16491	51.37733				0	50.17407	51.37086
			-1	50.16606	51.37652				-1	50.17522	51.37014
			-2	50.16949	51.37413				-2	50.19125	51.35999
			-3	50.17064	51.37304				-3	50.20099	51.35435
			-4	50.18782	51.36216				4	50.21244	51.34794
			-5	50.20099	51.35435				5	50.17293	51.37159
			-6	50.21301	51.34762				6	50.20614	51.35142
			-7	50.23248	51.33749				7	50.21187	51.34825
			-8	50.26626	51.32191				8	50.15690	51.38315
93	0	1/2	8	50.17064	51.37304	97	0	1/2	8	50.32009	51.30060
			7	50.18610	51.36325				7	50.22275	51.34245
			6	50.18839	51.36180				6	50.21072	51.34887
			5	50.16835	51.37492				5	50.18438	51.36434
			4	50.18037	51.36687				4	50.19411	51.35817
			3	50.19011	51.36071				3	50.20041	51.35468
			2	50.18553	51.36361				2	50.19068	51.36035
			1	50.17236	51.37195				1	50.17579	51.36978
			0	50.17293	51.37159				0	50.17465	51.37050
			1	50.17293	51.37159				-1	50.17579	51.36978
			-2	50.18724	51.36252				-2	50.19125	51.35999
			-3	50.19411	51.35817				-3	50.20213	51.35369
			-4	50.19583	51.35708				-4	50.21530	51.34639
			-5	50.15861	51.38187				5	50.17522	51.37014
			-6	50.18610	51.36325				6	50.21015	51.34919
			7	50.19068	51.36035				7	50.22389	51.34186
			-8	50.12597	51.40881				-8	50.16262	51.37896
94	0	1/2	8	50.18610	51.36325	98	0	1/2	8	50.21816	51.34486
			7	50.19927	51.35534				7	50.23534	51.33606
			6	50.19812	51.35601				6	50.21530	51.34639
			5	50.17522	51.37014				5	50.18724	51.36252
			4	50.18610	51.36325				4	50.19755	51.35634
			3	50.18896	51.36144				3	50.19984	51.35501
			2	50.18782	51.36216				2	50.18896	51.36144
			1	50.17350	51.37123				1	50.17350	51.37123
			0	50.17178	51.37231				0	50.17465	51.37050
			1	50.17350	51.37123				1	50.17293	51.37159
			2	50.18953	51.36107				-2	50.18953	51.36107
			-3	50.19698	51.35668				3	50.20099	51.35435
			-4	50.20328	51.35304				-4	50.22046	51.34365
			-5	50.16548	51.37692				5	50.17923	51.36760
			6	50.19583	51.35708				6	50.21702	51.34447
			7	50.20328	51.35304				7	50.24221	51.33271
			8	50.14029	51.39024				8	50.11968	51.41478

Run	x	y		P_p/P_{o_c}	M	Run	x	y		P_p/P_{o_s}	M
103	0	1/2	8	50.17639	51.36939	107	0	1/2	8	50.32409	51.29947
			7	50.20089	51.35467				7	50.31572	51.30219
			6	50.20091	51.35439				6	50.30914	51.30647
			5	50.17938	51.36750				5	50.31213	51.30349
			4	50.19015	51.36068				4	50.29897	51.30853
			3	50.19493	51.35786				3	50.26130	51.32406
			2	50.18536	51.36371				2	50.31213	51.30349
			1	50.17161	51.37242				1	50.31332	51.30306
			0	50.16563	51.37682				0	50.31093	51.30392
			1	50.16922	51.37432				1	50.30978	51.30435
			2	50.18536	51.36371				2	50.31930	51.30090
			3	50.19613	51.35690				3	50.28701	51.31325
			4	50.21287	51.34770				4	50.27745	51.31716
			5	50.17061	51.37318				5	50.31273	51.30327
			6	50.19792	51.35613				6	50.31452	51.30262
			7	50.20569	51.35167				7	50.31871	51.30111
			-8	50.12918	51.41143				8	50.29897	51.30853
104	0	3 1/2	8	50.21466	51.34673	108	0	1 1/2	8	50.32528	51.29874
			7	50.20510	51.35201				7	50.32289	51.29960
			6	50.20211	51.35370				6	50.31572	51.30219
			5	50.19453	51.35803				5	50.30316	51.30692
			4	50.17759	51.36864				4	50.29120	51.31157
			3	50.19194	51.35965				3	50.26130	51.32406
			2	50.18357	51.36500				2	50.28941	51.31229
			1	50.18058	51.36674				1	50.30196	51.30737
			0	50.20091	51.35439				0	50.30077	51.30783
			-1	50.18536	51.36371				1	50.30017	51.30806
			-2	50.18776	51.36220				-2	50.30316	51.30692
			3	50.19672	51.35683				-3	50.28522	51.31397
			-4	50.17998	51.36712				-4	50.27386	51.31866
			-5	50.20031	51.35474				-5	50.30555	51.30586
			-6	50.20091	51.35439				6	50.31751	51.30154
			-7	50.20510	51.35201				7	50.32469	51.29895
			-8	50.20689	51.35100				-8	50.32708	51.29809
105	0	-2 1/2	8	50.20390	51.35268	109	0	2 1/2	8	50.32050	51.30046
			7	50.20450	51.35234				7	50.32887	51.29744
			6	50.25532	51.32674				6	50.32349	51.29938
			5	50.17041	51.37318				5	50.30017	51.30806
			4	50.18417	51.36447				4	50.29180	51.31134
			3	50.18118	51.36636				3	50.29419	51.31039
			2	50.17460	51.37053				2	50.29180	51.31134
			1	50.16922	51.37432				1	50.29539	51.30992
			0	50.17699	51.36902				0	50.29598	51.30969
			-1	50.17520	51.37015				-1	50.29718	51.30922
			-2	50.17998	51.36712				-2	50.29539	51.30992
			-3	50.18296	51.36296				3	50.30495	51.30608
			-4	50.18118	51.36636				-4	50.30017	51.30806
			-5	50.18477	51.36409				5	50.28522	51.31397
			-6	50.18357	51.36500				-6	50.31871	51.30111
			-7	50.20211	51.35370				-7	50.33126	51.29658
			-8	50.19852	51.35578				-8	50.31930	51.30090
106	-16	1/2	8	50.19314	51.35879	110	0	3 1/2	8	50.32588	51.29852
			7	50.18716	51.36258				7	50.32170	51.30000
			6	50.18237	51.36561				6	50.32409	51.29917
			5	50.17938	51.36750				5	50.31572	51.30219
			4	50.17879	51.36788				4	50.29180	51.31134
			3	50.17819	51.36826				3	50.28522	51.31397
			2	50.18237	51.36561				2	50.25831	51.32538
			1	50.18118	51.36636				1	50.26967	51.32043
			0	50.18118	51.36636				0	50.27685	51.31741
			-1	50.24217	51.33273				1	50.27805	51.31691
			-2	50.24217	51.33273				2	50.27386	51.31866
			-3	50.17819	51.36826				3	50.29539	51.30992
			4	50.17998	51.36712				-4	50.30256	51.30714
			-5	50.16264	51.37894				5	50.31093	51.30392
			-6	50.18536	51.36371				6	50.32170	51.30000
			-7	50.19015	51.36068				7	50.32110	51.30025
			8	50.19433	51.35803				8	50.32708	51.29809

Run	x	y		P_p	P_{p_1}
111	0	1/2	8	50.33186	51.29676
			7	50.32887	51.29744
			6	50.33304	51.29693
			5	50.33664	51.29463
			4	50.30256	51.30714
			3	50.29479	51.31016
			2	50.28701	51.31325
			1	50.28213	51.31494
			0	50.27 [illegible]	51.31[illegible]
			1	50.27 [illegible]	51.31066
				50.28104	51.31568
				50.28343	51.31470
			4	50.29359	51.31063
			5	50.33485	51.29528
			6	50.33605	51.29485
			7	50.32648	51.29830
			8	50.33007	51.29701
112	-16	1/2	8	50.31631	51.30198
			7	50.33485	51.29528
			6	50.33126	51.29658
			5	50.32588	51.29852
			4	50.30615	51.30[illegible]
			3	50.29180	51.31134
			2	50.30077	51.30783
			1	50.30137	51.30760
			0	50.30734	51.30522
			1	50.30077	51.30783
			2	50.29838	51.30876
			3	50.31153	51.30370
			4	50.30137	51.30760
			5	50.32648	51.29830
			6	50.33246	51.29614
			7	50.33844	51.29398
			8	50.30854	51.30478
113	-16	3 1/2	8	50.32229	51.29982
			7	50.33545	51.29506
			6	50.33605	51.29485
			5	50.32588	51.29852
			4	50.30974	51.30435
			3	50.30017	51.30806
			2	50.29000	51.31205
			1	50.27924	51.31641
			0	50.28343	51.31470
			1	50.28104	51.31568
			2	50.29299	51.31086
			3	50.30555	51.30586
			4	50.31572	51.30219
			5	50.32170	51.30000
			6	50.33724	51.29441
			7	50.33724	51.29441
			8	50.33066	51.29679